

Seasonal Statistics of Shannon Capacity in a Dynamical Poisson-Voronoi Cellular Network

Sanjoy Kumar Jhavar and François Baccelli

Abstract—In this work we consider a dynamical cellular communication network in which mobile BSs are modeled as a homogeneous Poisson point process on \mathbb{R}^2 . Each base station moves at a constant speed in a random direction. A typical user connects to the nearest base station and it experiences variable signal and interference powers depending on the distance of all the stations. Along the motion of the stations, the user swaps its serving station, and such an event is called a *handover*. We are interested in the performance evaluation of the system under some classical and tropical metrics of interest at different time of events, inducing handovers, maximal proximity of serving station, nearest interferer at closest or farthest distance with respect to the user or at any typical time epoch. A comparison study of quality of service and Shannon capacity at these epochs is also provided, among the recurrence of such “good” or “bad” scenarios. We can make an analogy with seasons based on the fluctuations of signal and interference power. Strong or mild signal or interference power correspond to different seasons of Shannon capacity along the evolution of the system.

Index Terms—Wireless communication, handover, stochastic geometry, dynamical communications, performance evaluation, Shannon capacity, dimensioning, seasonal statistics, time series of Shannon capacity, tropical SINR.

I. INTRODUCTION

Modern wireless communication systems rely or will rely on the large scale deployment of vehicular and in particular non-terrestrial base stations (BS). Due to the mobility of such BSs, it is extremely important to assess the performance at all epochs of this process and find out ways to mitigate challenges posed by certain types of “good” or “bad” epochs or configurations in such systems. The most important performance metric for the quality of service (QoS) is the distribution of the Shannon rate experienced by a typical user in the system, which is a function of signal-to-interference-plus-noise-ratio (SINR) at any time instant.

To characterize the time evolution of Shannon capacity [1], we define a dynamical communication network model with random locations of BSs. This randomness is complemented by their random motion, and this makes the time evolution of the SINR a stochastic process. Stochastic geometry plays an important role in developing suitable models to understand many statistical features of key performance metrics in such systems. As we will see, it allows one to derive ensemble averages of the system properties, including at such specific epochs.

In this article we precisely focus on determining performance metrics of dynamical cellular communication systems at specific typical epochs of interest. For example, consider a time epoch when the power of the signal is maximum. This correspond to the time when the serving BS is at its minimal distance from the user in its motion. The SINR at this typical epoch is measured using the distance to the serving BS and that of all others. To measure the performance of the system, we take an average over all possible configurations of the system at such epochs, instead of taking averages at all times.

We first define the dynamical cellular communication model on \mathbb{R}^2 . The BSs are distributed as a homogeneous Poisson point process and all move at constant speed v and with a uniformly chosen and independent random direction. A user located at the origin (o) connects to the nearest BS at all time instants and changes its connection to whichever is the closest. This phenomenon is called a *handover*. Due to the motion of every station, the user encounters changes in the distance to the serving station, along the spatio-temporal evolution of the system. These temporal variations result in a continuous change in the performance metrics in terms of signal and interference power. We are in particular interested in determining the behavior of the system performance at specific time epochs whenever the user sees an abrupt change, for example at a handover epoch, at a time when the signal power is locally maximum, or at a time when the nearest interferer is at its closest or farthest distance.

Our investigation is based on analyzing the fluctuations of the SINR. We also use the maxitive (or tropical) interference, with a goal to capture the effect of the strongest interferer on the performance evaluation. As we will see, this is governed by the joint distribution of the distance to the nearest station, contributing to the signal power, as well as the distance to all other stations, contributing to the interference power. On the other hand, their comparison at different typical epochs is mainly governed by the comparison of the distribution of the distance to the serving BS or the closest interferer depending on the typical epochs.

As the title of this article suggests, one can better visualize this interplay between the evolving strong or weak signal and interference powers, as the evolution of seasons over time, where there is a unique source of signal power, and a joint source of interference power. The entire analysis is based on the identification of typical events corresponding to *max-signal*, *min-signal*, *min-interference* or *max-interference*, and probabilistic features of these seasonal statistics. Our

comparison results focus on the coverage probability and the Shannon capacity. Even though the time evolution of the interplay between strong or weak signal and interference power resembles the dynamics of seasons, in contrast, our spatio-temporal model is highly non-periodic. For instance, it can be seen to possibly possess two max-interference seasons without even having a max-signal in between. Also, there can be two max-signal seasons and a max-interference season in between, and vice versa. In our context, the temporal evolution or the time series of the Shannon capacity, can be better visualized in terms of Figure 2. In the tropical sense, the interference is considered to be from the maximum interferer only, and the effect of such a reduction can be seen in the entire analysis, from seasonal statistics to their comparison. Our analysis and results provide insight about the worst case scenarios at extreme seasons and can help the system designer to dimension the network based on this, rather on the typical time. This also prepares the system to be more proactive than reactive at such typical epochs.

The Figure 1 depicts a realization of the trajectories of the BSs and the evolution of the distance to the nearest and second nearest BSs, and the corresponding time series of the Shannon capacities (or rates) are shown in Figure 2, for the simple case of tropical SIR with power law attenuation for different attenuation exponent α and without fading. In the interference limited no-fading case, the Shannon capacity at time t is defined as

$$\mathcal{R}(t) := B \ln \left(1 + \frac{H(t)^{-\alpha}}{R(t)^{-\alpha}} \right),$$

where $H(t)$ and $R(t)$ are the distance to the nearest and second nearest BS, respectively, at time t , α is the exponent of the path-loss attenuation and $B = b/\ln 2$, with b being the bandwidth. Depending on the time-evolution of the ratio of the distance to the serving BS and nearest interferer there are high or low ‘seasons’ of Shannon capacity along the evolution of the system. We are interested in the characteristics of it at the seasons alluded before and depicted with vertical lines in Figure 2. The non-periodicity of the seasons and their sequential but random appearance are also evident even in the simple tropical model without noise and fading, whereas handover epochs are the worst seasons in terms of Shannon capacity experienced by the user. It can be seen as a one-to-one ‘tug of war’ between the signal and tropical interference power over time. The time series of the Shannon capacity turns out to be even more complex and infinitely dependent, while moving beyond tropical scenario with or without fading and noise. As we will see later in Remark 1, in a ‘dual dynamical model’ with a mobile user, which encounters the identical seasonality along its motion in a straight line, with BSs being fixed.

A. Motivation

Most of the literature about performance evaluation of wireless communication systems only deals with a snapshot analysis. For example, in a Poisson setting, we use a random variable for the distance to the nearest BS which is distributed as Rayleigh.

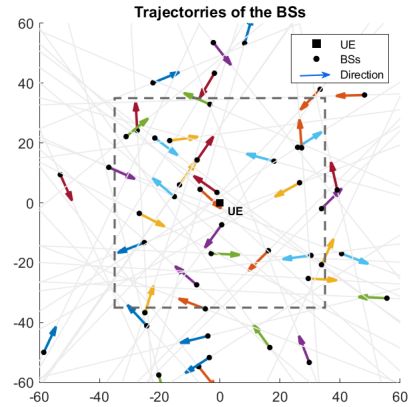


Fig. 1: Trajectory of BSs in a finite space and time window with respect to a fixed user at the origin. The black dots are the initial locations of the BSs and the arrows are for direction.

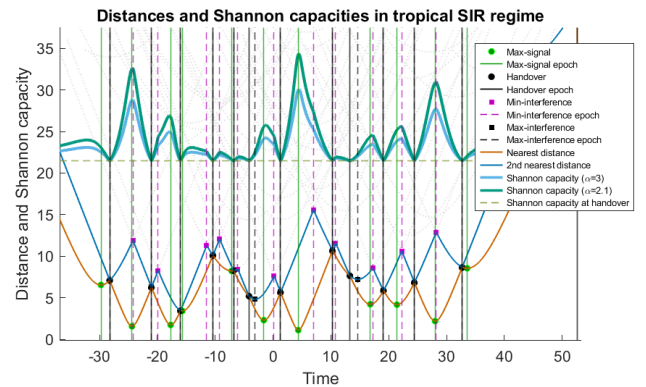


Fig. 2: Time series distance to the nearest (in red) and second nearest (in blue) BS(s) and that of Shannon capacities and typical epochs for $\alpha = 2.1$ (in light green) and 3 (in sky blue) in the tropical case without fading. The distance to all other BSs are shown with light grey curves in the background. The Shannon rate plots are vertically elevated for better visibility. The seasons are marked with vertical lines, and they appear non-periodically, for example: max-signal, handover, max-signal, min-interference, handover, max-interference and so on (counting from the left). The Shannon capacities are very prominent at handover and max-signal epochs, where as there is slight change of its slope at max-interference and min-interference epochs.

This is not the case at a handover epoch, as the system is conditioned on the existence of two BSs at equal distance from the typical user. As a result, the previous works fails to capture the performance of the system at such specific epochs, for example at a time when the signal or interference power is locally maximum or minimum. Our objective is to formally analyze a spatio-temporal model with the goal to capture the evolution of system performance at the typical epochs of interest listed before. As already mentioned, knowing a potentially extreme behavior at specific epochs can help the operator to prepare and dimension the system accordingly in all these best and perhaps more importantly worst case scenarios. From the system design perspective, it is also important to compare the performance at these time epochs.

B. Contributions

Below, we list out the main contributions made in this article. Most of our results are based on the power law attenuation function $\ell(r) = r^{-\alpha}$ and Rayleigh fading, where α is the path-loss exponent. As we will see later, it can be adapted to a more general class of attenuation functions and fading factors.

- 1) To set the stage for the performance evaluation, we identify and formalize the specific time epochs of interest within the spatio-temporal evolution of the system. This also includes the determination of the intensity of such epochs and the corresponding distance characteristics.
- 2) The mathematical analysis of the time epochs of locally minimum of distance to the interferer enables us to identify the handover point process for 2-Voronoi tessellation.
- 3) To determine the distribution of the interference power, we derive the distribution of the point process of BSs, other than the serving one at these epochs, which in our case turns out to be conditionally Poisson.
- 4) This leads to a determination of the coverage probability and Shannon rate at each of the typical epochs for both non-tropical and tropical scenarios. In some special cases, we manage to determine closed or integral form expressions for the coverage probability as well as the Shannon rate.
- 5) An analytic comparison of the performance metrics (coverage probability and Shannon rate) is also shown to hold between different typical epochs for both non-tropical and tropical scenarios. These comparisons are also validated by plotting these closed form or integral form expressions with respect to the user QoS parameter τ .
- 6) We establish Laplace transform order, moment generating order and likelihood ratio domination order relations between certain distances that contribute to the SINR. Our analysis is able to capture the fact that the Laplace transform order reflects onto a form of stochastic domination among the SINR at different typical epochs.
- 7) This also includes the comparison of interference power among different typical epochs, which is also consistent with our comparison of coverage probabilities.
- 8) We manage to establish some closed or integral form expressions for the coverage probabilities. A significant take away is that, in the interference limited regime with fading factor and with path-loss exponent $\alpha = 4$, the coverage probability at any of the typical epoch can be represented in terms of a non-linear function of the coverage probability at a typical time.
- 9) Some of the comparison results may hold true for the SINR defined using attenuation function other than the power law $\ell(r) = r^{-\alpha}$, for which we provide an example of bounded attenuation function $\ell(r) = (1 + r)^{-\alpha}$ and a counter example as well of step function with given

radius. The bounded attenuation function takes care of the singularity in the power law attenuation.

C. Literature

The first closed form expressions for Shannon capacity in cellular wireless communication systems using stochastic geometry were obtained in [2], when base stations are modelled as a Poisson point process. The analysis of cellular networks using tools from stochastic geometry gained significant traction following [2], and also [3]. Building on this foundation, performance evaluation of heterogeneous networks was explored in [4], [5], [6].

This was extended to the setting of satellite networks using stochastic geometry approach by Okati et. al. in [7] and [8] addressing the unique geometric and statistical challenges posed by non-terrestrial infrastructures. This line of work laid important groundwork for analyzing low Earth orbit (LEO) constellations, where the spatial distribution of satellites and their motion relative to ground users introduce non-trivial interference and coverage characteristics. The characterization of satellite constellations themselves has also received considerable attention. Choi et al. [9] proposed a constellation model grounded in stochastic geometry, enabling the analysis of coverage and connectivity for large-scale LEO deployments. This was further generalized to multi-altitude constellation architectures [10], where satellites operating at different heights create layered interference environments.

The dynamic nature of satellite on the orbits has motivated the development of dedicated mobility and motion models. Baccelli and Zuyev [11] introduced a dual dynamical model that jointly accounts for the motion of user and the stochastic geometry of static terrestrial network. Complementing this, the random direction model [12] provides a tractable abstraction for user or node mobility, and has found application in both terrestrial and non-terrestrial network analysis. Random geometric graph with similar mobility of random direction model is studied in [13].

The work [14] and [15] examines the impact of mobility on network performance, characterizing how node movement affects interference statistics and spatial reuse. Gong et al. [16] further incorporated fading in terms of mobility and channel randomness shapes coverage and outage probabilities. These contributions highlight that a complete performance analysis must account for both the spatial and temporal dimensions of network dynamics. A closely related thread concerns the temporal correlation of interference, which is of central importance when evaluating link-layer protocols and re-transmission schemes. Ganti and Haenggi [17] provided a rigorous treatment of this temporal correlation of interference and mitigation of the adversity provided by the later in Poisson networks. In a new paradigm, the effect mobility on the association policies in terms of Doppler shift and the performance evaluation is explored in [18]. Finally, questions of resource sharing and data rate allocation in spatially distributed networks have been addressed by Madadi et al. [19], who studied shared data rate models that account for the stochastic geometry of the network

alongside fairness and efficiency constraints. The notion of maximal power association in angular setting is studied in [20]. The current research is based on the handover analysis for the mobility model in [21] and as an initial ingredient about distance characteristics and Palm distributions are borrowed from there. The distance characteristics of similar interest in Poisson Voronoi tessellations are also studied in [22] and [23].

D. Organization of the article

This article starts with the initial description of the underlying system model and a set of questions of interest in Section II. Section III is dedicated to mathematical preliminaries, including a complete description of the system variables of interest. The proofs of the main results are presented in Appendix I. Section IV contains all the major results about the performance evaluation of the system at different typical events or equivalently seasons. This also includes the comparison among these QoS at typical events. Section V highlights some of the closed form or simple integral form expressions of the coverage probabilities in some of the regimes, due to specific values of the path-loss exponent α . We present the plots of the closed form or integral form expressions of coverage probabilities with respect to different threshold parameter τ . in Section VI. The proof of the main results about the performance evaluation and their expressions at different typical events are presented in Appendix II, for the case with fading. The proofs for the case without fading is presented in Appendix III. Appendix IV is dedicated to the proof of the comparison among the coverage probabilities at those typical epochs in cases with and without fading. The comparison of additive interference, as well as the tropical interference at different typical times is presented in Appendix V. Lastly, the proof for scale invariance property in the interference limited regime is given in Appendix VI.

II. SYSTEM MODEL AND PROBLEM FORMULATION

A. System Model

In this article, we work on a dynamical wireless communication network model based on a Poisson point process on \mathbb{R}^2 , as introduced in [21]. Consider a collection of BSs located at points of a homogeneous Poisson point process $\Phi_\lambda \equiv \Phi = \sum_i \delta_{X_i}$ on \mathbb{R}^2 with intensity λ . Suppose each of the BS moves at constant speed v , in a uniformly and independently chosen random direction. The BSs do not change their direction along the rest of the course. Suppose the directions are given by a collection of i.i.d. random variables $\{\Theta_i\}_i$. A user located at the origin stays connected to the nearest BS at any time, using a *distance based association rule*. During this connection period, the serving BS provides the down-link signal to the user and the rest of the BSs contribute to the total interference experienced by the user. The user changes its connection from one BS to next over time. Such a change of BS is called a *handover*. The time epochs of these handover events form a point process on the time axis.

For any BS starting at a location $X \in \Phi$ and moving in the direction Θ , it is located at $X^t := X + Vt$, at time t , where $V = v(\cos \Theta, \sin \Theta)$ and v is the modulus of the speed. We denote the point process corresponding to the new locations as $\Phi^t := \sum_i \delta_{X_i^t}$. It is well known from the displacement theorem [24, Section 5.5] that for all t , Φ^t is a homogeneous Poisson point process with intensity λ . We always write the location of the nearest BS as X_0^t . The time varying distance of a BS starting at $X = (|X| \cos \Psi, |X| \sin \Psi)$ is given by the function

$$d_X(t) := \|X^t\| = \left(\|X\|^2 + 2vt \cos \Xi + v^2 t^2 \right)^{\frac{1}{2}}, \quad (1)$$

where $\Xi := (\Theta - \Psi) \bmod(2\pi)$. Note that $\Xi \stackrel{d}{\sim} U[-\pi, \pi)$. The curve of the distance function will be used throughout the article. As we will see later, these curves are the branches of certain hyperbolas on the the upper half space $\mathbb{H}^+ := \mathbb{R} \times \mathbb{R}^+$.

Remark 1 (Dual dynamical model) *As it was shown in [21], this dynamical model is equivalent to the dual dynamical model, where the BSs are fixed but a mobile user is moving on a straight line at a constant speed. All the characteristics related to handovers, as seen in [21], at other typical epochs, and also the corresponding performance evaluations, are the same for both dynamical models.*

In the first model, in principle, at any time instant, the power of the signal emitted from each BS is a function of the distance from the user, using the power law attenuation function $\ell(\|X\|) = \|X\|^{-\alpha}$ for a BS located at X , where α is the path-loss exponent ranging between 2 and 4. In a more realistic scenario, one can incorporate a fading factor, given by a random variable with a given distribution. In the modelling of wireless communications, the performance of the serving BS is usually measured in terms of the SINR experienced by the user at time t , which is

$$\text{SINR}(t) := \frac{\rho \|X_0^t\|^{-\alpha}}{\sigma^2 + \sum_{Y \in \Phi^t \setminus \{X_0^t\}} \rho_Y \|Y\|^{-\alpha}}, \quad (2)$$

where σ^2 is the thermal noise power, $Y \in \Phi^t \setminus \{X_0^t\}$ are the locations of all other BSs at time t and ρ, ρ_Y are the i.i.d. fading factors. These can be considered as Rayleigh fading, but more general classes of fading distributions can cover a large set of use case. All other performance metrics, namely, *signal-to-noise-ratio* (SNR) and *signal-to-interference-ratio* (SIR) are defined similarly both in the fading and no-fading cases.

In addition, we also define a more restrictive version of the performance metrics using tropical interference, by this we mean that we replace the additive interference by maxitive interference over Φ^t , see [25] and [26]. In this case we are interested in the *signal-to-tropical interference-plus-noise-ratio* (STINR) defined as

$$\text{STINR}(t) := \frac{\rho \|X_0^t\|^{-\alpha}}{\sigma^2 + \max_{Y \in \Phi^t \setminus \{X_0^t\}} \rho_Y \|Y\|^{-\alpha}}, \quad (3)$$

and similarly for the no-fading case. We can define *signal-to-tropical interference-ratio* (STIR) similarly, both in the fading and no-fading cases. The Shannon rate is the metric of interest here, which is proportional to $\ln(1 + \text{SINR})$.

B. Problem formulation: performance metrics

In this article, building upon the theory developed in the previous work [21], we focus on the performance evaluation of the system using various metrics of interest. Suppose the user QoS requirement is $\tau > 0$. At any time t , we say that a typical user is τ -covered by the system with coverage probability

$$p^c(\tau, \mu, \lambda, \alpha)(t) := \mathbb{P}(\mathcal{S}(t) > \tau), \quad (4)$$

at time t , where $\mathcal{S} \in \{\text{SNR, SIR, SINR, STIR, STINR}\}$. In all these cases, we define the mean Shannon rate as

$$\mathcal{R}(\mu, \lambda, \alpha)(t) := \mathbb{E}[B \ln(1 + \mathcal{S}(t))], \quad (5)$$

at time t , where $B = b/\ln 2$, with b being the bandwidth. We use natural log \ln in the definition of the Shannon rate in (5), instead of \log_2 for convenience in later computational tractability.

The main results in the article are about the coverage probability and average data rate experienced by the user at the origin, at the different typical epochs alluded to above, namely, at a typical *min signal & max interference (mS-MI) epoch*, *max signal (MS) epoch*, *max interference (MI) epoch*, *min interference (mI) epoch* and at any *typical time epoch*. All these scenarios are described in Figure 3 using the collection of distance functions (1) described in [21]. We describe these scenarios in Table I in terms of proximity of the serving BS and all others, and also with in our seasonal analogy as follows:

- 1) **Min signal & max interference (mS-MI) epoch:** At a handover epoch the user experiences a comparable interference power component compared to the signal received from the serving station, which is a time of weakest signal and strongest interference.
- 2) **Max signal (MS) epoch:** At such an epoch, the power of the signal is maximal, as the serving BS is at its nearest position.
- 3) **Max interference (MI) epoch:** At such an epoch, the nearest interferer is at the closest position with respect to the user.
- 4) **Min interference (mI) epoch:** Such an epoch corresponds to the time when the nearest interferer gets swapped with another interferer. We will also call this event a *tropical interference handover*.
- 5) **Typical time epoch (t):** It correspond to the system at any other time epoch. At this time, there exists a BS at a Rayleigh distance. This leads to classical snapshot analysis of the system as in [2].

Table I summarizes the scenarios at different typical epochs, their correspondence with seasons, along with the notations for the variables for the distances used later in the signal and interference components. This article has three major parts. In the first part, we determine the probability distribution of several distance characteristics at various typical epochs, using the analysis in [21] and especially the Palm distribution, Theorem 5.4, therein. Next, using these distributions, we

Abbreviation	Meaning (Seasons)	Implication	Distance variables	Ext
<i>mS-MI</i>	Min signal and max interference	Signal handover	H_V $H_V, \{D_i\}_i$	v
<i>MS</i>	Max signal	Nearest position of the serving BS	H_S $R_S, \{D_i\}_i$	s
<i>MI</i>	Max interference	Nearest position of the closest interferer	R_I $H_I, \{D_i\}_i$	i
<i>mI</i>	Min interference	Tropical interference handover	R_X $H_X, H_X, \{D_i\}_i$	x
<i>t</i>	Typical time	-	R $\{D_i\}_i$	t

TABLE I: (a). In each cell of the variable column, the top variable corresponds to distance to the serving BS and the bottom variables correspond to distance to the interferers. (b). A typical epoch, denoted by t , correspond to the system at any typical time.

establish the coverage probability using a threshold parameter τ corresponding to the user QoS, under different metrics of interest. This also includes the average Shannon rate perceived by the user with respect to different metrics. The last part focuses on the comparison of coverage probabilities and Shannon rates for various regime at different typical epochs. Moreover, this also includes a scale invariance property of the performance metrics in the interference limited regime.

C. Strategy

The results in this article can be considered as a continuation of the theory developed in [21]. Along with the Palm probability distributions of quantities or distances useful for the distribution of SINR, in Section III, we identify and develop characteristics of few more ingredients of interest with the help of the spatio-temporal evolution of the distances of serving BS and other BSs. The distribution of these distances allows us to determine the distribution of SINR and Shannon rate at those typical events. Leveraging the properties of the Poisson point process, the probability generating functional (PGFL) of max-shot noise in particular, we provide integral form expressions or even closed form expressions in specific cases. We manage to compare the key performance indicators in terms of Laplace order or stochastic domination, with the help of the same ordering among some of the distances at typical epochs.

III. PRELIMINARIES

In the evaluation of the performance metrics at different time epochs, we need the probability distribution of system characteristics, for example, the distance to the serving station, to the nearest interferer(s) and that of all others at these epochs. This invites us to make use of the spatio-temporal evolution of the distance functions of all network participants, provided by the *radial bird particle process* developed in [21]. In the following subsections, we recall some of the constructions from there and devise new tools for deriving the distribution of the distances of interest at these different typical time epochs. Without loss of generality, we assume that $v = 1$, since the distance distribution is invariant with respect to the speed

parameter v , as seen in [21, Lemma 5.6], and also observed in (6) later in this article. We borrow some of the notation and names from the paper [21], or explicitly define some others otherwise. We consider this section as a preliminary to our main objective of this article.

A. Radial bird particle process

Consider the particle process $\mathcal{H}_c := \sum_i \delta_{C_i}$, on the upper half plane \mathbb{H}^+ where $C_i := \{(t, d_{X_i}(t)) : t \in \mathbb{R}\}$, and $d_{X_i}(\cdot)$ is the distance function of the BS starting at X_i , for a homogeneous Poisson point process $\Phi_\lambda = \Phi = \sum_i \delta_{X_i}$. We call the infinite closed set C_i a *radial bird* and

$$\mathcal{H}_c := \sum_i \delta_{C_i}$$

the *radial bird particle process*. For each $X \in \Phi$, we define

$$T_X := \arg \inf_{t \in \mathbb{R}} \{d_X(t)\} \text{ and } H_X := d_X(T_X).$$

It turns out that

$$(T_X, H_X) = (-|X| \cos \Xi, |X| |\sin \Xi|),$$

which is the time-space location corresponding to global minimum of the curve of $d_X(\cdot)$, where Ξ is the relative angle of motion of the BS starting at X . In case of $v \neq 1$, we have

$$(T_X, H_X) := \left(-\frac{|X|}{v} \cos \Xi, |X| |\sin \Xi| \right). \quad (6)$$

Using [21, Lemma 4.3], $\mathcal{H} := \sum_i \delta_{(T_i, H_i)}$, forms a homogeneous Poisson point process on \mathbb{H}^+ with intensity measure ν , where $(T_i, H_i) \equiv (T_{X_i}, H_{X_i})$ and $d\nu := dt \otimes 2\lambda dh$. We call \mathcal{H} the *head point process*.

We rewrite the radial bird particle process as $\mathcal{H}_c := \sum_i \delta_{(T_i, H_i), C_i}$ by associating the infinite set C_i to each point (T_i, H_i) of \mathcal{H} . The point process \mathcal{H} and the intricate properties of the distance function as a branch of a hyperbola work as the backbone of our analysis in the rest of the article. The following Figure 3 represents a local realization of the radial bird particle process \mathcal{H}_c , in which the intersection points on the vertical line at typical epochs represent the distance of the serving BS and the interferers.

B. Lower envelope

The lower envelope is defined as the random closed subset

$$\mathcal{L}_e := \{(t, L(t)) : t \in \mathbb{R}\},$$

of \mathbb{H} , where $L(t) := \inf_{i \in \mathbb{N}} \{d_{X_i}(t)\}$ for $t \in \mathbb{R}$. The lower envelope \mathcal{L}_e correspond to the lowest part of the radial bird particle process in Figure 3. Physically, \mathcal{L}_e represents the time evolution of the distance to the nearest BS from the user, which contributes to the signal component. It also encodes the information about the distance of the nearest interferer at handover events.

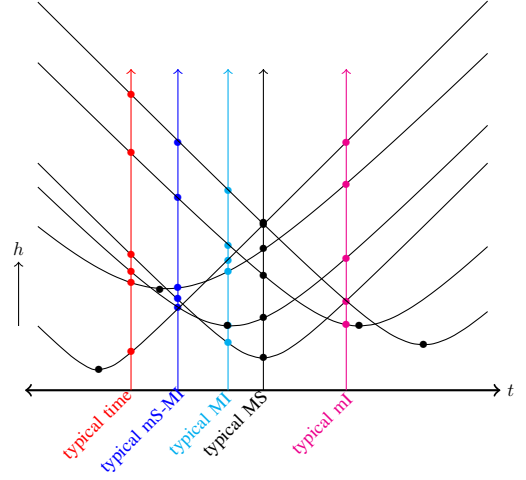


Fig. 3: The blue nodes (●), black nodes (●), red nodes (●), cyan nodes (●) and magenta nodes (●) respectively on individual vertical blue, black, red, cyan and magenta lines, form the point processes corresponding to the distance of all the mobile BSs at *min-signal max-interference*, *max-signal*, *typical time*, *max-interference* and *min-interference* epochs, respectively.

C. The k -th lower envelope and its characterization

Other than the lower envelope \mathcal{L}_e , it will be important to look at the second layer or the k -th layer above the lower envelope. The second layer is defined as

$$\mathcal{L}_e^{(2)} := \left\{ (t, L^{(2)}(t)) : t \in \mathbb{R} \right\},$$

where,

$$L^{(2)}(t) := \inf \left\{ \{d_{X_i}(t)\}_{i \in \mathbb{N}} \setminus \{L(t)\} \right\},$$

and we call it the *second lower envelope*. This is obtained by peeling off the part of the curves which lies on \mathcal{L}_e , see Figure 3. This object is interesting since the dominant contribution to the interference power is given by the distances measured with respect to $\mathcal{L}_e^{(2)}$. For $k \geq 2$ the k -th envelope is defined as

$$\mathcal{L}_e^{(k)} := \left\{ (t, L^{(k)}(t)) : t \in \mathbb{R} \right\},$$

where,

$$L^{(k)}(t) := \inf \left\{ \{d_{X_i}(t)\}_{i \in \mathbb{N}} \setminus \{L^{(i)}(t)\}_{1 \leq i \leq k-1} \right\},$$

where $L^{(1)}(t) := L(t)$ and $\mathcal{L}_e^{(1)} := \mathcal{L}_e$. For $(s, h) \in \mathbb{H}^+$, U_h^s denotes the upper half ball of radius h and center at (s, h) . Let us recall two main geometric properties from [21, Subsection 4.2 and the Observation 4.17] which can be summarized as follows:

- 1) Suppose $(s, h) \in C_{(T, H)}$, for the set particle $C_{(T, H)}$ located at a point $(T, H) \in \mathcal{H}$, corresponding to a BS starting at $X \in \Phi$. Then $(T, H) \in \partial U_h^s$, see Figure 4.
- 2) Let $(s, h), (T, H) \in \mathbb{H}^+$. Let $C_{(T, H)}$ be the radial bird with its head at (T, H) . Let \hat{h} be the height at which the radial bird $C_{(T, H)}$ intersects the vertical line $t = s$. Then $(T, H) \in U_h^s$ if and only if $\hat{h} < h$, as depicted in Figure 5.

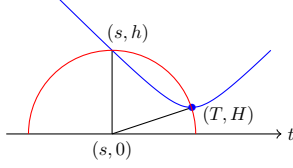


Fig. 4: $(s, h) \in C_{(T,H)} \Leftrightarrow (T, H) \in \partial U_h^s$.

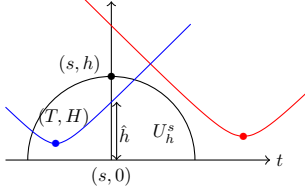


Fig. 5: All birds with head point inside and outside the half-ball of radius h , intersect the vertical line $t = s$ below and above the level h , respectively, as presented in Property 2

Remark 2 ($v \neq 1$) Without loss of generality, we perform all our analysis for $v = 1$. In case of $v \neq 1$, we have open upper half ellipse $E_h^{s,v}$, in place of the open upper half ball U_h^s , leading to slight change in the geometric arguments.

This leads to the following characterization of points lying on the k -th lower envelope $\mathcal{L}_e^{(k)}$, and the proof of which is given in Subsection I-A.

Proposition 1 Suppose $k \geq 1$. For any point $(s, h) \in \cup_{i \in \mathbb{N}} C_i$ that lies on $\mathcal{L}_e^{(k)}$:

- 1) there exist exactly $(k - 1)$ many head points in U_h^s , i.e., $\{(s, h) \in \mathcal{L}_e^{(k)}\} = \{\mathcal{H}(U_h^s) = k - 1\}$,
- 2) the fact that the point (s, h) is an intersection of two radial birds, implies that $\{(s, h) \in \mathcal{L}_e^{(k)}\} = \{\mathcal{H}(\overline{U}_h^s) = k + 1\}$.

D. Characteristics of min signal & max interference (mS-MI)

The time epochs of local minimum signal and local maximum interference (mS-MI) correspond to the handover point process, as seen in [21]. Therein the handover point process is defined as

$$\mathcal{V} := \sum_{(T_i, H_i) \in \mathcal{H}} \sum_{(T_j, H_j) \in \mathcal{H} : T_j < T_i} \delta_{\hat{S}} \mathbb{1}_{A(\hat{S}, \hat{H})}, \quad (7)$$

where $A(\hat{S}, \hat{H}) := \{\mathcal{H}(U_{\hat{H}}^{\hat{S}}) = 0\}$ and (\hat{S}, \hat{H}) is the intersection of two radial birds C_i and C_j corresponding to (T_i, H_i) and (T_j, H_j) , respectively. The intensity of \mathcal{V} is calculated in [21, Theorem 4.26] as $\lambda_{\mathcal{V}} = \frac{4\sqrt{\lambda}}{\pi}$.

At a handover event, there exist two BSs at equal distance from the user. One of them corresponds to the serving BS and the other one to the nearest interferer. From [21, Lemma 5.6], the typical handover distance, denoted by $H_{\mathcal{V}}$, follows a Nakagami distribution with parameter $(\frac{3}{2}, \frac{3}{2\lambda\pi})$, with density

$$f_{H_{\mathcal{V}}}(h) = 4\pi\lambda^{3/2}h^2e^{-\lambda\pi h^2}, \quad \text{for } h \geq 0. \quad (8)$$

E. Characteristics of max signal (MS)

At a typical time of maximum signal power, the serving BS is at its closest distance to the user. We denote the point process of max-signal epoch on the time axis by \mathcal{V}_s . Intensity of such a point process is $\lambda_s = \sqrt{\lambda}$, as derived in [21, Lemma 5.8]. We write the corresponding head point process \mathcal{H}_I as

$$\mathcal{H}_s := \sum_{j \in \mathbb{N}} \delta_{(T_j^s, H_j^s)} = \sum_{i \in \mathbb{N}} \delta_{(T_i, H_i)} \mathbb{1}_{\{(T_i, H_i) \in \mathcal{L}_e\}}.$$

Let H_s denote the distance to the nearest position of a BS. It is known from [21, Lemma 5.11] that H_s has a density

$$f_{H_s}(h) = 2\lambda^{\frac{1}{2}} e^{-\lambda\pi h^2}, \quad \text{for } h \geq 0.$$

Let R_s be the distance to the nearest interferer at a typical max-signal epoch. The following result is about the joint density of H_s^2 and R_s^2 and the proof of which is given in Appendix I-B.

Proposition 2 For any $\beta, \gamma \geq 0$, the joint distribution of H_s^2 and R_s^2 is given by the joint Laplace transform

$$\mathbb{E}_{\mathcal{V}_s}^0 \left[e^{-\gamma H_s^2 - \beta R_s^2} \right] = \left(1 + \frac{\beta}{\lambda\pi} \right)^{-1} \left(1 + \frac{\gamma + \beta}{\lambda\pi} \right)^{-1/2}.$$

The conditional probability density of R_s , given $H_s = h$ can be obtained using inverse Laplace transform.

Corollary 1 The conditional pdf of the random variable R_s given $H_s = h$ is

$$f_{R_s|H_s=h}(r) = \lambda^{\frac{1}{2}} r (r^2 - h^2)^{-\frac{1}{2}} e^{-\lambda\pi(r^2 - h^2)} \mathbb{1}_{\{r > h\}}.$$

Corollary 2 Under the Palm probability measure with respect to \mathcal{V}_s , the random variable R_s follows a Nakagami distribution with parameters $(\frac{3}{2}, \frac{3}{2\lambda\pi})$.

F. Characteristics of a typical time

Suppose R denotes the distance to the serving BS at a typical time. Using Poissonianity, it is well known that R is distributed as Rayleigh with pdf $f_R(r) := 2\lambda\pi r e^{-\lambda\pi r^2}$.

G. Characteristics of max interference (MI)

Recall that the head point process is $\mathcal{H} := \sum_{i \in \mathbb{N}} \delta_{(T_i, H_i)}$. Suppose $\mathcal{H}_I \leq \mathcal{H}$, i.e., $\text{Supp}(\mathcal{H}_I) \subset \text{Supp}(\mathcal{H})$, is the collection of points from \mathcal{H} restricted to the second lower envelope $\mathcal{L}_e^{(2)}$, i.e., $\mathcal{H}_I := \mathcal{H}|_{\mathcal{L}_e^{(2)}}$. In this case, in short, we use $_I$ in the subscript or superscript in our notation, to mean max interference. We write the corresponding head point process \mathcal{H}_I as

$$\mathcal{H}_I := \sum_{j \in \mathbb{N}} \delta_{(T_j^I, H_j^I)} = \sum_{i \in \mathbb{N}} \delta_{(T_i, H_i)} \mathbb{1}_{\{(T_i, H_i) \in \mathcal{L}_e^{(2)}\}}, \quad (9)$$

where we use the notation (T_j^I, H_j^I) for a head point on $\mathcal{L}_e^{(2)}$. Observe that from Proposition 1 with $k = 2$,

$$\{(T_i, H_i) \in \mathcal{L}_e^{(2)}\} = \{\mathcal{H}(U_{H_i}^{T_i}) = 1\},$$

see Figure 6. Also notice that, for $(T_i, H_i) \in \mathcal{L}_e^{(2)}$, it is not necessary for the radial bird at (T_i, H_i) to incur a handover. The sequence of points in \mathcal{H}_I gives rise to a stationary point process, say \mathcal{V}_I on \mathbb{R} , consisting of the abscissas of the points in \mathcal{H}_I . Formally,

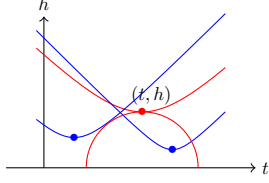


Fig. 6: The radial bird in red correspond to a BS that partly contributes the maximum interference to the user. The upper half ball U_h^t contains exactly one point of \mathcal{H} .

$$\mathcal{V}_I := \sum_{j \in \mathbb{N} : (T_j^I, H_j^I) \in \mathcal{H}_I} \delta_{T_j^I},$$

is the point process of the abscissas of the points from \mathcal{H}_I on the time axis. The time-stationarity of the point processes \mathcal{H}_I and \mathcal{V}_I is inherited from that of \mathcal{H} . We can re-write \mathcal{V}_I using (9) and (10) as

$$\mathcal{V}_I = \sum_{(T_i, H_i) \in \mathcal{H}} \delta_{T_i} \mathbf{1}_{\{(T_i, H_i) \in \mathcal{L}_e^{(2)}\}} = \sum_{(T_i, H_i) \in \mathcal{H}} \delta_{T_i} \mathbf{1}_{\{\mathcal{H}(U_{H_i}^{T_i})=1\}}. \quad (10)$$

In the following result, we determine the intensity of the point process \mathcal{V}_I , proof of which is provided in the Appendix (I-C).

Lemma 1 *The intensity of the point process \mathcal{V}_I is $\lambda_I = \frac{\sqrt{\lambda}}{2}$.*

This enables us to define the Palm distribution with respect to the point process \mathcal{V}_I , equivalently with respect to a typical max interference (MI) event. Let us denote the distance of the nearest interferer at typical epoch of MI as H_I . In the following, we derive the Palm probability distribution of H_I with respect to \mathcal{V}_I . The proof of this is given in Appendix I-D.

Proposition 3 *The Palm probability distribution of H_I with respect to \mathcal{V}_I is a Nakagami distribution with parameters $(\frac{3}{2}, \frac{3}{2\lambda\pi})$.*

Let R_I be the distance of the serving BS under the Palm probability of \mathcal{V}_I , where R_I and H_I are dependent. In the following, we give the joint Laplace transform of H_I^2, R_I^2 characterizing their joint distribution. The proof is given in Appendix I-E.

Proposition 4 *For any $\beta, \gamma \geq 0$, the joint distribution of H_I^2 and R_I^2 is given by the joint Laplace transform*

$$\mathbb{E}_{\mathcal{V}_I}^0 \left[e^{-\gamma H_I^2 - \beta R_I^2} \right] = \frac{2\lambda\pi}{\beta} \left[\left(1 + \frac{\gamma}{\lambda\pi} \right)^{-\frac{1}{2}} \left(1 + \frac{\gamma + \beta}{\lambda\pi} \right)^{-\frac{1}{2}} \right].$$

Corollary 3 *Conditioned on $H_I = h$, the random variable $h^{-2}R_I^2$ is uniformly distributed on $[0, 1]$.*

Corollary 4 *The marginal pdf of R_I is given by*

$$f_{R_I}(r) = 4\lambda\pi r \operatorname{erfc}(r\sqrt{\lambda\pi}),$$

for $r \geq 0$, where $\operatorname{erfc}(z) = \frac{2}{\sqrt{\pi}} \int_z^\infty e^{-z^2} dz$.

H. Characteristics of min interference (mI)

The tropical interference is the contribution from the second closest BS only. We are interested in analyzing the scenario when the tropical interference is minimum, and this happens at an epoch when the second closest BS is swapped. Two types of swaps can happen, namely, swaps given by pure handovers between nearest serving BS and nearest interferer, and swaps between second and third closest interferer. We call the first type a *signal handover* and second type a *tropical interference handover*. We denote the tropical interference handover point process by \mathcal{V}_T . In this case, in short, we use \mathcal{I} in the subscript or superscript in some of our notations as it corresponds to tropical interference.

We say that an intersection point (s, h) of two radial birds is a tropical interference handover if $(s, h) \in \mathcal{L}_e^{(2)}$. Using the characterization from Proposition 1, the tropical interference handover point process is defined as

$$\mathcal{V}_T := \sum_{(T_i, H_i) \in \mathcal{H}} \sum_{(T_j, H_j) \in \mathcal{H} : T_j < T_i} \delta_{\hat{S}} \mathbf{1}_{A_1(\hat{S}, \hat{H})}, \quad (11)$$

where $A_1(\hat{S}, \hat{H}) := \{\mathcal{H}(U_{\hat{H}}^{\hat{S}}) = 1\}$ similarly to (7). The following result is about the intensity of the point process \mathcal{V}_T , which is proved later in Appendix I-F.

Lemma 2 *The intensity of the point process \mathcal{V}_T is $\lambda_T = \frac{6\sqrt{\lambda}}{\pi}$.*

Remark 3 *This result about the intensity of \mathcal{V}_T , i.e., the frequency of tropical interference handovers is, $\lambda_T = \frac{6\sqrt{\lambda}}{\pi}$. It essentially derives the handover frequency in the 2-Voronoi tessellation of a Poisson point process, studied in [27] from the perspective of pairwise-cooperative cellular networks (COMP). Our technique can be used to generalize the results to the k -Voronoi tessellations for any $k > 2$.*

Let us denote the distance of a typical tropical interference handover as H_T . In the following, we give the Palm probability distribution of H_T with respect to \mathcal{V}_T and the proof is given in Appendix I-G.

Proposition 5 *The Palm probability distribution of H_T with respect to \mathcal{V}_T is a Nakagami distribution with parameters $(\frac{5}{2}, \frac{5}{2\lambda\pi})$.*

Let us denote the distance to the serving BS at this typical epoch by R_T , which is dependent on H_T . The following result is about the joint distribution of H_T^2, R_T^2 and the proof is given in Appendix I-H.

Proposition 6 For any $\beta, \gamma \geq 0$, the joint distribution of $H_{\mathcal{I}}^2$ and $R_{\mathcal{I}}^2$ is given by the joint Laplace transform

$$\mathbb{E}_{\mathcal{V}_{\mathcal{I}}}^0 \left[e^{-\gamma H_{\mathcal{I}}^2 - \beta R_{\mathcal{I}}^2} \right] = \frac{2\lambda\pi}{3\beta} \left[\left(1 + \frac{\gamma}{\lambda\pi} \right)^{-\frac{3}{2}} \left(1 + \frac{\gamma + \beta}{\lambda\pi} \right)^{-\frac{3}{2}} \right].$$

Corollary 5 Conditioned on $H_{\mathcal{I}} = h$, the random variable $h^{-2}R_{\mathcal{I}}^2$ is uniformly distributed on $[0, 1]$.

Corollary 6 The marginal pdf of $R_{\mathcal{I}}$ is given by

$$f_{R_{\mathcal{I}}}(r) = \frac{4\lambda\pi r}{3} \left(\operatorname{erfc}(r\sqrt{\lambda\pi}) + 2r\sqrt{\lambda\pi} e^{-\lambda\pi r^2} \right), \text{ for } r \geq 0.$$

I. Comparison of distances: Laplace transform and MGF order

Definition 1 (Laplace transform order \leq_L) We say that two non-negative random variables X, Y satisfy Laplace order

$$X \leq_L Y, \text{ if } \mathbb{E}_X [e^{-\gamma X}] \geq \mathbb{E}_Y [e^{-\gamma Y}],$$

for any $\gamma \geq 0$. The inequality is flipped because of the negative exponent.

Definition 2 (Moment generating function order \leq_{mgf})

We say that two non-negative random variables X, Y satisfy moment generating function order (MGF order)

$$X \leq_{\text{mgf}} Y, \text{ if } \mathbb{E}_X [e^{\gamma X}] \leq \mathbb{E}_Y [e^{\gamma Y}],$$

for any $\gamma \geq 0$.

Similarly to the Laplace order $H_{\mathcal{V}} \geq_L R \geq_L H_S$, form [21, Lemma 5.12], we also have the following orderings.

Lemma 3 The typical distances satisfy the following ordering

- 1) $H_{\mathcal{I}} \geq_L H_I$ and $R_{\mathcal{I}} \geq_L R_I$,
- 2) $H_{\mathcal{I}} \geq_{\text{mgf}} H_I$ and $R_{\mathcal{I}} \geq_{\text{mgf}} R_I$,
- 3) $H_{\mathcal{V}} \geq_{\text{mgf}} R \geq_{\text{mgf}} H_S$.

Definition 3 (Likelihood ratio dominance order \leq_{lr}^d) We say that two non-negative random variables X, Y satisfy likelihood ratio dominance order (LRD order),

$$X \leq_{\text{lr}}^d Y \text{ if } \frac{f_Y(z)}{f_X(z)} \text{ is an increasing function}$$

on their common support. Note that LRD order implies stochastic domination [28].

The following LRD ordering will be useful in comparing the coverage probabilities in the tropical case, without fading.

Lemma 4 The typical distances satisfy the following ordering $R_S \stackrel{d}{=} H_{\mathcal{V}} \leq_{\text{lr}}^d R_1$ and $H_I \leq_{\text{lr}}^d H_{\mathcal{I}}$.

Variable	Distribution	PDF
$H_{\mathcal{V}}$	$\text{Na} \left(\frac{3}{2}, \frac{3}{2\lambda\pi} \right)$	$f_{H_{\mathcal{V}}}(h) = 4\pi\lambda^{3/2}h^2 e^{-\lambda\pi h^2}$
H_S	$\text{Na} \left(\frac{1}{2}, \frac{1}{2\lambda\pi} \right)$	$f_{H_S}(h) = 2\lambda^{1/2}e^{-\lambda\pi h^2}$
R_S	$\text{Na} \left(\frac{3}{2}, \frac{3}{2\lambda\pi} \right)$	$f_{R_S H_S=h}(r) = \frac{\lambda^{1/2} r e^{-\lambda\pi(r^2-h^2)}}{(r^2-h^2)^{1/2}} \mathbb{1}_{\{r>h\}}$ $f_{R_S}(h) = 4\pi\lambda^{3/2}h^2 e^{-\lambda\pi h^2}$
$R_{\mathcal{I}}^2$	$\text{U}[0, H_{\mathcal{I}}^2]$	$f_{R_{\mathcal{I}}^2 H_{\mathcal{I}}=h}(r) = h^{-2} \mathbb{1}_{[0, h^2]}(r)$
R_I	$\text{Na} \left(\frac{3}{2}, \frac{3}{2\lambda\pi} \right)$	$f_{R_I}(r) = 4\lambda\pi r \operatorname{erfc}(r\sqrt{\lambda\pi})$
H_I	$\text{Na} \left(\frac{3}{2}, \frac{3}{2\lambda\pi} \right)$	$f_{H_I}(h) = 4\pi\lambda^{3/2}h^2 e^{-\lambda\pi h^2}$
$R_{\mathcal{I}}^2$	$\text{U}[0, H_{\mathcal{I}}^2]$	$f_{R_{\mathcal{I}}^2 H_{\mathcal{I}}=h}(r) = h^{-2} \mathbb{1}_{[0, h^2]}(r)$
$R_{\mathcal{I}}$	$\text{Na} \left(\frac{5}{2}, \frac{5}{2\lambda\pi} \right)$	$f_{R_{\mathcal{I}}}(r) = \frac{4\lambda\pi r}{3} \left(\operatorname{erfc}(r\sqrt{\lambda\pi}) + 2r\sqrt{\lambda\pi} e^{-\lambda\pi r^2} \right)$
$H_{\mathcal{I}}$	$\text{Na} \left(\frac{5}{2}, \frac{5}{2\lambda\pi} \right)$	$f_{H_{\mathcal{I}}}(h) = \frac{8}{3}\pi^2\lambda^{5/2}h^4 e^{-\lambda\pi h^2}$
R	$\text{Ray} \left(\frac{1}{\sqrt{2\lambda\pi}} \right)$	$f_R(h) = 2\lambda\pi h e^{-\lambda\pi h^2}$
R_1	$\text{Ray} \left(\frac{1}{\sqrt{2\lambda\pi}} \right)$	$f_{R_1 R=r}(h) = 2\lambda\pi h e^{-\lambda\pi(h^2-r^2)} \mathbb{1}_{\{h \geq r\}}$ $f_{R_1}(h) = 2\lambda^2\pi^2 h^3 e^{-\lambda\pi h^2}$

TABLE II: Densities of various typical distances. The notations (a). $\text{Na}(m, \omega)$ stands for the Nakagami distributed random variable with parameters (m, ω) , (b). $\text{Ray}(\theta)$ stands for the Rayleigh distributed random variable with parameter θ , (c). $\text{U}[a, b]$ stands for the uniform random variable on $[a, b]$.

J. Summary of densities of the typical distances

For ease of reading and navigation, we provide the list (Table II) for probability densities of the distances of interest and which will be essential in the performance evaluation.

K. Distances of all other stations

Given the distance $H \in \{H_{\mathcal{V}}, H_S, H_I, H_{\mathcal{I}}, R\}$ at different typical epochs, let us define the distances of all other BSs can be represented as a one dimensional point process $\eta_H = \sum_i \delta_{D_i}$, on (H, ∞) . The following result can be shown to hold using arguments similar to those in [21, Lemma 4.34]:

Lemma 5 Conditioned on $H = h$, under the Palm probability measure of the respective typical epoch, the point process η_h is a Poisson point process on (h, ∞) with intensity measure of density $2\pi\lambda r dr$.

IV. PERFORMANCE EVALUATION & COMPARISON

For simplicity, let us assume that the both transmit power of each of the transmitter and the combined channel gain is 1.

A. System with fading

1) *Performance metrics:* The main quantities of interest are SINR and its tropical version, STINR, at the typical epochs, defined by

$$\text{SINR} := \frac{S}{\sigma^2 + I}, \quad \text{STINR} := \frac{S}{\sigma^2 + \mathcal{T}},$$

aligning with the definition (2) and (3), where σ^2 is the thermal noise power, S is the received signal power to the user at the corresponding typical epoch

$$S := \begin{cases} \rho H_{\mathcal{V}}^{-\alpha} & \text{at typical mS-MI epoch,} \\ \rho H_S^{-\alpha} & \text{at typical MS epoch,} \\ \rho R_I^{-\alpha} & \text{at typical MI epoch,} \\ \rho R_{\mathcal{I}}^{-\alpha} & \text{at typical mI epoch,} \\ \rho R^{-\alpha} & \text{at any typical epoch,} \end{cases} \quad (12)$$

using the random variable for the distance to the serving station, listed in Table I, and I and \mathcal{T} are the additive and maxitive (or tropical) interference power. Given $H = H_V, H_S, R_I, R_X, R$, the interference I and the tropical interference \mathcal{T} are defined in terms of the distances H_I or H_X to the nearest interferer(s), and distances $\{D_i\}_{i \in \mathbb{N}}$ to all others, at the respective places in the proof of our results. The signal-to-interference-ratio (SIR), signal-to-tropical interference-ratio (STIR) and signal-to-noise-ratio (SNR) are defined naturally.

The factors ρ used for the signal and $\{\rho_i\}_{i \in \mathbb{N}}$ that will be used for the interference correspond to the fading of the channels from the transmitters, which are assumed to be i. i. d. and distributed as $\text{Exp}(\mu)$, for $\mu > 0$.

At all the typical epochs, the coverage probability and Shannon rate or data rate are defined using $\mathcal{S} \in \{\text{SINR}, \text{STINR}, \text{SNR}, \text{SIR}, \text{STIR}\}$ as

$$p^c(\tau, \mu, \lambda, \alpha) := \mathbb{P}(\mathcal{S} \geq \tau),$$

and

$$\mathcal{R}(\mu, \lambda, \alpha) := \mathbb{E}[B \ln(1 + \mathcal{S})],$$

respectively, where $B = b \log_2 e$, with b being the bandwidth of the channel, which we assume to be a constant.

Remark 4 (Shannon rate) *Note that for any metric \mathcal{S} , the Shannon rate \mathcal{R} can be written in general in terms of the coverage probability as derived in [2]*

$$\mathcal{R} = B \int_0^\infty \frac{1}{1+z} \mathbb{P}(\mathcal{S} \geq z) dz. \quad (13)$$

We treat this as the formula for the Shannon rate, without stating explicitly in our results and hence it is enough to determine the coverage probabilities in all these cases in both cases with and without fading.

In the following, we determine the coverage probability and the average data rate using different performance metrics $\mathcal{S} \in \{\text{SNR}, \text{SIR}, \text{SINR}, \text{STIR}, \text{STINR}\}$, at typical mS-MI, MS and typical time epoch. We present the proof in Appendix II.

Theorem 1 *The coverage probability with respect to Palm probability distribution of the typical mS-MI, MS and typical time epoch is given by*

$$p^c(\tau, \mu, \lambda, \alpha) = \mathbb{E}_H^0 \left[e^{-\mu\tau H^\alpha \sigma^2} \mathcal{L}_{I_H}(\mu\tau H^\alpha) \right], \quad (14)$$

where $H \in \{H_V, H_S, R\}$.

In the case of typical max-interference (MI) and typical min-interference (mI), there exists an interferer at distance $H \in \{H_I, H_X\}$ and a serving BS is at distance $R \in \{R_I, R_X\}$ such that $R \leq H$ a.s., and all other BSs are farther than H . Subsequently the performance metrics are given by the following result, the proof of which is given in Section II.

Theorem 2 *The coverage probability with respect to Palm probability distribution of typical mI and MI epoch is given by*

$$p^c(\tau, \mu, \lambda, \alpha) = \mathbb{E}_{H,R}^0 \left[e^{-\mu\tau R^\alpha \sigma^2} \mathcal{L}_{I_H}(\mu\tau R^\alpha) \right], \quad (15)$$

where $R \in \{R_I, R_X\}$, $H \in \{H_I, H_X\}$.

Remark 5 *In this case, the interference I_H (or \mathcal{T}_H for tropical interference) is computed slightly differently with respect to the distance $H \in \{H_I, H_X\}$ to the nearest interferer. All our computations are based on determining the Laplace transform $\mathcal{L}_{I_h}(\gamma)$ of the interference or its tropical version $\mathcal{L}_{\mathcal{T}_h}(\gamma)$ for some parameter γ , given $H = h$, the distribution of H , along with the help of Lemma 5.*

B. System without fading

The main quantities of interest are the SINR and its tropical version STINR, at the typical epochs, are given by

$$\text{SINR} := \frac{S}{\sigma^2 + I}, \quad \text{STINR} := \frac{S}{\sigma^2 + \mathcal{T}},$$

aligning with the definition (2) and (3), where the power of the received signal is defined as

$$S := \begin{cases} H_V^{-\alpha} & \text{at typical mS-MI epoch,} \\ H_S^{-\alpha} & \text{at typical MS epoch,} \\ R_I^{-\alpha} & \text{at typical MI epoch,} \\ R_X^{-\alpha} & \text{at typical mI epoch,} \\ R^{-\alpha} & \text{at any typical epoch,} \end{cases} \quad (16)$$

using the random variable for the distance to the serving station, listed in Table I, H_V, H_S, R_I, R_X, R , for the corresponding cases, respectively. The additive interference I and the maxitive or tropical interference \mathcal{T} are introduced similarly to the case with fading, at the respective places in the proof of our results.

In the following, we determine the coverage probability and the Shannon rate using different performance metrics $\mathcal{S} \in \{\text{SINR}, \text{STINR}, \text{SNR}, \text{SIR}, \text{STIR}\}$, at different typical epochs of mS-MI, MS and typical time, as follows:

Theorem 3 *The coverage probability with respect to Palm probability distribution of epoch of interest, is given by*

$$p^c(\tau, \lambda, \alpha) = \mathbb{E}_H^0 \left[F_{I_H} \left(0 \vee (H^{-\alpha}/\tau - \sigma^2) \right) \right], \quad (17)$$

where $H \in \{H_V, H_S, R\}$ in the non-tropical case and $H = H_V$ in the tropical case, are the distance to the serving station.

Theorem 4 *The coverage probability with respect to Palm probability distribution of typical time and typical max-signal in the tropical case are given by*

$$p^c(\tau, \lambda, \alpha) = \mathbb{E}_{H,X}^0 \left[F_{\mathcal{T}} \left(0 \vee (R^{-\alpha}/\tau - \sigma^2) \right) \right], \quad (18)$$

for the tropical interference $\mathcal{T} = X^{-\alpha}$, where $X \in \{R_I, R_S\}$ and $H \in \{R, H_S\}$.

In the case of typical max-interference (MI) and typical min-interference (mI), there exists an interferer at distance $H \in \{H_I, H_X\}$ and a serving BS at a distance $R \in \{R_I, R_X\}$ such that $R \leq H$ almost surely. All other BSs are farther than H and the locations of the latter are Poisson distributed. In this case, the interference I_H (or \mathcal{T}_H for tropical interference) is computed slightly differently with respect to the distance H to the nearest interferer. The performance metrics are given in:

Theorem 5 *The coverage probability with respect to Palm probability distribution of epoch of interest, is given by*

$$p^c(\tau, \lambda, \alpha) = \mathbb{E}_{H,R}^0 [F_{I_H} (0 \vee (R^{-\alpha}/\tau - \sigma^2))], \quad (19)$$

where $R \in \{R_I, R_X\}$ and $H \in \{H_I, H_X\}$.

In all our computations, we derive the distribution F_{I_h} or $F_{\mathcal{T}_h}$ of the additive interference or tropical interference, respectively, given the distance $H = h$ in different typical epochs. Due to the absence of fading factor, the proofs are much simpler.

Remark 6 *We derive the expression for the coverage probabilities at different typical epochs in Appendix II and Appendix III, including some closed form expressions in the special cases highlighted in Section V. The system performance for all other metrics, namely, SIR and STIR, can be derived by adapting the formulas (14), (15), (17) and (19) accordingly, by setting $\sigma = 0$. On the other hand, the coverage probability in the SNR regime can be derived directly from the distribution of the distance to the serving BS at the corresponding typical epochs of interest.*

For ease of reading, we present a table of notation for the coverage probabilities and the data rate with respect to different time epochs, in continuation of Table I and Table II.

Epoch	Variables	Distribution (Table II)	Interference Tropical -interference	Cov. prob. (additive) (Tropical)	Data rate (additive) (Tropical)
<i>mS-MI</i>	H_V H_V	$\text{Na}(\frac{3}{2}, \frac{3}{2\lambda\pi})$	I_{H_V} \mathcal{T}_{H_V}	p_V^c $p_{V;\mathcal{T}}^c$	\mathcal{R}_V $\mathcal{R}_{V;\mathcal{T}}$
<i>MS</i>	H_S R_S	$\text{Na}(\frac{1}{2}, \frac{1}{2\lambda\pi})$ $\text{Na}(\frac{3}{2}, \frac{3}{2\lambda\pi})$	I_{H_S} \mathcal{T}_{H_S}	p_S^c $p_{S;\mathcal{T}}^c$	\mathcal{R}_S $\mathcal{R}_{S;\mathcal{T}}$
<i>MI</i>	R_I H_I	$\text{U}[0, H_I^2]$ $\text{Na}(\frac{3}{2}, \frac{3}{2\lambda\pi})$	I_{H_I} \mathcal{T}_{H_I}	p_I^c $p_{I;\mathcal{T}}^c$	\mathcal{R}_I $\mathcal{R}_{I;\mathcal{T}}$
<i>mI</i>	R_X H_X, H_X	$\text{U}[0, H_X^2]$ $\text{Na}(\frac{5}{2}, \frac{5}{2\lambda\pi})$	I_{H_X} \mathcal{T}_{H_X}	p_X^c $p_{X;\mathcal{T}}^c$	\mathcal{R}_X $\mathcal{R}_{X;\mathcal{T}}$
<i>t</i>	R	Rayleigh $\frac{1}{\sqrt{2\lambda\pi}}$	I_R \mathcal{T}_R	p_t^c $p_{t;\mathcal{T}}^c$	\mathcal{R}_t $\mathcal{R}_{t;\mathcal{T}}$

TABLE III: (a). Here in the second column, we just mention the variables corresponding to the signal and nearest interferer(s) and the distance of the rest of the interference is given by $\{D_i\}_i$. (b). $\text{Na}(m, \omega)$ stands for the Nakagami random variable with parameters (m, ω) . (c). In the third column, I stands for interference and \mathcal{T} for tropical interference. (d). The notation for coverage probability and data rate p_*^c, \mathcal{R}_* denotes the non-tropical case and $p_{*;\mathcal{T}}^c, \mathcal{R}_{*;\mathcal{T}}$ with an extra subscript \mathcal{T} to denote the tropical case, where $* \in \{v, s, i, x, t\}$.

Remark 7 (Alternative definition of HoPP \mathcal{V}) *In the no fading case, under the interference limited regime, observe that at a handover epoch, the STIR is equal to 1, whereas $\text{STIR}(t) > 1$ at any other time instant t , almost surely. It signifies that one can alternatively define the handover point process \mathcal{V} as*

$$\mathcal{V} := \sum_{t \in \mathbb{R}} \delta_t \mathbb{1}_{\{\text{STIR}(t)=1\}}.$$

C. Comparison of performance metrics

We now state another important result of this work that compares the coverage probability and the average data rates among different typical epochs, the proof of which is given in Appendix IV

Theorem 6 *The following comparison of the coverage probabilities holds true for any QoS $\tau \geq 0$:*

- 1) *with or without fading: $p_V^c \leq p_t^c \leq p_S^c$ and $p_X^c \leq p_I^c$,*
- 2) *with fading: $p_{V;\mathcal{T}}^c \leq p_{t;\mathcal{T}}^c \leq p_{S;\mathcal{T}}^c$ and $p_{X;\mathcal{T}}^c \leq p_{I;\mathcal{T}}^c$,*
- 3) *without fading: $p_{X;\mathcal{T}}^c \leq p_{I;\mathcal{T}}^c$.*

Remark 8 *In the tropical no-fading scenario, there are different orderings among $p_{V;\mathcal{T}}^c, p_{t;\mathcal{T}}^c, p_{S;\mathcal{T}}^c$ for different combination of values of the parameters τ, λ, α , which can be seen through their corresponding plots provided in Figure 13 and also proven at the end of Appendix IV.*

Remark 9 *The first result is a consequence of the Laplace order $H_V \geq_L R \geq_L H_S$. The second results in Theorem 6 may look a bit counter-intuitive, as in view of the Laplace transform order $H_X \geq_L H_I$ shown in Lemma 3, at the typical max interference epoch (MI) seem to exert lower coverage. The coverage is even lower in typical tropical interference handover (mI), because there are two equally strong interferers present at a typical tropical handover epoch. The later fact again reflects onto the comparison of rates as established in the second part Corollary 7.*

Corollary 7 *The following comparisons of the average Shannon rates hold true:*

- 1) *with or without fading: $\mathcal{R}_V \leq \mathcal{R}_t \leq \mathcal{R}_S$ and $\mathcal{R}_X \leq \mathcal{R}_I$,*
- 2) *with fading: $\mathcal{R}_{V;\mathcal{T}} \leq \mathcal{R}_{t;\mathcal{T}} \leq \mathcal{R}_{S;\mathcal{T}}$ and $\mathcal{R}_{X;\mathcal{T}} \leq \mathcal{R}_{I;\mathcal{T}}$,*
- 3) *without fading: $\mathcal{R}_{X;\mathcal{T}} \leq \mathcal{R}_{I;\mathcal{T}}$.*

Let us now write the performance metrics as \mathcal{S}_* for SINR and $\mathcal{S}_{*;\mathcal{T}}$ for STINR, where $* \in \{v, s, i, x, t\}$. A natural stochastic domination \leq_{st} among these metrics follows from Theorem 6, when their distributions are compared under their respective Palm probability spaces.

Corollary 8 *The following stochastic domination between SINR and STINR holds true for both the non-tropical and tropical cases:*

- 1) with or without fading: $\mathcal{S}_v \leq_{\text{st}} \mathcal{S}_t \leq_{\text{st}} \mathcal{S}_s$ and $\mathcal{S}_I \leq_{\text{st}} \mathcal{S}_I$,
- 2) with fading: $\mathcal{S}_{v;\tau} \leq_{\text{st}} \mathcal{S}_{t;\tau} \leq_{\text{st}} \mathcal{S}_{s;\tau}$ and $\mathcal{S}_{I;\tau} \leq_{\text{st}} \mathcal{S}_{I;\tau}$,
- 3) without fading: $\mathcal{S}_{I;\tau} \leq_{\text{st}} \mathcal{S}_{I;\tau}$.

Note that for any of the performance metrics \mathcal{S} , the Laplace transform of \mathcal{S} can be written for any $\gamma \geq 0$ as

$$\begin{aligned} \mathbb{E}_{\#}^0 [e^{-\gamma \mathcal{S}}] &= \gamma \int e^{-\gamma x} F_{\mathcal{S}}(x) dx \\ &= \gamma \int e^{-\gamma x} (1 - p^c(x)) dx, \end{aligned} \quad (20)$$

where $\# \in \{v, s, I, \mathcal{I}, t\}$, $p^c(x) = p_{*}^c(x, \mu, \lambda, \alpha)$ or $p_{*;\tau}^c(x, \mu, \lambda, \alpha)$ for the system with fading and $p^c(x) = p_{*}^c(x, \lambda, \alpha)$ or $p_{*;\tau}^c(x, \lambda, \alpha)$ for the system without fading and $* \in \{v, s, I, \mathcal{I}, t\}$. Laplace order comparison of the performance metrics \mathcal{S}_* for SINR and $\mathcal{S}_{*;\tau}$ for STINR follows from (20), Theorem 6, and also from the stochastic domination in Corollary 8.

Corollary 9 *The following Laplace orderings between SINR and STINR, compared under their respective Palm probability spaces, hold true for both the non-tropical and tropical cases:*

- 1) with or without fading: $\mathcal{S}_v \leq_{\text{L}} \mathcal{S}_t \leq_{\text{L}} \mathcal{S}_s$ and $\mathcal{S}_I \leq_{\text{L}} \mathcal{S}_I$,
- 2) without fading: $\mathcal{S}_{v;\tau} \leq_{\text{L}} \mathcal{S}_{t;\tau} \leq_{\text{L}} \mathcal{S}_{s;\tau}$ and $\mathcal{S}_{I;\tau} \leq_{\text{L}} \mathcal{S}_{I;\tau}$,
- 3) without fading: $\mathcal{S}_{I;\tau} \leq_{\text{L}} \mathcal{S}_{I;\tau}$.

Remark 10 *The comparison of mean Shannon capacity in Corollary 7 can be seen as a consequence of the Laplace order in Corollary 9, with the help of Hamdi's lemma [29] stated as*

$$\mathbb{E}[\ln(1 + X)] = \int_0^{\infty} \frac{1}{z} (1 - \mathbb{E}[e^{-zX}]) e^{-z} dz,$$

for any non-negative random variable X , using the analytical fact that $\int_0^{\infty} \frac{1}{z} (1 - e^{-zx}) e^{-z} dz = \ln(1 + x)$.

D. Comparison of interference power: Stochastic domination & Laplace transform order

Let us denote the additive interference power as I_* and maxitive interference power as \mathcal{T}_* , for $* \in \{v, s, I, \mathcal{I}, t\}$. Then we have the following ordering, the proof of which is given in Appendix V.

Theorem 7 *The interference power in the non-tropical and tropical cases satisfies the following orderings:*

- 1) with or without fading: $I_v \geq_{\text{L}} I_t \geq_{\text{L}} I_s$ and $I_I \geq_{\text{L}} I_I$,
- 2) with fading: $\mathcal{T}_v \geq_{\text{st}} \mathcal{T}_t \geq_{\text{st}} \mathcal{T}_s$ and $\mathcal{T}_I \geq_{\text{st}} \mathcal{T}_I$,
- 3) without fading: $\mathcal{T}_v \stackrel{d}{=} \mathcal{T}_s \geq_{\text{lr}} \mathcal{T}_t$ and $\mathcal{T}_I \geq_{\text{lr}} \mathcal{T}_I$,

compared under their respective Palm probability spaces.

Remark 11 *These orderings are natural and remain consistent with the ordering among the coverage probabilities at different typical epochs in Theorem 6. The LRD ordering can be proved as a corollary of Lemma 4.*

E. Scale invariance in the interference limited regime

We have the following scale invariance property of the coverage probability and data rate with respect to the intensity λ of the BSs and the fading parameter μ (in an environment with fading), in the interference limited regime, i.e., $\sigma = 0$. In all these cases, the ratio $\frac{H^{-\alpha}}{I_H}$ is scale invariant with respect to λ , where H is the distance to the nearest BS and I_H is the additive or maxitive interference. As a result we have the scale invariance property of the coverage probabilities at different typical epochs, in the interference limited regime. The proof is given in Appendix VI.

Theorem 8 *For any of the typical epochs, the coverage probabilities p_{*}^c and $p_{*;\tau}^c$, are scale invariant with respect to the intensity parameter λ (also with respect to fading parameter μ in the scenario with fading), where $* \in \{v, s, I, \mathcal{I}, t\}$.*

Corollary 10 *For any of the typical epochs, the average data rates \mathcal{R}_* and $\mathcal{R}_{*;\tau}$ satisfy the scale invariance property in the interference limited scenario, with respect to the intensity parameter λ (also with respect to fading parameter μ in the environment with fading), where $* \in \{v, s, I, \mathcal{I}, t\}$.*

F. Attenuation functions: example and counter example

1) **Bounded path-loss function:** All our comparison results in Theorem 6, Corollary 7, Corollary 9 and Theorem 7 can be shown to hold true for the bounded path-loss function

$$\ell(r) = (1 + r)^{-\alpha},$$

as in [30]. Our results can be verified along the same type of analysis, see Appendix VII for an instance. The type of attenuation function is very useful to eliminate the question of singularity of infinite signal power from a BS infinitesimally close to the user, in case of power law attenuation. In general, the bounded path-loss model naturally lacks the scale invariance property of the performance metrics in the interference limited regime, due to the extra additive term inside the attenuation function.

2) **Step attenuation function:** On the other hand, the comparison results do not hold true for other attenuation functions, for example

$$\ell(r) = p \mathbb{1}_{\{r \leq d\}},$$

where p is a constant power and d is a fixed cut-off distance. For example, a disordered behavior, depending on the user QoS τ , among p_v^c, p_t^c, p_s^c and p_I^c, p_I^c with additive interference, and also for the tropical interference case, is shown in Appendix VII. As we will see therein, we also lose the scale invariance property, in this case.

V. CLOSED FORMS FOR COVERAGE PROBABILITIES

Much of our computations are focused on the determination of closed forms or simple integral forms for the coverage probabilities at various typical epochs. We list out all such expressions in different regimes and typical epochs, with or without fading, and having specific values of the path-loss exponent α . Nevertheless, the coverage probabilities in all these cases can be simulated numerically.

A. With fading

These closed forms are mainly for SINR, SIR and SNR regimes in the presence of fading.

1) *SINR regime*: In the SINR regime, for the specific case of $\alpha = 2$ we have $p_*^c = 0$, in any of the typical epochs, i.e., $* \in \{v, s, I, \mathcal{I}, t\}$. For $\alpha = 4$ we have

$$p_*^c = \frac{1}{(1+\tau)\mathbb{1}_{\{*\neq v\}}} \mathbb{E}_{H_*}^0 \left[e^{-\mu\tau H_*^4 \sigma^2 - \pi\lambda H_*^2 \kappa(\tau, 4)} \right],$$

where $\kappa(\tau, 4) = \tau^{\frac{1}{2}} \arctan(\tau^{\frac{1}{2}})$ and $* \in \{v, s, t\}$. In the other two typical epochs,

$$p_*^c = \frac{\tau^{-1/4}}{4} \int_0^\tau \frac{z^{-3/4}}{(1+z)^{1+\mathbb{1}_{\{*\neq z\}}}} \mathbb{E}_{H_*}^0 \left[e^{-\mu z H_*^4 \sigma^2 - \pi\lambda H_*^2 \kappa(z, 4)} \right] dz,$$

where $\kappa(z, 4) = z^{\frac{1}{2}} \arctan(z^{\frac{1}{2}})$ and $* \in \{I, \mathcal{I}\}$.

2) *SIR regime*: For $\alpha=2$, we have $p_*^c=0$, at any typical epoch, i.e., $* \in \{v, s, I, \mathcal{I}, t\}$. For $\alpha = 4$, we have

$$p_v^c = (1+\tau)^{-1} \left(1 + \tau^{\frac{1}{2}} \arctan(\tau^{\frac{1}{2}}) \right)^{-3/2},$$

$$p_s^c = \left(1 + \tau^{\frac{1}{2}} \arctan(\tau^{\frac{1}{2}}) \right)^{-1}, \quad p_s^c = \left(1 + \tau^{\frac{1}{2}} \arctan(\tau^{\frac{1}{2}}) \right)^{-1/2},$$

$$p_I^c = \frac{\tau^{-1/2}}{2} \int_0^\tau \frac{z^{-1/2}}{1+z} \left(1 + z^{\frac{1}{2}} \arctan(z^{\frac{1}{2}}) \right)^{-3/2} dz,$$

$$p_{\mathcal{I}}^c = \frac{\tau^{-1/2}}{2} \int_0^\tau \frac{z^{-1/2}}{(1+z)^2} \left(1 + z^{\frac{1}{2}} \arctan(z^{\frac{1}{2}}) \right)^{-5/2} dz.$$

The formula of p_t^c naturally matches that in [2]. Moreover, we have the following relations among the coverage probabilities in terms of $p_t^c(\tau)$, in the interference limited regime, as

$$p_v^c(\tau) = \frac{(p_t^c(\tau))^{3/2}}{1+\tau}, \quad p_s^c(\tau) = (p_t^c(\tau))^{1/2},$$

$$p_I^c(\tau) = \frac{\tau^{-1/2}}{2} \int_0^\tau \frac{z^{-1/2}}{1+z} (p_t^c(z))^{3/2} dz,$$

$$p_{\mathcal{I}}^c(\tau) = \frac{\tau^{-1/2}}{2} \int_0^\tau \frac{z^{-1/2}}{(1+z)^2} (p_t^c(z))^{5/2} dz,$$

by writing them as a function of τ only.

3) *SNR regime*: In particular, for the coverage probability in the SNR regime with $\alpha = 2$, we have from (14) that

$$p_*^c = \mathbb{E}_H^0 \left[e^{-\mu\tau H^2 \sigma^2} \right] = \left(1 + \frac{\mu\tau\sigma^2}{\lambda\pi} \right)^{-\zeta},$$

where $* \in \{v, s, t\}$, $\zeta = 3/2, 1/2, 1$ for $H = H_v, H_s, R$, using the Laplace transform of H_v^2, H_s^2, R^2 , under their respective Palm probability spaces. Also from (15), Proposition 4 and Proposition 6, we have

$$p_*^c = \mathbb{E}_H^0 \left[e^{-\mu\tau H^2 \sigma^2} \right] = \frac{2\lambda\pi}{\mu\tau\sigma^2} \left[1 - \left(1 + \frac{\mu\tau\sigma^2}{\lambda\pi} \right)^{-\zeta} \right],$$

where $* \in \{I, \mathcal{I}\}$, $\zeta = 1/2$ and $3/2$, for $H = R_I$ and $R_{\mathcal{I}}$, respectively.

B. Without fading

In no-fading scenario, the closed form or integral form expressions we have are for any value of α , and these are mainly for the STINR, STIR and SNR regimes.

1) *STINR regime*:

$$p_{v; \tau}^c = \begin{cases} F_{H_v}^0 \left(\left(\frac{1-\tau}{\tau\sigma^2} \right)^{\frac{1}{\alpha}} \right) & \text{if } \tau < 1 \\ 0 & \text{otherwise.} \end{cases}$$

At typical max-interference and min-interference we have, for $* \in \{I, \mathcal{I}\}$

$$p_{*; \tau}^c = \tau^{-\frac{2}{\alpha}} \mathbb{E}_{H_*}^0 \left[\left(1 + \mathbb{1}_{\{*\neq \mathcal{I}\}} + \sigma^2 H_*^\alpha \right)^{-\frac{2}{\alpha}} \right].$$

2) *STIR regime*: For any $\tau \geq 0$

$$p_{v; \tau}^c = \begin{cases} 1 & \text{if } \tau < 1, \\ 0 & \text{if } \tau \geq 1, \end{cases} \quad p_{t; \tau}^c = \begin{cases} \tau^{-2/\alpha} & \text{if } \tau > 1 \\ 1 & \text{if } \tau \leq 1 \end{cases},$$

$$p_{s; \tau}^c = \begin{cases} \frac{1}{2\sqrt{\pi}} \mathbb{E}_{H_s}^0 \left[\Gamma \left(0, \lambda\pi(\tau^{2/\alpha} - 1)H_s^2 \right) \right] & \text{if } \tau > 1 \\ 1 & \text{if } \tau \leq 1. \end{cases}$$

For any $\tau \geq 1$, $p_{I; \tau}^c = \tau^{-2/\alpha}$, $p_{\mathcal{I}; \tau}^c = (2\tau)^{-2/\alpha}$.

Remark 12 Based on the alternative definition of handover using STIR in Remark 7, and the coverage probability $p_{v; \tau}^c$, we see that, at handover epochs, the user is covered almost surely, unless the QoS requirement is $\tau \geq 1$ and the user is not covered almost surely in that case.

3) *SNR regime*: The coverage probability, in general written as p_*^c , is given by

$$p_*^c = \mathbb{P}^0 \left(H \leq (\tau\sigma^2)^{-\frac{1}{\alpha}} \right),$$

for $H = H_v, H_s, R_I, R_{\mathcal{I}}, R$ and $* \in \{v, s, I, \mathcal{I}, t\}$, under their respective Palm probability measures \mathbb{P}^0 .

VI. NUMERICAL RESULTS AND DISCUSSIONS

In this part we present the numerical illustrations of our results on the performance evaluation in terms of coverage probabilities and their comparison at different typical epochs, in both cases with and without fading. The closed form or semi explicit integral form derived by leveraging the Poissonianity, enable us to create plots of these performance metrics quite conveniently. The coverage probabilities are plotted against the user QoS requirement variable τ in dB scale. The system parameters are the intensity of BSs λ , the exponent α of the path-loss attenuation function, μ the fading parameter and σ the parameter for the thermal noise. The plots and their comparisons are made for different λ and α values. Figure 7 plots coverage probabilities against the SINR threshold τ in dB scale, at typical handover, typical time and typical max-signal, when $\alpha = 3, 4$, $\mu = 2$, $\sigma^2 = 10^{-6}$ and $\lambda = 10^{-4}, 10^{-2}$ and 1, respectively. Figure 8 is similar for the cases of typical max-interference and min-interference. In the interference limited regime, the coverage probabilities are plotted in Figure 7 (d) and Figure 8 (d) for $\alpha = 3, 4$, $\mu = 2$, and the intensity $\lambda = 1$ only, due to the scale invariance. A similar comparison of plots

is also provided in Figure 9 and Figure 10 with the same values of the parameters.

In the tropical cases, we have similar comparison plots of coverage probabilities in Figure 11 and Figure 12 in the case with fading, Figure 13 and Figure 14 in the case without fading. All these plots validate our comparison of coverage probabilities stated in Theorem 6, except for the comparison of coverage probabilities $p_{\mathcal{V},\tau}^c, p_{t,\tau}^c$ and $p_{s,\tau}^c$ at typical handover, typical time and typical max-signal, respectively, for the case of tropical SINR and SIR without fading, as shown at the end of Appendix IV and also validated in Figure 13. Our plot shows a different comparison among $p_{\mathcal{V},\tau}^c, p_{s,\tau}^c$ and $p_{t,\tau}^c$ holds for the threshold parameter $\tau \geq 0$ [dB]. Performance is better at the typical time epoch for high density (λ) of the BSs, which is not the case in low density regimes.

For brevity we have presented the numerical comparison just for the coverage probabilities (Theorem 6), but not for the mean Shannon capacities (Corollary 7) and the interferences (Theorem 7).

VII. CONCLUSIONS AND FUTURE RESEARCH

This work addresses the question of performance evaluation in a Poisson based dynamical cellular communication system at various typical epochs, at which a UE tend to suffer or benefit from the presence of interferer(s) or server close or far from the UE. Building on top of the mobility model described in [21], using stochastic geometry, we have derived the coverage probabilities at these epochs, depending on the system parameter and made comparison between them. Our approach based on the determination of the characteristics of several typical distances that are essential for the performance evaluation. The ergodic data rate among different typical epochs correspond to different seasons for capacity with respect to our seasonal analogy of the system performance. This article contains a complete study of system performance in a Poisson BSs setting in the absence of fading and noise or in their presence, along with simple assumption of Rayleigh fading and classical use case of power law path-loss attenuation function. The in-built tractability of the Poisson analysis allows one to analyze many other fading distribution and path-loss attenuation function.

As a future direction of research, we plan to investigate the performance evaluation and their comparisons in other dynamical wireless system models, mentioned in [21], for example 3D Poisson setting, 2D & 3D Cox setting, Poisson and Cox setting under the spherical set up.

APPENDIX I PROOFS: PRELIMINARIES

A. Proof of Proposition 1

The result is a corollary of Property 2. Indeed, if there are more than $(k-1)$ point in U_h^s , then the radial bird at those points intersects the vertical line $t = s$ at a level below h ,

contradicting the fact that $(s, h) \in \mathcal{L}_e^{(k)}$. For part 2, if (s, h) is an intersection point of two radial birds, then \overline{U}_h^s will contain two extra points corresponding to the two radial birds. \square

B. Proof of Proposition 2

Here we use the intensity of the point process $\mathcal{V}_s, \lambda_s = \sqrt{\lambda}$ from [21, Lemma 5.8]. The joint Laplace transform of H_s^2, R_s^2 with parameter γ, β under the Palm probability measure of \mathcal{V}_s is

$$\begin{aligned} & \mathbb{E}_{\mathcal{V}_s}^0 \left[e^{-\gamma H_s^2 - \beta R_s^2} \right] \\ &= \frac{1}{\lambda_s} \mathbb{E} \left[\sum_{(T_i^s, H_i^s) \in \mathcal{H}_s: T_i^s \in [0,1]} e^{-\gamma (H_i^s)^2 - \beta (R_i^s)^2} \right] \\ &= \frac{1}{\sqrt{\lambda}} \mathbb{E} \left[\sum_{(T_i, H_i) \in \mathcal{H}: T_i \in [0,1]} e^{-\gamma H_i^2 - \beta (R_i^s)^2} \mathbb{1} \left\{ \mathcal{H}(U_{H_i}^{T_i}) = 0 \right\} \right. \\ & \quad \left. \times \mathbb{1} \left\{ \exists (T_j, H_j) \in \mathcal{H} : (T_i, H_i) \in U_{R_i^s}^{T_i} \right\} \right] \\ &= \frac{1}{\sqrt{\lambda}} \mathbb{E} \left[\sum_{(T_i, H_i) \in \mathcal{H}: T_i \in [0,1]} e^{-\gamma H_i^2} \mathbb{1} \left\{ \mathcal{H}(U_{H_i}^{T_i}) = 0 \right\} \sum_{(T_j, H_j) \in \mathcal{H} \setminus (U_{H_i}^{T_i})^c} e^{-\beta R_{i,j}^2} \right. \\ & \quad \left. \times \mathbb{1} \left\{ \mathcal{H} \left(U_{R_{i,j}}^{T_i} \setminus U_{H_i}^{T_i} \right) = 1 \right\} \right] \\ &= \frac{1}{\sqrt{\lambda}} \mathbb{E} \left[\sum_{\substack{(T_i, H_i) \in \mathcal{H} \\ T_i \in [0,1]}} e^{-\gamma H_i^2} \sum_{(T_j, H_j) \in \mathcal{H} \setminus (U_{H_i}^{T_i})^c} e^{-\beta R_{i,j}^2} \mathbb{1} \left\{ \mathcal{H}(U_{R_{i,j}}^{T_i}) = 1 \right\} \right], \end{aligned}$$

where $R_{i,j}^2 = (T_i - T_j)^2 + H_j^2$. By applying the multivariate Campbell-Mecke formula for the factorial power of order 2 of \mathcal{H} , i.e., $\mathcal{H}^{2,\neq}$, we get

$$\begin{aligned} & \mathbb{E}_{\mathcal{V}_s}^0 \left[e^{-\gamma H_s^2 - \beta R_s^2} \right] \\ &= \frac{4\lambda^2}{\sqrt{\lambda}} \int_0^1 \int_0^\infty \int_{(U_{h_i}^{t_i})^c} e^{-\gamma h_i^2} e^{-(\beta + \lambda\pi)((t_i - t_j)^2 + h_j^2)} dh_j dt_j dh_i dt_i \\ &= 4\lambda^{\frac{3}{2}} \int_0^\infty \int_{(U_{h_i}^0)^c} e^{-\gamma h_i^2} e^{-(\beta + \lambda\pi)(t^2 + h_j^2)} dh_j dt dh_i \\ &= 2\lambda^{3/2} \pi \int_0^\infty e^{-\gamma h_i^2} K_{\beta + \lambda\pi}(h_i) dh_i, \end{aligned} \quad (21)$$

where

$$\begin{aligned} K_{\beta + \lambda\pi}(h_i) &:= \frac{2}{\pi} \int_{(U_{h_i}^0)^c} e^{-(\beta + \lambda\pi)(t^2 + h_j^2)} dh_j dt \\ &= \frac{2}{\pi} \int_0^\pi \int_{h_i}^\infty e^{-(\beta + \lambda\pi)r^2} r dr d\theta \\ &= \frac{1}{\beta + \lambda\pi} e^{-(\beta + \lambda\pi)h_i^2}. \end{aligned} \quad (22)$$

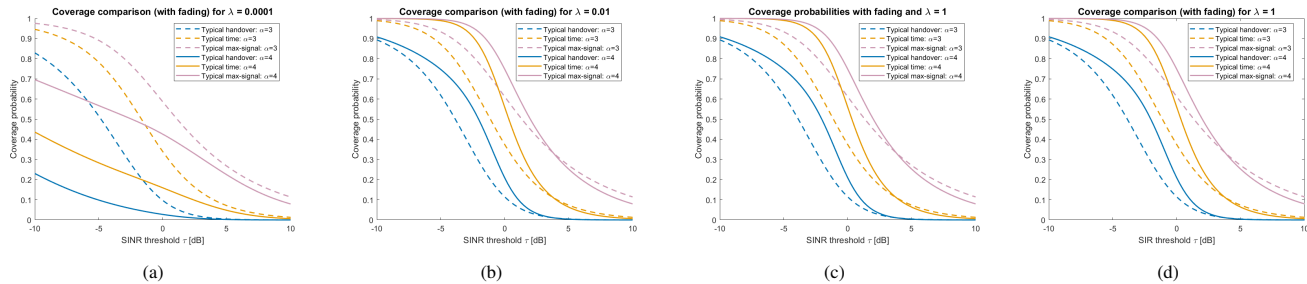


Fig. 7: Non-tropical case (with fading): Comparison of coverage probabilities at typical min-signal max-interference (handover), typical time, typical max-signal, with respect to SINR threshold or user QoS requirement τ in dB unit, in the case: (a) $\lambda = 10^{-4}$, (b) $\lambda = 10^{-2}$, (c) $\lambda = 1$ for $\alpha = 3$ and 4 in the case with fading, between -10 to 10 dB. Figure (d) is for intensity $\lambda = 1$, for $\alpha = 3$ and 4, in the interference limited regime.

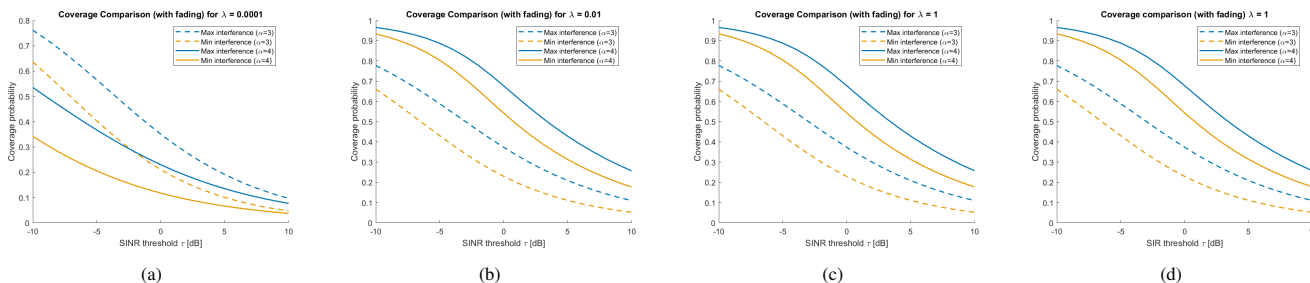


Fig. 8: Non-tropical case (with fading): Comparison of coverage probabilities at typical max-interference, typical min-interference, with respect to SINR threshold or user QoS requirement τ in dB unit, in the case: (a) $\lambda = 10^{-4}$, (b) $\lambda = 10^{-2}$, (c) $\lambda = 1$ for $\alpha = 3$ and 4 in the case with fading, between -10 to 10 dB. Figure (d) is for intensity $\lambda = 1$, for $\alpha = 3$ and 4, in the interference limited regime.

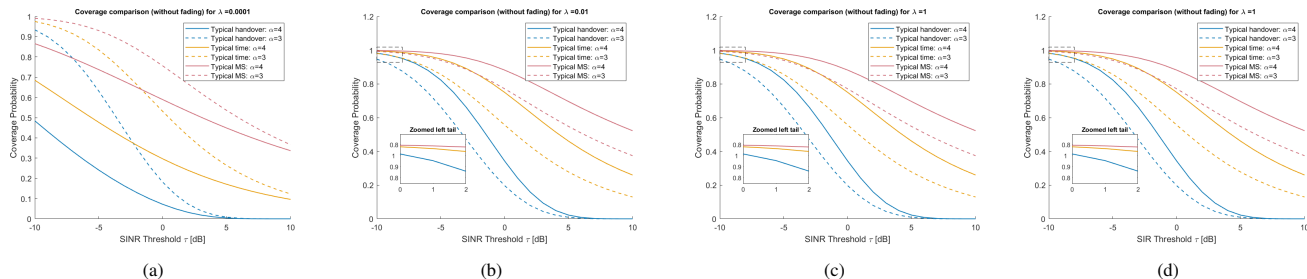


Fig. 9: Non-tropical case (without fading): Comparison of coverage probabilities at typical min-signal max-interference (handover), typical time and typical max-signal, with respect to SINR threshold or user QoS requirement τ in dB unit, in the case: (a) $\lambda = 10^{-4}$, (b) $\lambda = 10^{-2}$, (c) $\lambda = 1$ for $\alpha = 3$ and 4 in the case without fading. Figure (d) is for intensity $\lambda = 1$, for $\alpha = 3$ and 4, in the interference limited regime.

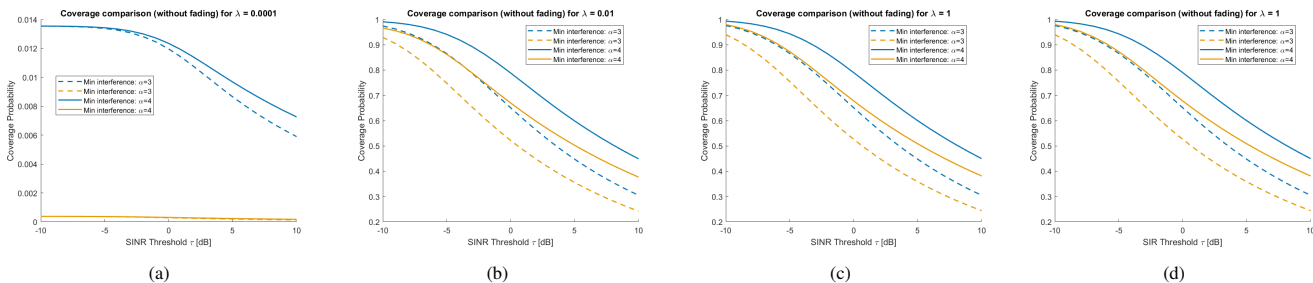


Fig. 10: Non-tropical case (without fading): Comparison of coverage probabilities at typical max-interference and typical min-signal, with respect to SINR threshold or user QoS requirement τ in dB unit, in the case: (a) $\lambda = 10^{-4}$, (b) $\lambda = 10^{-2}$, (c) $\lambda = 1$ for $\alpha = 3$ and 4 in the case without fading. Figure (d) is for intensity $\lambda = 1$, for $\alpha = 3$ and 4, in the interference limited regime.

Substituting from (22) to (21), we get

$$\begin{aligned}\mathbb{E}_{\mathcal{V}_S}^0 \left[e^{-\gamma H_S^2 - \beta R_S^2} \right] &= \frac{2\lambda^{3/2}\pi}{\beta + \lambda\pi} \int_0^\infty e^{-(\gamma + \beta + \lambda\pi)h_i^2} dh_i \\ &= \frac{\lambda^{3/2}\pi^{3/2}}{\beta + \lambda\pi} (\gamma + \beta + \lambda\pi)^{-\frac{1}{2}} \\ &= \left(1 + \frac{\beta}{\lambda\pi}\right)^{-1} \left(1 + \frac{\gamma + \beta}{\lambda\pi}\right)^{-\frac{1}{2}}.\end{aligned}$$

Note that for $\gamma = 0$, we have $\mathbb{E}_{\mathcal{V}_S}^0 \left[e^{-\beta R_S^2} \right] = \left(1 + \frac{\beta}{\lambda\pi}\right)^{-3/2}$ and hence R_S has a Nakagami distribution with parameters $\left(\frac{3}{2}, \frac{3}{2\lambda\pi}\right)$. \square

C. Proof of Lemma 1

Using the alternative definition of \mathcal{V}_I in (10) the intensity of the point process \mathcal{V}_I is

$$\lambda_I = \mathbb{E} \left[\sum_{T_j^I \in \mathcal{V}_I : 0 \leq T_j^I \leq 1} 1 \right] = \mathbb{E} \left[\sum_{\substack{(T_i, H_i) \in \mathcal{H} \\ 0 \leq T_i \leq 1}} \mathbb{1}_{\{\mathcal{H}(U_{H_i}^{T_i})=1\}} \right].$$

Applying Campbell-Mecke formula, we have

$$\begin{aligned}\lambda_I &= 2\lambda \int_0^1 \int_0^\infty \lambda\pi h^2 e^{-\lambda\pi h^2} dh dt \\ &= 2\lambda \int_0^\infty \lambda\pi h^2 e^{-\lambda\pi h^2} dh \\ &= \lambda \int_0^\infty x e^{-x} \frac{1}{\sqrt{\lambda\pi x}} dx = \sqrt{\frac{\lambda}{\pi}} \int_0^\infty x^{\frac{3}{2}-1} e^{-x} dx = \frac{\sqrt{\lambda}}{2}. \square\end{aligned}$$

D. Proof of Proposition 3

The Laplace transform of H_I^2 under the Palm probability measure of \mathcal{V}_I is

$$\begin{aligned}\mathbb{E}_{\mathcal{V}_I}^0 \left[e^{-\gamma H_I^2} \right] &= \frac{1}{\lambda_I} \mathbb{E} \left[\sum_{(T_j^I, H_j^I) \in \mathcal{H}_I : T_j^I \in [0,1]} e^{-\gamma (H_j^I)^2} \right] \\ &= \frac{1}{\lambda_I} \mathbb{E} \left[\sum_{(T_i, H_i) \in \mathcal{H} : T_i \in [0,1]} e^{-\gamma H_i^2} \mathbb{1}_{\{\mathcal{H}(U_{H_i}^{T_i})=1\}} \right]. \quad (23)\end{aligned}$$

Applying the Campbell-Mecke formula and using $\lambda_I = \frac{1}{2}\sqrt{\lambda}$ from Lemma 1, the last term in (23) equals

$$\begin{aligned}\frac{2\lambda}{\lambda_I} \int_0^1 \int_0^\infty \lambda\pi h^2 e^{-(\gamma + \lambda\pi)h^2} dh dt \\ &= 4\sqrt{\lambda} \int_0^\infty \lambda\pi h^2 e^{-(\gamma + \lambda\pi)h^2} dh \\ &= 4\sqrt{\lambda} \frac{\lambda\pi}{\gamma + \lambda\pi} \int_0^\infty x e^{-x} \frac{1}{2\sqrt{(\gamma + \lambda\pi)x}} dx \\ &= 2\pi \left(\frac{\lambda}{\gamma + \lambda\pi} \right)^{\frac{3}{2}} \Gamma\left(\frac{3}{2}\right) = \left(1 + \frac{\gamma}{\lambda\pi}\right)^{-\frac{3}{2}}.\end{aligned}$$

This shows that H_I follows a Nakagami distribution with parameters $\left(\frac{3}{2}, \frac{3}{2\lambda\pi}\right)$. \square

E. Proof of Proposition 4

Given $(T_i^I, H_i^I) \in \mathcal{H}_I$, if $(T_j, H_j) \in \mathcal{H}|_{U_{H_i^I}^{T_i^I}}$, then $R_i^I :=$

$\left(\left(T_i^I - T_j\right)^2 + H_j^2\right)^{\frac{1}{2}} \leq H_i^I$. The joint Laplace transform of H_I^2, R_I^2 is given by

$$\begin{aligned}\mathbb{E}_{\mathcal{V}_I}^0 \left[e^{-\gamma H_I^2 - \beta R_I^2} \right] &= \frac{1}{\lambda_I} \mathbb{E} \left[\sum_{(T_i^I, H_i^I) \in \mathcal{H}_I : T_i^I \in [0,1]} e^{-\gamma (H_i^I)^2 - \beta (R_i^I)^2} \right] \\ &= \frac{1}{\lambda_I} \mathbb{E} \left[\sum_{\substack{(T_i, H_i) \in \mathcal{H} \\ T_i \in [0,1]}} e^{-\gamma H_i^2 - \beta (R_i^I)^2} \mathbb{1}_{\{\mathcal{H}(U_{H_i}^{T_i})=1\}} \right. \\ &\quad \left. \times \mathbb{1}_{\{\exists (T_j, H_j) \in \mathcal{H} : (T_j, H_j) \in U_{H_i}^{T_i}\}} \right] \\ &= \frac{1}{\lambda_I} \mathbb{E} \left[\sum_{\substack{(T_i, H_i) \in \mathcal{H} \\ T_i \in [0,1]}} e^{-\gamma H_i^2} \mathbb{1}_{\{\mathcal{H}(U_{H_i}^{T_i})=1\}} \sum_{(T_j, H_j) \in \mathcal{H}|_{U_{H_i}^{T_i}}} e^{-\beta R_{i,j}^2} \right],\end{aligned}$$

where, $R_{i,j}^2 = (T_i - T_j)^2 + H_j^2$. By applying the multivariate Campbell-Mecke formula for the factorial power of order 2 of \mathcal{H} , i.e., $\mathcal{H}^{2,\neq}$ similar to the Palm distribution in [21, Theorem 5.4], we obtain that

$$\begin{aligned}\mathbb{E}_{\mathcal{V}_I}^0 \left[e^{-\gamma H_I^2 - \beta R_I^2} \right] &= \frac{4\lambda^2}{\lambda_I} \int_0^1 \int_0^\infty \int_{U_{h_i}^{t_i}} e^{-(\gamma + \lambda\pi)h_i^2} e^{-\beta((t_i - t_j)^2 + h_j^2)} dh_j dt_j dh_i dt_i \\ &= 8\lambda^{\frac{3}{2}} \int_0^\infty \int_{U_{h_i}^0} e^{-(\gamma + \lambda\pi)h_i^2} e^{-\beta(t^2 + h_j^2)} dh_j dt dh_i \\ &= 4\lambda^{3/2}\pi \int_0^\infty e^{-(\gamma + \lambda\pi)h_i^2} J_\beta(h_i) dh_i, \quad (24)\end{aligned}$$

where

$$\begin{aligned}J_\beta(h_i) &:= \frac{2}{\pi} \int_{U_{h_i}^0} e^{-\beta(t^2 + h_j^2)} dh_j dt \\ &= \frac{2}{\pi} \int_0^\pi \int_0^{h_i} e^{-\beta r^2} r dr d\theta = \frac{1}{\beta} \left(1 - e^{-\beta h_i^2}\right). \quad (25)\end{aligned}$$

This implies that, conditioned on $H_I = h_i$, R_I^2 is uniformly distributed on $[0, h_i^2]$. Hence, from (24) and (25), we have

$$\begin{aligned}\mathbb{E}_{\mathcal{V}_I}^0 \left[e^{-\gamma H_I^2} e^{-\beta R_I^2} \right] &= \frac{4\lambda^{3/2}\pi}{\beta} \int_0^\infty e^{-(\gamma + \lambda\pi)h_i^2} \left(1 - e^{-\beta h_i^2}\right) dh_i \\ &= \frac{4\lambda^{3/2}\pi}{\beta} \left[\int_0^\infty e^{-(\gamma + \lambda\pi)h_i^2} dh_i - \int_0^\infty e^{-(\gamma + \lambda\pi + \beta)h_i^2} dh_i \right] \\ &= \frac{2\lambda^{3/2}\pi^{3/2}}{\beta} \left[(\gamma + \lambda\pi)^{-\frac{1}{2}} - (\gamma + \lambda\pi + \beta)^{-\frac{1}{2}} \right] \\ &= \frac{2\lambda\pi}{\beta} \left[\left(1 + \frac{\gamma}{\lambda\pi}\right)^{-\frac{1}{2}} - \left(1 + \frac{\gamma + \beta}{\lambda\pi}\right)^{-\frac{1}{2}} \right],\end{aligned}$$

as required in this result. \square

F. Proof of Lemma 2

For any two points $(t_1, h_1), (t_2, h_2)$ with $t_2 < t_1$, we have that the square of the distance to the intersection of two radial birds at $(t_1, h_1), (t_2, h_2)$ is given by

$$\hat{h}^2 = \frac{1}{4} \left[(t_1 - t_2)^2 + 2(h_1^2 + h_2^2) + \frac{(h_2^2 - h_1^2)^2}{(t_1 - t_2)^2} \right]. \quad (26)$$

Applying the multivariate Campbell-Mecke formula for the factorial power of order 2 of \mathcal{H} , i.e., $\mathcal{H}^{2, \neq}$, the intensity of \mathcal{V}_x is

$$\begin{aligned} \lambda_x &= 4\lambda^2 \int_0^1 \int_0^\infty \int_0^\infty \int_{-\infty}^{t_1} \lambda\pi \hat{h}^2 e^{-\lambda\pi \hat{h}^2} dt_2 dh_2 dh_1 dt_1 \\ &= 4\lambda^2 \int_0^\infty \int_0^\infty \int_0^\infty \lambda\pi \hat{h}^2 e^{-\lambda\pi \hat{h}^2} dt dh_1 dh_2, \end{aligned} \quad (27)$$

where \hat{h} is a function of $t = t_1 - t_2$, h_1 and h_2 . We write the inner integral as

$$\begin{aligned} &\int_0^\infty \lambda\pi \hat{h}^2 e^{-\lambda\pi \hat{h}^2} dt \\ &= e^{-\frac{\lambda\pi}{2}(h_1^2 + h_2^2)} \left(I(a, b) + \frac{\lambda\pi}{2} (h_1^2 + h_2^2) J(a, b) \right), \end{aligned} \quad (28)$$

where $a = \frac{\lambda\pi}{4}$ and $b = \frac{\lambda\pi}{4} (h_2^2 - h_1^2)^2$ and

$$I(a, b) = \int_0^\infty \left(at^2 + \frac{b}{t^2} \right) e^{-(at^2 + \frac{b}{t^2})} dt, \quad (29)$$

$$J(a, b) = \int_0^\infty e^{-(at^2 + \frac{b}{t^2})} dt = \frac{\sqrt{\pi}}{2\sqrt{ab}} e^{-2\sqrt{ab}}. \quad (30)$$

The integral $J(a, b)$ in (30) is computed using Cauchy-Schlömilch transformation [31]. We first compute an integral of the form (29). Using Leibniz's rule for differentiation under the integral sign for two parameter a and b , we have

$$\begin{aligned} I(a, b) &= -a \frac{\partial}{\partial a} J(a, b) - b \frac{\partial}{\partial b} J(a, b) \\ &= -\frac{\sqrt{\pi}}{2} e^{-2\sqrt{ab}} \left[a \left(-\frac{1}{2} a^{-3/2} - \sqrt{b}/a \right) + b \left(-\frac{1}{\sqrt{b}} \right) \right] \\ &= \frac{\sqrt{\pi}}{2} e^{-2\sqrt{ab}} \left[\frac{1}{2} a^{-1/2} + 2\sqrt{b} \right] \\ &= \frac{\sqrt{\pi}}{4\sqrt{a}} e^{-2\sqrt{ab}} (1 + 4\sqrt{ab}). \end{aligned}$$

Then using $a = \frac{\lambda\pi}{4}$ and $b = \frac{\lambda\pi}{4} (h_2^2 - h_1^2)^2$ in (28), we have

$$\begin{aligned} &\int_0^\infty \lambda\pi \hat{h}^2 e^{-\lambda\pi \hat{h}^2} dt \\ &= e^{-\frac{\lambda\pi}{2}(h_1^2 + h_2^2)} e^{-2\sqrt{ab}} \frac{\sqrt{\pi}}{4\sqrt{a}} (1 + 4\sqrt{ab} + \lambda\pi (h_1^2 + h_2^2)) \\ &= e^{-\frac{\lambda\pi}{2}(h_1^2 + h_2^2 + |h_1^2 - h_2^2|)} \frac{1}{2\sqrt{\lambda}} [1 + \lambda\pi (|h_1^2 - h_2^2| + h_1^2 + h_2^2)] \\ &= \frac{1}{2\sqrt{\lambda}} e^{-\lambda\pi (h_1^2 \vee h_2^2)} (1 + 2\lambda\pi (h_1^2 \vee h_2^2)). \end{aligned} \quad (31)$$

Using the value of the inner integral from (31) in (27) we have

$$\begin{aligned} \lambda_x &= 2\lambda^{3/2} \int_0^\infty \int_0^\infty e^{-\lambda\pi (h_1^2 \vee h_2^2)} (1 + 2\lambda\pi (h_1^2 \vee h_2^2)) dh_1 dh_2 \\ &= \frac{2\sqrt{\lambda}}{\pi} \int_0^\infty \int_0^\infty e^{-h_1^2 \vee h_2^2} (1 + 2(h_1^2 \vee h_2^2)) dh_1 dh_2. \end{aligned} \quad (32)$$

Since the integrand is a symmetric function of h_1, h_2 , it is enough to compute the integral for $h_2 \in [0, \infty)$ and $h_1 \in [0, h_2]$. Using this, it can be proved that

$$\int_{(\mathbb{R}^+)^2} e^{-(h_1^2 \vee h_2^2)} dh_1 dh_2 = 1 = \int_{(\mathbb{R}^+)^2} (h_1^2 \vee h_2^2) e^{-(h_1^2 \vee h_2^2)} dh_1 dh_2.$$

This shows from (32) that $\lambda_x = \frac{6\sqrt{\lambda}}{\pi}$. \square

G. Proof of Proposition 5

The Laplace transform of H_x^2 is obtained under the Palm probability measure of \mathcal{V}_x similarly to the Palm distribution in [21, Theorem 5.4] as follows:

$$\begin{aligned} &\mathbb{E}_{\mathcal{V}_x}^0 \left[e^{-\gamma H_x^2} \right] \\ &= \frac{1}{\lambda_x} \mathbb{E} \left[\sum_{\substack{(T_i, H_i) \in \mathcal{H} \\ T_i \in [0, 1]}} \sum_{\substack{(T_j, H_j) \in \mathcal{H} \\ T_j < T_i}} e^{-\gamma \hat{H}^2} \mathbf{1}_{\{\mathcal{H}(U_{\hat{H}}^{\hat{S}}) = 1\}} \right] \\ &= \frac{4\lambda^2}{\lambda_x} \int_0^1 \int_0^\infty \int_0^\infty \int_{-\infty}^{t_1} \lambda\pi \hat{h}^2 e^{-(\gamma + \lambda\pi) \hat{h}^2} dt_2 dh_2 dh_1 dt_1 \\ &= \frac{2\lambda^{3/2}\pi}{3} \int_0^\infty \int_0^\infty \int_0^\infty \lambda\pi \hat{h}^2 e^{-(\gamma + \lambda\pi) \hat{h}^2} dt dh_2 dh_1, \end{aligned} \quad (33)$$

by applying the multivariate Campbell-Mecke formula for the factorial power of order 2 of \mathcal{H} , where $\lambda_x = \frac{6\sqrt{\lambda}}{\pi}$, from Lemma 2, and \hat{h} is function of $t = t_1 - t_2, h_1$ and h_2 as derived in (26). We evaluate the inner integral in (33) as

$$\begin{aligned} &\frac{\lambda\pi}{\gamma + \lambda\pi} \int_0^\infty (\gamma + \lambda\pi) \hat{h}^2 e^{-(\gamma + \lambda\pi) \hat{h}^2} dt \\ &= \frac{\sqrt{\pi}}{2\sqrt{\gamma + \lambda\pi}} e^{-(\gamma + \lambda\pi)(h_1^2 \vee h_2^2)} (1 + 2(\gamma + \lambda\pi)(h_1^2 \vee h_2^2)) \\ &= \frac{1}{2\sqrt{\lambda}} \left(\frac{\lambda\pi}{\gamma + \lambda\pi} \right)^{1/2} e^{-(\gamma + \lambda\pi)(h_1^2 \vee h_2^2)} (1 + 2(\gamma + \lambda\pi)(h_1^2 \vee h_2^2)), \end{aligned} \quad (34)$$

using similar computation up to (31). Substituting from (34) to (33), we have

$$\begin{aligned} \mathbb{E}_{\mathcal{V}_x}^0 \left[e^{-\gamma H_x^2} \right] &= \frac{\lambda\pi}{3} \left(\frac{\lambda\pi}{\gamma + \lambda\pi} \right)^{3/2} \int_0^\infty \int_0^\infty e^{-(\gamma + \lambda\pi)(h_1^2 \vee h_2^2)} \\ &\quad \times (1 + 2(\gamma + \lambda\pi)(h_1^2 \vee h_2^2)) dh_2 dh_1 \\ &= \frac{\lambda\pi}{3} \left(\frac{\lambda\pi}{\gamma + \lambda\pi} \right)^{3/2} \frac{3}{\gamma + \lambda\pi} = \left(1 + \frac{\gamma}{\lambda\pi} \right)^{-5/2}, \end{aligned} \quad (35)$$

since the double integral in the first step in (35) equals to $\frac{3}{\gamma + \lambda\pi}$ similarly to (32). \square

H. Proof of Proposition 6

The joint distribution of H_x^2, R_x^2 is given by the joint Laplace transform obtained similarly to the Palm distribution in [21,

Theorem 5.4], as follows:

$$\begin{aligned}
& \mathbb{E}_{\mathcal{V}_x}^0 \left[e^{-\gamma H_x^2 - \beta R_x^2} \right] \\
&= \frac{1}{\lambda_x} \mathbb{E} \left[\sum_{\substack{(T_i, H_i) \in \mathcal{H} \\ T_i \in [0, 1]}} \sum_{\substack{(T_j, H_j) \in \mathcal{H} \\ T_j < T_i}} e^{-\gamma H_x^2 - \beta R_x^2} \mathbb{1} \left\{ \mathcal{H}(U_{\hat{H}}^{\hat{S}}) = 1 \right\} \right. \\
&\quad \left. \times \mathbb{1} \left\{ \exists (T_k, H_k) \in \mathcal{H} \Big|_{U_{\hat{H}}^{\hat{S}}} \right\} \right] \\
&= \frac{1}{\lambda_x} \mathbb{E} \left[\sum_{\substack{(T_i, H_i) \in \mathcal{H} \\ T_i \in [0, 1]}} \sum_{\substack{(T_j, H_j) \in \mathcal{H} \\ T_j < T_i}} e^{-\gamma H_x^2} \mathbb{1} \left\{ \mathcal{H}(U_{\hat{H}}^{\hat{S}}) = 1 \right\} \right. \\
&\quad \left. \times \sum_{(T_k, H_k) \in \mathcal{H} \Big|_{U_{\hat{H}}^{\hat{S}}}} e^{-\beta R_{\hat{S}, k}^2} \right] \\
&= \frac{4\lambda^2}{\lambda_x} \int_0^1 \int_0^\infty \int_0^\infty \int_{-\infty}^{t_1} e^{-(\gamma + \lambda\pi)\hat{h}^2} \lambda\pi J_\beta(\hat{s}, \hat{h}) dt_2 dh_2 dh_1 dt_1, \tag{36}
\end{aligned}$$

where $R_x^2 = R_{\hat{S}, k}^2 := (\hat{S} - T_k)^2 + H_k^2$, $J_\beta(\hat{s}, \hat{h}) = \frac{2}{\pi} \int_{U_{\hat{h}}^{\hat{s}}} e^{-\beta \hat{r}^2} dt_3 dh_3$, $\hat{r}^2 = (\hat{s} - t_3)^2 + h_3^2$ is a realisation of R_x and $\hat{s} = \frac{t_1^2 + h_1^2 - t_2^2 - h_2^2}{2(t_1 - t_2)}$.

Let $\hat{s} - t_3 = u \cos \theta$ and $h_3 = u \sin \theta$. Then similarly to (25) we can compute the integral

$$\begin{aligned}
J_\beta(\hat{s}, \hat{h}) &= \frac{2}{\pi} \int_{U_{\hat{h}}^{\hat{s}}} e^{-\beta \hat{r}^2} dt_3 dh_3 \\
&= \frac{2}{\pi} \int_0^\pi \int_0^{\hat{h}} e^{-\beta u^2} u du d\theta = \frac{1}{\beta} (1 - e^{-\beta \hat{h}^2}). \tag{37}
\end{aligned}$$

Conditioned on $H_x = \hat{h}$, we have R_x^2 is uniform on $[0, \hat{h}^2]$. Then the integral in (36) becomes

$$\begin{aligned}
& \mathbb{E}_{\mathcal{V}_x}^0 \left[e^{-\gamma H_x^2} e^{-\beta R_x^2} \right] \\
&= \frac{4\lambda^3 \pi}{\lambda_x \beta} \int_0^\infty \int_0^\infty \int_0^\infty e^{-(\gamma + \lambda\pi)\hat{h}^2} (1 - e^{-\beta \hat{h}^2}) dt dh_2 dh_1 \\
&= \frac{2\lambda\pi}{3\beta} \left[\left(1 + \frac{\gamma}{\lambda\pi}\right)^{-3/2} - \left(1 + \frac{\gamma + \beta}{\lambda\pi}\right)^{-3/2} \right],
\end{aligned}$$

using the fact that $\lambda_x = \frac{6\sqrt{\lambda}}{\pi}$ from Lemma 2 and for any $\eta \geq 0$

$$\pi\lambda^{3/2} \int_0^\infty \int_0^\infty \int_0^\infty e^{-(\lambda\pi + \eta)\hat{h}^2} dt dh_2 dh_1 = \left(1 + \frac{\eta}{\lambda\pi}\right)^{-3/2}. \square$$

APPENDIX II PROOFS: CASE WITH FADING

This section contains the proof of Theorem 1 and the derivation of these performance metrics for individual typical epochs with SINR and STINR, with respect to the corresponding Palm probability measure.

A. Proof of Theorem 1

The coverage probability with respect to the Palm probability distribution of the epoch of interest is

$$p^c(\tau, \mu, \lambda, \alpha) = \mathbb{E}_H^0 [\mathbb{P}(\mathcal{S} > \tau | H)]. \tag{38}$$

Conditioned on $H = h$ the inner term (38) is

$$\begin{aligned}
\mathbb{P}(\mathcal{S} > \tau | H = h) &= \mathbb{E}_{I_h} [\mathbb{P}(\mathcal{S} > \tau | I_h)] \\
&= \mathbb{E}_{I_h} [\mathbb{P}(\rho > \tau h^\alpha (\sigma^2 + I_h))] \\
&= \mathbb{E}_{I_h} \left[e^{-\mu\tau h^\alpha (\sigma^2 + I_h)} \right] \\
&= e^{-\mu\tau h^\alpha \sigma^2} \mathcal{L}_{I_h}(\mu\tau h^\alpha).
\end{aligned}$$

Then the coverage probability is given by the formula

$$p^c(\tau, \mu, \lambda, \alpha) = \mathbb{E}_H^0 \left[e^{-\mu\tau H^\alpha \sigma^2} \mathcal{L}_{I_H}(\mu\tau H^\alpha) \right]. \quad \square$$

B. Proof of Theorem 2

The proof follows the same steps as in Theorem 1, together with taking into account the randomness due to the distance H to the nearest interferer as well, jointly with the distance R to the serving BS. Given $H = h$ and $R = r$, the coverage probability is

$$\begin{aligned}
\mathbb{P}(\mathcal{S} > \tau | H = h, R = r) &= \mathbb{E}_{I_h} [\mathbb{P}(\mathcal{S} > \tau | I_h)] \\
&= \mathbb{E}_{I_h} [\mathbb{P}(\rho > \tau r^\alpha (\sigma^2 + I_h))] \\
&= \mathbb{E}_{I_h} \left[e^{-\mu\tau r^\alpha (\sigma^2 + I_h)} \right] \\
&= e^{-\mu\tau r^\alpha \sigma^2} \mathcal{L}_{I_h}(\mu\tau r^\alpha).
\end{aligned}$$

Jointly averaging of H and R , we have

$$p^c(\tau, \mu, \lambda, \alpha) = \mathbb{E}_{H, R}^0 \left[e^{-\mu\tau R^\alpha \sigma^2} \mathcal{L}_{I_H}(\mu\tau R^\alpha) \right]. \quad \square$$

For each of the typical epoch of interest, *ms-MI*, *MS*, *MI*, *ml* and *t*, in each of the subsections, we just state the expression of the metrics before proving them using the formula obtained in Theorem 1 and Theorem 2, without formally stating them as a theorem or corollary. From now on, for simplicity we write $p_*^c \equiv p_*^c(\tau, \mu, \lambda, \alpha)$, $p_{*,\tau}^c \equiv p_{*,\tau}^c(\tau, \mu, \lambda, \alpha)$ and $\mathcal{R}_* \equiv \mathcal{R}_*(\mu, \lambda, \alpha)$, $\mathcal{R}_{*,\tau} \equiv \mathcal{R}_{*,\tau}(\mu, \lambda, \alpha)$, which are understood to a function of the set of parameters $\{\tau, \mu, \lambda, \alpha\}$ and $\{\mu, \lambda, \alpha\}$, respectively, where $*$ $\in \{v, s, I, t\}$.

Remark 13 *In all our proofs, we just derive the expression for $p_*^c(\tau, \mu, \lambda, \alpha)$ and $p_{*,\tau}^c(\tau, \mu, \lambda, \alpha)$, and use it in the general formula in (13) for both $\mathcal{R}_*(\mu, \lambda, \alpha)$ and $\mathcal{R}_{*,\tau}(\mu, \lambda, \alpha)$, where $*$ $\in \{v, s, I, t\}$.*

C. Min-signal-max-interference (mS-MI): typical handover

In this case the distance to the serving BS is given by the handover distance H_v . The Palm probability distribution of a typical handover distance H_v is given by a Nakagami distribution with parameter $(\frac{3}{2}, \frac{3}{2\lambda\pi})$, having density (8) established in [21, Lemma 5.6].

Conditioned on the typical handover distance $H_v = h$, the distance of all other BSs is given by a Poisson point process $\eta_h = \sum_i \delta_{D_i}$ on $[h, \infty)$ with intensity measure having density

$2\pi\lambda r dr$, as seen in Lemma 5 (see also [21, Lemma 4.34]). Here is a result about the probability of coverage. In the following, we use the subscript \mathcal{V} to denote the typical handover.

1) *Theorem 1 (for SINR at typical mS-MI)*: The probability of coverage in the system with threshold τ at a typical handover is given by

$$p_{\mathcal{V}}^c = \frac{1}{1+\tau} \mathbb{E}_{H_{\mathcal{V}}}^0 \left[e^{-\mu\tau H_{\mathcal{V}}^{\alpha} \sigma^2 - \pi\lambda H_{\mathcal{V}}^2 \kappa(\tau, \alpha)} \right], \quad (39)$$

where $\kappa(\tau, \alpha) := \tau^{2/\alpha} \int_{\tau^{-2/\alpha}}^{\infty} \frac{1}{1+z^{\alpha/2}} dz$ as in (94).

Proof: Using the formula (14) we have

$$p_{\mathcal{V}}^c = \int_0^{\infty} e^{-\mu\tau h^{\alpha} \sigma^2} \mathcal{L}_{I_h}(\mu\tau h^{\alpha}) f_{H_{\mathcal{V}}}(h) dh, \quad (40)$$

where $\mathcal{L}_{I_h}(\gamma)$ is the Laplace transform of the total interference

$$I_h := \rho h^{-\alpha} + \sum_i \rho_i D_i^{-\alpha},$$

given the handover distance $H_{\mathcal{V}} = h$. Using the Poisson point process η_h of distances of all other stations, we compute the Laplace transform of I_h as follows:

$$\begin{aligned} \mathbb{E}_{I_h} [e^{-\gamma I_h}] &= \mathbb{E}_{\eta_h, \rho, \{\rho_i\}} \left[\mathbb{E} [e^{-\gamma I_h} | \eta_h, \rho, \{\rho_i\}] \right] \\ &= \mathbb{E}_{\rho} \left[e^{-\gamma \rho h^{-\alpha}} \right] \mathbb{E}_{\eta_h, \{\rho_i\}} \left[e^{-\gamma \sum_{i \in \mathbb{N}} \rho_i D_i^{-\alpha}} \right] \\ &= \frac{\mu}{\mu + \gamma h^{-\alpha}} \mathbb{E}_{\eta_h, \{\rho_i\}} \left[\prod_{i \in \mathbb{N}} e^{-\gamma \rho_i D_i^{-\alpha}} \right] \\ &= \frac{\mu}{\mu + \gamma h^{-\alpha}} \mathbb{E}_{\eta_h} \left[\prod_{i \in \mathbb{N}} \mathbb{E}_{\rho_i} [e^{-\gamma \rho_i D_i^{-\alpha}}] \right]. \end{aligned} \quad (41)$$

Computing the PGFl with respect to the point process η_h , we have

$$\begin{aligned} &\mathbb{E}_{\eta_h} \left[\prod_{i \in \mathbb{N}} \mathbb{E}_{\rho_i} [e^{-\gamma \rho_i D_i^{-\alpha}}] \right] \\ &= \exp \left(-2\pi\lambda \int_h^{\infty} \left(1 - \mathbb{E}_{\rho} [e^{-\gamma \rho r^{-\alpha}}] \right) r dr \right) \\ &= \exp \left(-2\pi\lambda \int_h^{\infty} \frac{\gamma r^{-\alpha}}{\mu + \gamma r^{-\alpha}} r dr \right). \end{aligned} \quad (42)$$

Substituting the Laplace transform of I_h with $\gamma = \mu\tau h^{\alpha}$ from (41) to (40), we get

$$\begin{aligned} p_{\mathcal{V}}^c &= \int_0^{\infty} e^{-\mu\tau h^{\alpha} \sigma^2} \mathcal{L}_{I_h}(\mu\tau h^{\alpha}) f_{H_{\mathcal{V}}}(h) dh \\ &= \frac{1}{1+\tau} \int_0^{\infty} e^{-\mu\tau h^{\alpha} \sigma^2 - 2\pi\lambda \int_h^{\infty} \frac{\tau h^{\alpha}}{\tau\alpha + \tau h^{\alpha}} r dr} f_{H_{\mathcal{V}}}(h) dh \\ &= \frac{1}{1+\tau} \int_0^{\infty} e^{-\mu\tau h^{\alpha} \sigma^2 - \pi\lambda h^2 \kappa(\tau, \alpha)} f_{H_{\mathcal{V}}}(h) dh, \end{aligned}$$

where we have computed the integral

$$\int_h^{\infty} \frac{\tau h^{\alpha}}{r^{\alpha} + \tau h^{\alpha}} r dr = \frac{1}{2} h^2 \kappa(\tau, \alpha), \quad (43)$$

where $\kappa(\tau, \alpha) := \tau^{2/\alpha} \int_{\tau^{-2/\alpha}}^{\infty} \frac{1}{1+z^{\alpha/2}} dz$ as in (94). \square

Remark 14 (Special case: $\alpha = 2$ and 4) For the attenuation exponent $\alpha = 2$, we have

$$\kappa(\tau, 2) = \tau \int_{\tau^{-1}}^{\infty} \frac{1}{1+z} dz = \infty.$$

As a result the coverage probability $p_{\mathcal{V}}^c(\tau, \mu, \lambda, 2) = 0$. Also for $\alpha = 4$, we have that

$$\kappa(\tau, 4) = \tau^{\frac{1}{2}} \int_{\tau^{-\frac{1}{2}}}^{\infty} \frac{1}{1+z^2} dz = \tau^{\frac{1}{2}} \arctan(\tau^{\frac{1}{2}}).$$

Using this, the coverage probability in (39) simplifies to

$$p_{\mathcal{V}}^c(\tau, \mu, \lambda, 4) = \frac{1}{1+\tau} \mathbb{E}_{H_{\mathcal{V}}}^0 \left[e^{-\mu\tau H_{\mathcal{V}}^{\alpha} \sigma^2 - \pi\lambda H_{\mathcal{V}}^2 \tau^{\frac{1}{2}} \arctan(\tau^{\frac{1}{2}})} \right],$$

in the fading environment with $\alpha = 4$.

Remark 15 In an interference limited regime with fading exponent $\alpha = 4$, the coverage probability has a exact closed form expression as

$$\begin{aligned} p_{\mathcal{V}, \tau}^c &= \frac{1}{1+\tau} \mathbb{E}_{H_{\mathcal{V}}}^0 \left[e^{-\pi\lambda H_{\mathcal{V}}^2 \tau^{\frac{1}{2}} \arctan(\tau^{\frac{1}{2}})} \right] \\ &= (1+\tau)^{-1} \left(1 + \tau^{\frac{1}{2}} \arctan(\tau^{\frac{1}{2}}) \right)^{-3/2}, \end{aligned} \quad (44)$$

using the Laplace transform of $H_{\mathcal{V}}^2$ from [21, Lemma 5.6]. Note from Theorem 8 that, $p_{\mathcal{V}}^c$ is scale invariant with respect to λ, μ .

2) *Theorem 1 (for tropical SINR at typical mS-MI)*: Under the tropical regime of SINR, the coverage probability at a threshold τ at a typical handover are

$$\begin{aligned} p_{\mathcal{V}, \tau}^c &= \mathbb{E}_{H_{\mathcal{V}}}^0 \left[e^{-\mu\tau H_{\mathcal{V}}^{\alpha} \sigma^2} \mu\tau H_{\mathcal{V}}^{\alpha} \int e^{-\mu\tau H_{\mathcal{V}}^{\alpha} x} \left(1 - e^{-\mu H_{\mathcal{V}}^{\alpha} x} \right) \right. \\ &\quad \left. \times e^{-2\lambda\pi K_{\alpha}(\mu, x, H_{\mathcal{V}})} dx \right]. \end{aligned}$$

Proof. In this case the tropical interference, given $H_{\mathcal{V}} = h$, is $\mathcal{T}_h := \rho h^{-\alpha} \vee \max_i \rho_i D_i^{-\alpha}$. Using the formula (14) in Theorem 1, we have

$$p_{\mathcal{V}, \tau}^c = \int_0^{\infty} e^{-\mu\tau h^{\alpha} \sigma^2} \mathcal{L}_{\mathcal{T}_h}(\mu\tau h^{\alpha}) f_{H_{\mathcal{V}}}(h) dh.$$

Given a handover at a distance h , the probability distribution of the tropical interference is

$$\begin{aligned} &\mathbb{P}(\mathcal{T}_h \leq x) \\ &= \mathbb{E}_{\eta_h, \rho, \{\rho_i\}} \left[\mathbb{P}(I_h \leq x) | \eta_h, \rho, \{\rho_i\} \right] \\ &= \mathbb{E}_{\eta_h} \left[\mathbb{E}_{\rho, \{\rho_i\}} \left(\mathbb{1}_{\rho h^{-\alpha} \leq x} \prod_{i \in \mathbb{N}} \mathbb{1}_{\rho_i D_i^{-\alpha} \leq x} \right) | \eta_h \right] \\ &= \mathbb{P}_{\rho}(\rho h^{-\alpha} \leq x) \mathbb{E}_{\eta_h} \left[\prod_{i \in \mathbb{N}} \exp \left(\log \mathbb{E}_{\rho_i} \left[\mathbb{1}_{\rho_i D_i^{-\alpha} \leq x} \right] \right) | \eta_h \right] \\ &= \mathbb{P}_{\rho}(\rho \leq h^{\alpha} x) \mathbb{E}_{\eta_h} \left[\exp \left(\sum_{i \in \mathbb{N}} \log \mathbb{E}_{\rho_i} \left[\mathbb{1}_{\rho_i D_i^{-\alpha} \leq x} \right] \right) | \eta_h \right] \\ &= \left(1 - e^{-\mu h^{\alpha} x} \right) \exp \left(-2\lambda\pi \int_h^{\infty} \left(1 - \mathbb{P}_{\rho}(\rho r^{-\alpha} \leq x) \right) r dr \right) \\ &= \left(1 - e^{-\mu h^{\alpha} x} \right) \exp \left(-2\lambda\pi \int_h^{\infty} e^{-\mu r^{\alpha} x} r dr \right) \\ &= \left(1 - e^{-\mu h^{\alpha} x} \right) e^{-2\lambda\pi K_{\alpha}(\mu, x, h)}, \end{aligned} \quad (45)$$

where $K_\alpha(\mu, x, h)$ is as defined in (98). Thus the Laplace transform of the interference \mathcal{T}_h is

$$\mathcal{L}_{\mathcal{T}_h}(\gamma) = \gamma \int e^{-\gamma x} F_{\mathcal{T}_h}(x) dx. \quad (46)$$

Then from (46) with $\gamma = \mu\tau h^\alpha$ and (14), the coverage probability is

$$p_{t;\tau}^c = \int_0^\infty e^{-\mu\tau h^\alpha \sigma^2} \mu\tau h^\alpha \int e^{-\mu\tau h^\alpha x} (1 - e^{-\mu h^\alpha x}) \times e^{-2\lambda\pi K_\alpha(\mu, x, h)} dx f_{H_V}(h) dh. \quad \square$$

Remark 16 (Special case: $\alpha = 2$ and 4) For $\alpha = 2$, we have $K_2(\mu, x, h) = \frac{1}{2\mu x} e^{-\mu h^2 x}$. For $\alpha = 4$ we have $K_4(\mu, x, h) = \frac{1}{4\sqrt{\mu x}} \Gamma\left(\frac{1}{2}, \mu h^4 x\right)$.

D. Typical time

At any typical time, let R be the random variable for the nearest BS from the user. It is well known in literature that R follows a Rayleigh distribution with parameter $1/\sqrt{2\pi\lambda}$, i.e., it has density

$$f_R(r) := 2\lambda\pi r e^{-\lambda\pi r^2}.$$

1) *Theorem 1 (for SINR at a typical time):* In this case the coverage probability with user QoS τ is

$$p_t^c = \mathbb{E}_R^0 \left[e^{-\mu\tau R^\alpha \sigma^2 - \pi\lambda R^2 \kappa(\tau, \alpha)} \right],$$

where the function κ is as defined in (94).

Proof. To apply the formula for the τ -coverage probability (14) we determine the Laplace transform $\mathcal{L}_{I_r}(\gamma)$ with $\gamma = \mu\tau r^\alpha$ as

$$\begin{aligned} \mathcal{L}_{I_r}(\mu\tau r^\alpha) &= \exp\left(-2\pi\lambda \int_r^\infty \frac{\mu\tau r^\alpha v^{-\alpha}}{\mu + \mu\tau r^\alpha v^{-\alpha}} v dv\right) \\ &= \exp\left(-2\pi\lambda \int_r^\infty \frac{\tau r^\alpha}{v^\alpha + \tau r^\alpha} v dv\right) = e^{-\pi\lambda r^2 \kappa(\tau, \alpha)}, \end{aligned}$$

where κ is as in (94). Then, from (14), the coverage probability is

$$p_t^c = \int_0^\infty e^{-\mu\tau r^\alpha \sigma^2} e^{-\pi\lambda r^2 \kappa(\tau, \alpha)} f_R(r) dr. \quad \square$$

Remark 17 Similarly to (44) we also obtain closed form in the interference limited regime for the case $\alpha = 4$ as $p_t^c = \left(1 + \tau^{\frac{1}{2}} \arctan(\tau^{\frac{1}{2}})\right)^{-1}$, using the fact that $\mathbb{E}\left[e^{-\gamma R^2}\right] = \left(1 + \frac{\gamma}{\lambda\pi}\right)^{-1}$.

2) *Theorem 1 (for STINR at a typical time):* At a typical time, the probability of coverage with user QoS τ is given by

$$p_{t;\tau}^c = \mu\tau \mathbb{E}_R^0 \left[R^\alpha \int e^{-\mu\tau R^\alpha (\sigma^2 + x) - 2\lambda\pi K_\alpha(\mu, x, R)} dx \right]. \quad (47)$$

Proof: We find the coverage probability using the formula (14) we first determine the Laplace transform of \mathcal{T}_r given $R = r$. For this, the probability distribution of \mathcal{T}_r is

$$\begin{aligned} \mathbb{P}(\mathcal{T}_r \leq x) &= \mathbb{E}_{\eta_r, \{\rho_i\}} [\mathbb{P}(\mathcal{T}_r \leq x) | \eta_r, \{\rho_i\}] \\ &= \mathbb{E}_{\eta_r} \left[\mathbb{E}_{\{\rho_i\}} \left[\left(\prod_{i \in \mathbb{N}} \mathbb{1}_{\rho_i D_i^{-\alpha} \leq x} \right) | \eta_r \right] \right] \\ &= \mathbb{E}_{\eta_r} \left[\prod_{i \in \mathbb{N}} \exp\left(\log \mathbb{E}_{\rho_i} \left[\mathbb{1}_{\rho_i D_i^{-\alpha} \leq x} \right]\right) | \eta_r \right] \\ &= \mathbb{E} \left[\exp\left(\sum_{i \in \mathbb{N}} \log \mathbb{E}_{\rho_i} \left[\mathbb{1}_{\rho_i D_i^{-\alpha} \leq x} \right]\right) | \eta_r \right]. \end{aligned}$$

Using the PGFl of the Poisson point process η_r , we have

$$\begin{aligned} \mathbb{P}(\mathcal{T}_r \leq x) &= \exp\left(-2\lambda\pi \int_r^\infty (1 - \mathbb{P}_\rho(\rho v^{-\alpha} \leq x)) v dv\right) \\ &= \exp\left(-2\lambda\pi \int_r^\infty \mathbb{P}_\rho(\rho > v^\alpha x) v dv\right) \\ &= e^{-2\lambda\pi \int_r^\infty e^{-\mu v^\alpha x} v dv} = e^{-2\lambda\pi K_\alpha(\mu, x, h)}, \quad (48) \end{aligned}$$

where the function $K_\alpha(\mu, x, h)$ is defined in (98). The Laplace transform of the tropical interference is

$$\begin{aligned} \mathbb{E}_{\mathcal{T}_r} [e^{-\gamma \mathcal{T}_r}] &= \gamma \int e^{-\gamma x} \mathbb{P}(\mathcal{T}_r \leq x) dx \\ &= \gamma \int e^{-\gamma x} e^{-2\lambda\pi K_\alpha(\mu, x, r)} dx, \quad (49) \end{aligned}$$

using $\gamma = \mu\tau r^\alpha$, the coverage probability turns out to be

$$p_{t;\tau}^c = \mu\tau \int_0^\infty r^\alpha e^{-\mu\tau r^\alpha \sigma^2} \int e^{-\mu\tau r^\alpha x - 2\lambda\pi K_\alpha(\mu, x, r)} dx f_R(r) dr. \quad \square$$

E. Typical max-signal (MS)

Let H_S be the distance to the typical visible head point. It follows from [21, Lemma 5.11] that the distance H_S to the typical visible head follows a Nakagami distribution with parameter $(\frac{1}{2}, \frac{1}{2\lambda\pi})$, i.e., $f_{H_S}(h) = 2\sqrt{\lambda} e^{-\lambda\pi h^2}$.

1) *Theorem 1 (for SINR at a typical MS):* The τ -coverage probability is

$$p_S^c = \mathbb{E}_{H_S}^0 \left[e^{-\mu\tau H_S^\alpha \sigma^2 - \pi\lambda H_S^2 \kappa(\tau, \alpha)} \right]. \quad (50)$$

Proof: To find the τ -coverage probability using (14) we first compute the Laplace transform of the interference I_h given $H_S = h$ as

$$\begin{aligned} \mathbb{E}_{I_h} [e^{-\gamma I_h}] &= \mathbb{E}_{\eta_h, \{\rho_i\}} \left[e^{-\gamma \sum_{i \in \mathbb{N}} \rho_i D_i^{-\alpha}} | \eta_h, \{\rho_i\} \right] \\ &= \mathbb{E}_{\eta_h} \left[\prod_{i \in \mathbb{N}} \mathbb{E}_{\rho_i} [e^{-\gamma \rho_i D_i^{-\alpha}}] | \eta_h \right]. \quad (51) \end{aligned}$$

Applying the PGFl with respect to the point process η_h in (51), we have

$$\begin{aligned}\mathbb{E}_{I_h}[e^{-\gamma I_h}] &= \exp\left(-2\pi\lambda \int_h^\infty \left(1 - \mathbb{E}_\rho[e^{-\gamma\rho r^{-\alpha}}]\right) r dr\right) \\ &= \exp\left(-2\pi\lambda \int_h^\infty \frac{\gamma r^{-\alpha}}{\mu + \gamma r^{-\alpha}} r dr\right) \quad (52) \\ &\stackrel{(\gamma = \mu\tau h^\alpha)}{=} \exp\left(-2\pi\lambda \int_h^\infty \frac{\tau h^\alpha r^{-\alpha}}{1 + \tau h^\alpha r^{-\alpha}} r dr\right) \\ &= e^{-2\pi\lambda \int_h^\infty \frac{\tau h^\alpha}{r^\alpha + \tau h^\alpha} r dr} = e^{-\pi\lambda h^2 \kappa(\tau, \alpha)}, \quad (53)\end{aligned}$$

where κ as in (94). Then using (14), the τ -coverage probability is

$$p_S^c = \int_0^\infty e^{-\mu\tau h^\alpha \sigma^2 - \pi\lambda h^2 \kappa(\tau, \alpha)} f_{H_S}(h) dh.$$

□

Remark 18 Similarly to (44) we also obtain a closed form in the interference limited regime for the case $\alpha = 4$ as

$$p_S^c = \left(1 + \tau^{\frac{1}{2}} \arctan(\tau^{\frac{1}{2}})\right)^{-1/2},$$

using the fact from [21, Lemma 5.11] that $\mathbb{E}\left[e^{-\gamma H_S^2}\right] = \left(1 + \frac{\gamma}{\lambda\pi}\right)^{-\frac{1}{2}}$.

2) *Theorem 1 (for STINR at a typical MS)*: In this case the τ -coverage probability is

$$p_{S;\tau}^c = \mathbb{E}_{H_S}^0 \left[e^{-\mu\tau H_S^\alpha \sigma^2} \mu\tau H_S^\alpha \int e^{-\mu\tau H_S^\alpha x - 2\lambda\pi K_\alpha(\mu, x, H_S)} dx \right].$$

Proof: Given $H_S = h$, the tropical interference is $\mathcal{T}_h = \max_i \rho_i D_i^{-\alpha}$ and its distribution is

$$\begin{aligned}\mathbb{P}(\mathcal{T}_h \leq x) &= \mathbb{E}_{\eta_h, \{\rho_i\}} [\mathbb{P}(\mathcal{T}_h \leq x) | \eta_h, \{\rho_i\}] \\ &= \mathbb{E}_{\eta_h} \left[\mathbb{E}_{\{\rho_i\}} \left(\prod_{i \in \mathbb{N}} \mathbb{1}_{\rho_i D_i^{-\alpha} \leq x} \right) | \eta_h \right] \\ &= \mathbb{E}_{\eta_h} \left[\prod_{i \in \mathbb{N}} \mathbb{E}_{\rho_i} \left[\mathbb{1}_{\rho_i D_i^{-\alpha} \leq x} \right] | \eta_h \right] \\ &= \exp\left(-2\lambda\pi \int_h^\infty \mathbb{P}_\rho(\rho > v^\alpha x) v dv\right) \\ &= \exp\left(-2\lambda\pi \int_h^\infty e^{-\mu v^\alpha x} v dv\right) \\ &= e^{-2\lambda\pi K_\alpha(\mu, x, h)}. \quad (54)\end{aligned}$$

where $K_\alpha(\mu, x, h)$ is defined in (98). Using the distribution of \mathcal{T}_h (54), we obtain the Laplace transform of \mathcal{T}_h as

$$\mathcal{L}_{I_h}(\mu\tau h^\alpha) = \mu\tau h^\alpha \int e^{-\mu\tau h^\alpha x - 2\lambda\pi K_\alpha(\mu, x, h)} dx.$$

We obtain the coverage probability by using (14). □

F. Typical max-interference (MI)

Recall that the distance to the nearest interferer and the serving BS is denoted by H_I and R_I , where $H_I \stackrel{d}{\sim} \text{Na}\left(\frac{3}{2}, \frac{3}{2\lambda\pi}\right)$ from Proposition 3 and, from Proposition 4, $R_I^2 \stackrel{d}{\sim} \text{U}[0, h^2]$, given $H_I = h$.

1) *Theorem 2 (for SINR at a typical MI)*: The coverage probability for user QoS τ is

$$p_I^c = \frac{2\tau^{-2/\alpha}}{\alpha} \int_0^\tau \frac{z^{2/\alpha-1}}{1+z} \mathbb{E}_{H_I}^0 \left[e^{-\mu z H_I^\alpha \sigma^2 - \pi\lambda H_I^2 \kappa(z, \alpha)} \right] dz.$$

Proof: In this case, the total interference is

$$I_{H_I} := \rho H_I^{-\alpha} + \sum_{i \in \mathbb{N}} \rho_i D_i^{-\alpha},$$

where H_I is the distance to the nearest interferer. Given $H_I = h$ and distance to the serving BS $R_I = r$, the Laplace transform of the interference is

$$\begin{aligned}\mathbb{E}_{I_h} [e^{-\gamma I_h}] &= \mathbb{E}_{\eta_h, \rho, \{\rho_i\}} \left[e^{-\gamma(\rho h^{-\alpha} + \sum_{i \in \mathbb{N}} \rho_i D_i^{-\alpha})} | \eta_h, \rho, \{\rho_i\} \right] \\ &= \mathbb{E}_\rho \left[e^{-\gamma \rho h^{-\alpha}} \right] \mathbb{E}_{\eta_h, \{\rho_i\}} \left[\prod_{i \in \mathbb{N}} e^{-\gamma \rho_i D_i^{-\alpha}} | \eta_h, \{\rho_i\} \right]\end{aligned}$$

$$\begin{aligned}&= \frac{\mu}{\mu + \gamma h^{-\alpha}} \mathbb{E}_{\eta_h} \left[\prod_{i \in \mathbb{N}} \mathbb{E}_{\rho_i} \left[e^{-\gamma \rho_i D_i^{-\alpha}} \right] | \eta_h \right] \\ &= \frac{\mu}{\mu + \gamma h^{-\alpha}} e^{-2\pi\lambda \int_h^\infty \frac{\gamma u^{-\alpha}}{\mu + \gamma u^{-\alpha}} u du} \quad (55)\end{aligned}$$

$$\begin{aligned}&\stackrel{\gamma = \mu\tau r^\alpha}{=} \frac{1}{1 + \tau r^\alpha h^{-\alpha}} e^{-2\pi\lambda \int_h^\infty \frac{\tau r^\alpha u^{-\alpha}}{1 + \tau r^\alpha u^{-\alpha}} u du} \\ &= \frac{h^\alpha}{h^\alpha + \tau r^\alpha} e^{-2\pi\lambda \int_h^\infty \frac{\tau r^\alpha}{u^\alpha + \tau r^\alpha} u du}. \quad (56)\end{aligned}$$

Hence the coverage probability is

$$p_I^c = \mathbb{E}_{H_I, R_I}^0 \left[\frac{H_I^\alpha}{H_I^\alpha + \tau R_I^\alpha} e^{-\mu\tau R_I^\alpha \sigma^2 - 2\pi\lambda \int_{H_I}^\infty \frac{\tau R_I^\alpha}{u^\alpha + \tau R_I^\alpha} u du} \right]. \quad (57)$$

Considering the random variable R_I^2 , the integral in the exponent in (56) equals

$$\int_h^\infty \frac{\tau r^{\alpha/2}}{u^\alpha + \tau r^{\alpha/2}} u du = \frac{h^2}{2} \kappa\left(\tau(r/h^2)^{\alpha/2}, \alpha\right), \quad (58)$$

using (97). Hence the coverage probability turns out to be

$$\begin{aligned}p_I^c &= \int_0^\infty \int_0^{h^2} \frac{e^{-\mu\tau r^{\alpha/2} \sigma^2}}{1 + \tau(r/h^2)^{\alpha/2}} e^{-\pi\lambda h^2 \kappa(\tau(r/h^2)^{\alpha/2}, \alpha)} \\ &\quad \times \frac{1}{h^2} dr f_{H_I}(h) dh \\ &\stackrel{\frac{r}{h^2} = w}{=} \int_0^1 \int_0^1 \frac{e^{-\mu\tau h^\alpha w^{\alpha/2} \sigma^2}}{1 + \tau w^{\alpha/2}} e^{-\pi\lambda h^2 \kappa(\tau w^{\alpha/2}, \alpha)} f_{H_I}(h) dh dw \\ &= \int_0^1 \frac{1}{1 + \tau w^{\alpha/2}} \mathbb{E}_{H_I}^0 \left[e^{-\mu\tau w^{\alpha/2} H_I^\alpha \sigma^2 - \pi\lambda H_I^2 \kappa(\tau w^{\alpha/2}, \alpha)} \right] dw \\ &= \frac{2\tau^{-2/\alpha}}{\alpha} \int_0^\tau \frac{z^{2/\alpha-1}}{1+z} \mathbb{E}_{H_I}^0 \left[e^{-\mu z H_I^\alpha \sigma^2 - \pi\lambda H_I^2 \kappa(z, \alpha)} \right] dz, \quad (59)\end{aligned}$$

by taking $\tau w^{\alpha/2} = z$. □

2) *Theorem 2 (for STINR at a typical MI)*: In this case the τ -coverage probability is

$$p_{I;\tau}^c = \mathbb{E}_{H_I, R_I}^0 \left[e^{-\mu\tau R_I^\alpha \sigma^2} \mu\tau R_I^\alpha \int e^{-\mu\tau R_I^\alpha x} \left(1 - e^{-\mu H_I^\alpha x}\right) \times e^{-2\lambda\pi K_\alpha(\mu, x, H_I)} dx \right].$$

Proof: Given the distance to the nearest interferer $H_I = h$, the tropical interference is $\mathcal{T}_h = \rho h^{-\alpha} \vee \max_i \rho_i D_i^{-\alpha}$. The probability distribution of \mathcal{T}_h is

$$\begin{aligned} \mathbb{P}(\mathcal{T}_h \leq x) &= \mathbb{E}_{\eta_h, \rho, \{\rho_i\}} [\mathbb{P}(\mathcal{T}_h \leq x) | \eta_h, \{\rho_i\}] \\ &= \mathbb{E}_{\eta_h} \left[\mathbb{E}_{\rho, \{\rho_i\}} \left(\rho h^{-\alpha} \prod_{i \in \mathbb{N}} \mathbb{1}_{\rho_i D_i^{-\alpha} \leq x} \right) | \eta_h \right] \\ &= \mathbb{P}_\rho(\rho h^{-\alpha} \leq x) \mathbb{E}_{\eta_h} \left[\prod_{i \in \mathbb{N}} \mathbb{E}_{\rho_i} [\mathbb{1}_{\rho_i D_i^{-\alpha} \leq x}] | \eta_h \right] \\ &= (1 - e^{-\mu h^\alpha x}) e^{-2\lambda\pi \int_h^\infty \mathbb{P}_\rho(\rho > v^\alpha x) v dv} \\ &= (1 - e^{-\mu h^\alpha x}) e^{-2\lambda\pi \int_h^\infty e^{-\mu v^\alpha x} v dv} \\ &= (1 - e^{-\mu h^\alpha x}) e^{-2\lambda\pi K_\alpha(\mu, x, h)}, \end{aligned} \quad (60)$$

where K_α is as defined in (98). We compute the Laplace transform $\mathcal{L}_{\mathcal{T}_h}(\gamma)$, for $\gamma = \mu\tau r^\alpha$ given $R_I = r$, similarly to (46) as

$$\mathbb{E}[e^{-\gamma \mathcal{T}_h}] = \mu\tau r^\alpha \int e^{-\mu\tau r^\alpha x} (1 - e^{-\mu h^\alpha x}) e^{-2\lambda\pi K_\alpha(\mu, x, h)} dx. \quad (61)$$

We obtain the coverage probability using the Laplace transform (61) in the formula (15) as

$$\begin{aligned} p_{I, \tau}^c &= \mathbb{E}_{H_I, R_I}^0 \left[e^{-\mu\tau R_I^\alpha \sigma^2} \mu\tau R_I^\alpha \int e^{-\mu\tau R_I^\alpha x} (1 - e^{-\mu H_I^\alpha x}) \right. \\ &\quad \left. \times e^{-2\lambda\pi K_\alpha(\mu, x, H_I)} dx \right] \\ &= \int_0^1 \mathbb{E}_{H_I} \left[e^{-\mu\tau H_I^\alpha w^{\alpha/2} \sigma^2} \mu\tau H_I^\alpha w^{\alpha/2} \int e^{-\mu\tau H_I^\alpha w^{\alpha/2} x} \right. \\ &\quad \left. \times (1 - e^{-\mu H_I^\alpha x}) e^{-2\lambda\pi K_\alpha(\mu, x, H_I)} dx \right] dw, \end{aligned}$$

by taking R_I^2/h^2 as a uniform random variable on $[0, 1]$, given $H_I = h$. \square

G. Typical min-interference (mI): typical tropical interference handover

Recall that the distance to the nearest interferer and the serving BS is denoted by H_x and R_x , where $H_x \stackrel{d}{\sim} \text{Na}(\frac{3}{2}, \frac{3}{2\lambda\pi})$ from Proposition 5 and, from Proposition 6, $R_x^2 \stackrel{d}{\sim} \text{U}[0, h^2]$, given $H_x = h$.

1) *Theorem 2 (for SINR at a typical mI):* In this case, the τ -coverage probability is

$$p_x^c = \frac{2\tau^{-2/\alpha}}{\alpha} \int_0^\tau \frac{z^{2/\alpha-1}}{(1+z)^2} \mathbb{E}_{H_x}^0 \left[e^{-\mu z H_x^\alpha \sigma^2 - \pi\lambda H_x^2 \kappa(z, \alpha)} \right] dz.$$

Proof: Suppose the distance to the typical handover is H_x . Given $H_x = h$, let R_x be the distance to serving station. In this case the total interference is

$$I_h := (\rho^+ + \rho^-) h^{-\alpha} + \sum_{i \in \mathbb{N}} \rho_i D_i^{-\alpha}.$$

Given $H_x = h$ and $R_x = r$, the Laplace transform of the interference is

$$\begin{aligned} \mathbb{E}[e^{-\gamma I_h}] &= \left(\frac{\mu}{\mu + \gamma h^{-\alpha}} \right)^2 e^{-2\pi\lambda \int_h^\infty \frac{\gamma v^{-\alpha}}{\mu + \gamma v^{-\alpha}} v dv} \\ &= \left(\frac{h^\alpha}{h^\alpha + \tau r^\alpha} \right)^2 e^{-2\pi\lambda \int_h^\infty \frac{\tau r^\alpha}{v^\alpha + \tau r^\alpha} v dv}, \end{aligned} \quad (62)$$

by substituting $\gamma = \mu\tau r^\alpha$. Using the formula (15), the coverage probability is

$$p_x^c = \mathbb{E}_{H_x, R_x}^0 \left[\left(\frac{H_x^\alpha}{H_x^\alpha + \tau R_x^\alpha} \right)^2 e^{-\mu\tau R_x^\alpha \sigma^2 - 2\pi\lambda \int_{H_x}^\infty \frac{\tau R_x^\alpha}{v^\alpha + \tau R_x^\alpha} v dv} \right]. \quad (63)$$

By considering the random variable R_x^2 and performing an analysis similarly to (59), we have

$$\begin{aligned} p_x^c &= \int_0^1 \frac{1}{(1+\tau w^{\alpha/2})^2} \mathbb{E}_{H_x}^0 \left[e^{-\mu\tau w^{\alpha/2} H_x^\alpha \sigma^2 - \pi\lambda H_x^2 \kappa(\tau w^{\alpha/2}, \alpha)} \right] dw \\ &= \frac{2\tau^{-2/\alpha}}{\alpha} \int_0^\tau \frac{z^{2/\alpha-1}}{(1+z)^2} \mathbb{E}_{H_x}^0 \left[e^{-\mu z H_x^\alpha \sigma^2 - \pi\lambda H_x^2 \kappa(z, \alpha)} \right] dz, \end{aligned}$$

where $\tau w^{\alpha/2} = z$ and $\kappa(z, \alpha)$ is defined in using (97). \square

2) *Theorem 2 (for STINR at a typical mI):* The τ -coverage probability is

$$\begin{aligned} p_{x, \tau}^c &= \mathbb{E}_{H_x, R_x}^0 \left[e^{-\mu\tau R_x^\alpha \sigma^2} \mu\tau R_x^\alpha \int e^{-\mu\tau R_x^\alpha x} (1 - e^{-\mu H_x^\alpha x})^2 \right. \\ &\quad \left. \times e^{-2\lambda\pi K_\alpha(\mu, x, H_x)} dx \right]. \end{aligned}$$

Proof: Given $H_x = h$, let R_x be the distance to serving station. In this case the tropical interference is

$$\mathcal{T}_h := \rho^+ h^{-\alpha} \vee \rho^- h^{-\alpha} \vee \max_{i \in \mathbb{N}} \rho_i D_i^{-\alpha}.$$

We compute the distribution of \mathcal{T}_h , given $H_x = h$ similarly to (60), as

$$\mathbb{P}(\mathcal{T}_h \leq x) = (1 - e^{-\mu h^\alpha x})^2 e^{-2\lambda\pi K_\alpha(\mu, x, h)}.$$

Hence, similarly to (61), the Laplace transform of \mathcal{T}_h is

$$\mathbb{E}[e^{-\gamma \mathcal{T}_h}] = \mu\tau r^\alpha \int e^{-\mu\tau r^\alpha x} (1 - e^{-\mu h^\alpha x})^2 e^{-2\lambda\pi K_\alpha(\mu, x, h)} dx.$$

We obtain the coverage probability using the Laplace transform of the interference \mathcal{T}_h in the formula (15), with $\gamma = \mu\tau r^\alpha$, given $(H_x, R_x) = (h, r)$, as

$$\begin{aligned} p_{x, \tau}^c &= \mathbb{E}_{H_x, R_x}^0 \left[e^{-\mu\tau R_x^\alpha \sigma^2} \mu\tau R_x^\alpha \int e^{-\mu\tau R_x^\alpha x} (1 - e^{-\mu H_x^\alpha x})^2 \right. \\ &\quad \left. \times e^{-2\lambda\pi K_\alpha(\mu, x, H_x)} dx \right]. \end{aligned} \quad \square$$

APPENDIX III PROOFS: CASE WITHOUT FADING

As an opening remark for this section, we use the same set of notations for the distance variables, coverage probabilities and data rates, as in the case with fading. Recall from Lemma 5 that at any of the typical epochs of interest, the point process η_h of the distance of all other BS is Poisson on (h, ∞) with intensity measure $\hat{\mu}$ with density $d\hat{\mu} := 2\pi\lambda r dr$, given $H = h$, for $H \in \{H_v, H_s, R_t, R_x, R\}$.

A. Proof of Theorem 3

The coverage probability is given by

$$p^c(\tau, \lambda, \alpha) = \mathbb{E}_H^0[\mathbb{P}(\mathcal{S} > \tau|H)], \quad (64)$$

where, given $H = h$, the inner term in (64) is

$$\begin{aligned} \mathbb{P}(\mathcal{S} > \tau|H = h) &= \mathbb{E}_{I_h}[\mathbb{P}(\mathcal{S} > \tau|I_h)] \\ &= \mathbb{P}_{I_h}(\tau(\sigma^2 + I_h) < h^{-\alpha}) \\ &= \mathbb{P}_{I_h}(I_h < h^{-\alpha}/\tau - \sigma^2) \\ &= F_{I_h}(0 \vee (h^{-\alpha}/\tau - \sigma^2)). \end{aligned}$$

Then the baseline formula for the coverage probability is

$$p^c(\tau, \lambda, \alpha) = \mathbb{E}_H^0[F_{I_H}(0 \vee (H^{-\alpha}/\tau - \sigma^2))]. \quad \square$$

B. Proof of Theorem 5

The proof follows the same steps as those in Theorem 3 by considering the distance R to the serving BS and the distance H to the nearest interferer as well. Given $H = h$ and $R = r$, the coverage probability is

$$\begin{aligned} \mathbb{P}(\mathcal{S} > \tau|H = h, R = r) &= \mathbb{E}_{I_h}[\mathbb{P}(\mathcal{S} > \tau|h, I_h)] \\ &= \mathbb{P}_{I_h}(\tau(\sigma^2 + I_h) < r^{-\alpha}) \\ &= \mathbb{P}_{I_h}(I_h < r^{-\alpha}/\tau - \sigma^2) \\ &= F_{I_h}(0 \vee (r^{-\alpha}/\tau - \sigma^2)). \end{aligned} \quad (65)$$

By jointly averaging over the distances R and H , from (65), we have

$$p^c(\tau, \lambda, \alpha) = \mathbb{E}_{H,R}^0[F_{I_H}(0 \vee (R^{-\alpha}/\tau - \sigma^2))]. \quad \square$$

C. Proof of Theorem 4

The result can be proved similarly to the last one. \square

Remark 19 In the SNR regime, the coverage probability turns out to be

$$p^c(\tau, \lambda, \alpha) = \mathbb{P}^0\left(H \leq (\tau\sigma^2)^{-1/\alpha}\right),$$

for $H = H_v, H_s, R_I, R_x, R$, under their respective Palm probability measures \mathbb{P}^0 .

For simplicity we write $p_*^c \equiv p_*^c(\tau, \lambda, \alpha)$, $p_{*;\tau}^c \equiv p_{*;\tau}^c(\tau, \lambda, \alpha)$ and $\mathcal{R}_* \equiv \mathcal{R}_*(\lambda, \alpha)$, $\mathcal{R}_{*;\tau} \equiv \mathcal{R}_{*;\tau}(\lambda, \alpha)$, which are understood to a function of the set of parameters $\{\tau, \lambda, \alpha\}$ and $\{\lambda, \alpha\}$, respectively, where $*$ $\in \{v, s, I, x, t\}$.

Remark 20 In all our proofs, we just derive the expression for $p_*^c(\tau, \lambda, \alpha)$ and $p_{*;\tau}^c(\tau, \lambda, \alpha)$. The average data rate can be derived using the general formula in (13) for both $\mathcal{R}_*(\lambda, \alpha)$ and $\mathcal{R}_{*;\tau}(\lambda, \alpha)$, where $*$ $\in \{v, s, I, x, t\}$.

Remark 21 Suppose the contribution of the total interference created by the BSs beyond distance h , for some $h \geq 0$, is $I'_h := \sum_{i \in \mathbb{N}} D_i^{-\alpha}$. The distribution of I'_h is the same at all

typical epochs. Indeed, the Laplace transform of which is given by

$$\mathbb{E}\left[e^{-\nu I'_h}\right] = \mathbb{E}_{\eta_h}\left[\prod_{i \in \mathbb{N}} e^{-\nu D_i^{-\alpha}} | \eta_h\right] = e^{-2\pi\lambda \int_h^\infty (1 - e^{-\nu r^{-\alpha}}) r dr}. \quad (66)$$

Using the integral inside the exponent as in (99) we have

$$\mathcal{L}_{I'_h}(\nu) = e^{-\pi\lambda L_\nu(h, \alpha)}, \quad (67)$$

where $L_\nu(h, \alpha) := -h^2(1 - e^{-\nu h^{-\alpha}}) + \nu^{2/\alpha}\gamma(1 - \frac{2}{\alpha}, \nu h^{-\alpha})$.

Remark 22 Note from (99) that for $\alpha = 2$ and 4 we have

$$L_\nu(h, 2) = -h^2(1 - e^{-\nu h^{-2}}) + \nu\gamma(0, \nu h^{-2}),$$

$$L_\nu(h, 4) = -h^2(1 - e^{-\nu h^{-4}}) + \nu^{1/2}\gamma(1/2, \nu h^{-4}),$$

in terms of the incomplete gamma function defined as $\gamma(a, b) := \int_0^b z^{a-1} e^{-z} dz$.

D. Min-signal-max-interference (mS-MI): typical handover

The typical handover distance H_v is given by a Nakagami distribution with parameter $(\frac{3}{2}, \frac{3}{2\lambda\pi})$ and with density (8).

1) *Theorem 3 (for SINR at typical mS-MI)*: In this case the interference is $I_h := h^{-\alpha} + \sum_i D_i^{-\alpha}$, given $H_v = h$. Suppose F_{I_h} is the distribution of the interference I_h . By applying the formula (17) the coverage probability is

$$p_v^c = \mathbb{E}_{H_v}^0[F_{I_{H_v}}(0 \vee (H_v^{-\alpha}/\tau - \sigma^2))], \quad (68)$$

where the distribution of $I_h = h^{-\alpha} + I'_h$, given $H_v = h$, can be found using the Laplace transform

$$\mathcal{L}_{I_h}(\nu) = e^{-\nu h^{-\alpha}} \mathcal{L}_{I'_h}(\nu) \stackrel{(67)}{=} e^{-\nu h^{-\alpha} - \pi\lambda L_\nu(h, \alpha)}. \quad (69)$$

2) *Theorem 3 (for STINR at typical mS-MI)*: Given a handover at a distance $H_v = h$, the tropical interference in this case is given by the other BS at a distance h , i.e., $\mathcal{T}_h = h^{-\alpha}$. The coverage probability is

$$\begin{aligned} p_{v;\tau}^c &= \int_0^\infty \mathbb{1}_{h^{-\alpha} > \tau(\sigma^2 + h^{-\alpha})} f_{H_v}(h) dh \\ &= \int_0^\infty \mathbb{1}_{h < (\frac{1-\tau}{\tau\sigma^2})^{\frac{1}{\alpha}}} f_{H_v}(h) dh = F_{H_v}\left(\left(\frac{1-\tau}{\tau\sigma^2}\right)^{\frac{1}{\alpha}}\right). \end{aligned} \quad (70)$$

which is computed using the density of H_v from (8).

E. Typical time

The distance to the nearest BS follows a Rayleigh density

$$f_R(r) := 2\lambda\pi r e^{-\lambda\pi r^2}.$$

1) *Theorem 3 (for SINR at typical time)*: In this case the distance R to the nearest point is Rayleigh distributed and the interference is

$$I_r := \sum_i D_i^{-\alpha},$$

given $R = r$. The coverage probability is given by the formula (17) as

$$p_t^c = \int_0^\infty F_{I_r} \left(\left(\frac{r^{-\alpha}}{\tau} - \sigma^2 \right) \vee 0 \right) f_R(r) dr. \quad (71)$$

where F_{I_r} is the distribution of I_r when $R = r$, is given by the Laplace transform as in (67)

$$\mathcal{L}_{I_r}(\nu) = e^{-\pi\lambda L_\nu(r, \alpha)}.$$

2) *Theorem 4 (for STINR at typical time)*: In the tropical case the interference is given by the second closest station. Let R_1 be the distance to the second closest station. In this case the tropical interference is given by $\mathcal{T} = R_1^{-\alpha}$. From (18) the coverage probability turns out to be

$$\begin{aligned} p_{t;\tau}^c &= \int_0^\infty F_{\mathcal{T}} \left((r^{-\alpha}/\tau - \sigma^2) \vee 0 \right) f_R(r) dr \\ &= \int_0^\infty \mathbb{P}_{R_1|r} \left(R_1 > \left((r^{-\alpha}/\tau - \sigma^2) \vee 0 \right)^{-\frac{1}{\alpha}} \vee r \right) f_R(r) dr \\ &= \int_0^{(\tau\sigma^2)^{-1/\alpha}} \mathbb{P}_{R_1|r} \left(R_1 > (r^{-\alpha}/\tau - \sigma^2)^{-1/\alpha} \vee r \right) f_R(r) dr \\ &= \int_0^{(\tau\sigma^2)^{-1/\alpha}} \int_{(h^{-\alpha}/\tau - \sigma^2)^{-1/\alpha} \vee h} f_{R_1|h}(r) dr f_R(h) dh. \end{aligned} \quad (72)$$

Note that $h^{-\alpha}/\tau - \sigma^2 < h^{-\alpha}$ for all $\tau \geq 1$ and under this case we have

$$p_{t;\tau}^c = \int_0^{(\tau\sigma^2)^{-1/\alpha}} \int_{(h^{-\alpha}/\tau - \sigma^2)^{-1/\alpha}} f_{R_1|h}(r) dr f_R(h) dh.$$

For $\tau < 1$, $h^{-\alpha}/\tau - \sigma^2 \geq h^{-\alpha}$ if and only if $h \leq \left(\frac{\sigma^2\tau}{1-\tau} \right)^{-1/\alpha}$ and hence

$$\begin{aligned} p_{t;\tau}^c &= \int_0^{\left(\frac{\sigma^2\tau}{1-\tau} \right)^{-1/\alpha}} \int_h^\infty f_{R_1|h}(r) dr f_R(h) dh \\ &\quad + \int_{\left(\frac{\sigma^2\tau}{1-\tau} \right)^{-1/\alpha}}^{(\tau\sigma^2)^{-1/\alpha}} \int_{(h^{-\alpha}/\tau - \sigma^2)^{-1/\alpha}}^\infty f_{R_1|h}(r) dr f_R(h) dh \\ &= \mathbb{P} \left(R \leq (1-\tau)^{1/\alpha} (\sigma^2\tau)^{-1/\alpha} \right) \\ &\quad + \int_{\left(\frac{\sigma^2\tau}{1-\tau} \right)^{-1/\alpha}}^{(\tau\sigma^2)^{-1/\alpha}} \int_{(h^{-\alpha}/\tau - \sigma^2)^{-1/\alpha}}^\infty f_{R_1|h}(r) dr f_R(h) dh, \end{aligned}$$

since $\left(\frac{\sigma^2\tau}{1-\tau} \right)^{-1/\alpha} \leq (\sigma^2\tau)^{-1/\alpha}$ for $\tau < 1$.

F. Typical max-signal (MS)

Let H_S be the distance to the typical visible head point. It follows from [21, Lemma 5.11] that the distance H_S to the typical visible head follows a Nakagami distribution with parameter $\left(\frac{1}{2}, \frac{1}{2\lambda\pi} \right)$, i.e.,

$$f_{H_S}(h) = 2\lambda^{\frac{1}{2}} e^{-\lambda\pi h^2}.$$

1) *Theorem 3 (for SINR at typical MS)*: Given the distance to the serving BS $H_S = h$, the total interference is $I_h = \sum_i D_i^{-\alpha}$, and suppose its distribution is F_{I_h} given by the Laplace transform

$$\mathcal{L}_{I_h}(\nu) = e^{-\pi\lambda L_\nu(h, \alpha)}.$$

We determine the coverage probability using (17) as

$$p_s^c = \int_0^\infty F_{I_h} \left(0 \vee \left(\frac{h^{-\alpha}}{\tau} - \sigma^2 \right) \right) f_{H_S}(h) dh. \quad (74)$$

2) *Theorem 4 (for STINR at typical MS)*: The tropical interference is given by the second closest station, distance of which is R_S . Given $H_S = h$, we have $\mathcal{T}_h = R_S^{-\alpha}$, where $R_S \geq h$ is the distance to the nearest interferer. The distribution of interference is

$$\mathbb{P}(\mathcal{T}_h \leq x) = \mathbb{P}(R_S^{-\alpha} \leq x) = \mathbb{P}(R_S > x^{-1/\alpha}).$$

From (18) the coverage probability $p_{s;\tau}^c$ turns out to be

$$\begin{aligned} &\mathbb{P} \left(R_S > \left((H_S^{-\alpha}/\tau - \sigma^2) \vee 0 \right)^{-1/\alpha} \vee H_S \right) \\ &= \int_0^\infty \mathbb{P}_{R_S|h} \left(R_S > \left((h^{-\alpha}/\tau - \sigma^2) \vee 0 \right)^{-1/\alpha} \vee h \right) f_{H_S}(h) dh \\ &= \int_0^{(\tau\sigma^2)^{-1/\alpha}} \mathbb{P}_{R_S|h} \left(R_S > (h^{-\alpha}/\tau - \sigma^2)^{-1/\alpha} \vee h \right) f_{H_S}(h) dh \\ &= \int_0^{(\tau\sigma^2)^{-1/\alpha}} \int_{(h^{-\alpha}/\tau - \sigma^2)^{-1/\alpha} \vee h} f_{R_S|h}(r) dr f_{H_S}(h) dh. \end{aligned} \quad (75)$$

Note that $h^{-\alpha}/\tau - \sigma^2 < h^{-\alpha}$ for all $\tau \geq 1$ and in this case, we have

$$p_{s;\tau}^c = \int_0^{(\tau\sigma^2)^{-1/\alpha}} \int_{(h^{-\alpha}/\tau - \sigma^2)^{-1/\alpha}}^\infty f_{R_S|h}(r) dr f_{H_S}(h) dh.$$

For $\tau < 1$, $h^{-\alpha}/\tau - \sigma^2 \geq h^{-\alpha}$ if $h \leq \left(\frac{\sigma^2\tau}{1-\tau} \right)^{-1/\alpha}$ and hence

$$\begin{aligned} p_{s;\tau}^c &= \int_0^{\left(\frac{\sigma^2\tau}{1-\tau} \right)^{-1/\alpha}} \int_h^\infty f_{R_S|h}(r) dr f_{H_S}(h) dh \\ &\quad + \int_{\left(\frac{\sigma^2\tau}{1-\tau} \right)^{-1/\alpha}}^{(\tau\sigma^2)^{-1/\alpha}} \int_{(h^{-\alpha}/\tau - \sigma^2)^{-1/\alpha}}^\infty f_{R_S|h}(r) dr f_{H_S}(h) dh \\ &= \mathbb{P} \left(H_S \leq (1-\tau)^{1/\alpha} (\sigma^2\tau)^{-1/\alpha} \right) \\ &\quad + \int_{\left(\frac{\sigma^2\tau}{1-\tau} \right)^{-1/\alpha}}^{(\tau\sigma^2)^{-1/\alpha}} \int_{(h^{-\alpha}/\tau - \sigma^2)^{-1/\alpha}}^\infty f_{R_S|h}(r) dr f_{H_S}(h) dh, \end{aligned}$$

since $\left(\frac{\sigma^2\tau}{1-\tau} \right)^{-1/\alpha} \leq (\sigma^2\tau)^{-1/\alpha}$ for $\tau < 1$.

G. Typical max-interference (MI)

Suppose the nearest BS and the nearest interferer are at distance R_t and H_I , respectively.

1) *Theorem 5 (for SINR at typical MI)*: In this case given H_I , the distance to the closest interferer at its nearest position, the total interference is

$$I_{H_I} := H_I^{-\alpha} + \sum_{i \in \mathbb{N}} D_i^{-\alpha},$$

and given $R_I = r$, we have $D_i \geq H_I \geq r$, for all $D_i \in \eta_h$. Given the typical invisible head at distance $H_I = h$ the Laplace transform of I_h is

$$\mathcal{L}_{I_h}(\nu) \stackrel{(67)}{=} e^{-\nu h^{-\alpha} - \pi \lambda L_\nu(h, \alpha)}. \quad (76)$$

Let F_{I_h} be the distribution of the interference I_h . Using that and the formula (19) we find the coverage probability as

$$p_I^c = \mathbb{E}_{H_I, R_I}^0 \left[F_{I_{H_I}} \left(\left(\frac{R_I^{-\alpha}}{\tau} - \sigma^2 \right) \vee 0 \right) \right]. \quad (77)$$

2) *Theorem 5 (for STINR at typical MI)*: In this case, we can only consider the case where $\tau \geq 1$. The tropical interference is given by the distance to the second closest BS H_I , $\mathcal{T} = H_I^{-\alpha}$. The distribution of interference is

$$F_{\mathcal{T}}(x) = \mathbb{P}(H_I^{-\alpha} \leq x) = \mathbb{P}(H_I \geq x^{-1/\alpha}).$$

From formula (19), we have

$$\begin{aligned} p_{I, \tau}^c &= \mathbb{E}_{H_I, R_I}^0 \left[F_{\mathcal{T}} \left(\left(\frac{R_I^{-\alpha}}{\tau} - \sigma^2 \right) \vee 0 \right) \right] \\ &= \mathbb{P}^0 \left(H_I \geq \left(\left(\frac{R_I^{-\alpha}}{\tau} - \sigma^2 \right) \vee 0 \right)^{-1/\alpha} \right) \\ &= \mathbb{P}^0 \left(H_I \geq \left(\left(\frac{R_I^{-\alpha}}{\tau} - \sigma^2 \right) \vee 0 \right)^{-1/\alpha}; R_I^{-\alpha} \leq \sigma^2 \tau \right) \\ &\quad + \mathbb{P}^0 \left(H_I \geq \left(\left(\frac{R_I^{-\alpha}}{\tau} - \sigma^2 \right) \vee 0 \right)^{-1/\alpha}; R_I^{-\alpha} \geq \sigma^2 \tau \right) \\ &= \mathbb{P}^0(H_I = \infty; R_I^{-\alpha} \leq \sigma^2 \tau) \\ &\quad + \mathbb{P}^0(R_I \leq (\tau(H_I^{-\alpha} + \sigma^2))^{-1/\alpha}; R_I^{-\alpha} \geq \sigma^2 \tau) \\ &= \mathbb{P}^0(R_I \leq (\tau(H_I^{-\alpha} + \sigma^2))^{-1/\alpha}). \end{aligned} \quad (78)$$

Note that

$$\begin{aligned} &\mathbb{P}^0(R_I \leq (\tau(H_I^{-\alpha} + \sigma^2))^{-1/\alpha}) \\ &= \tau^{-2/\alpha} \mathbb{E}_{H_I}^0 \left[H_I^{-2} (H_I^{-\alpha} + \sigma^2)^{-2/\alpha} \right] \\ &= \tau^{-2/\alpha} \mathbb{E}_{H_I}^0 \left[(1 + \sigma^2 H_I^\alpha)^{-2/\alpha} \right]. \end{aligned} \quad (79)$$

H. Typical min-interference (mI): tropical interference handover

Suppose the nearest BS and nearest interferer are at distance R_x and H_x .

1) *Theorem 5 (for SINR at typical mI)*: In this case, given H_x , the total interference is

$$I_{H_x} := 2H_x^{-\alpha} + \sum_{i \in \mathbb{N}} D_i^{-\alpha}.$$

Then using (19), the coverage probability is given by

$$p_x^c = \mathbb{E}_{H_x, R_x}^0 \left[F_I \left(\frac{R_x^{-\alpha}}{\tau} - \sigma^2 \right) \right], \quad (80)$$

where the distribution of the interference I_h given $H_x = h$, is computed similarly to (76) using the Laplace transform as

$$\mathcal{L}_{I_h}(\nu) \stackrel{(67)}{=} e^{-2\nu h^{-\alpha} - \pi \lambda L_\nu(h, \alpha)}.$$

2) *Theorem 5 (for STINR at typical mI)*: This is only under the case where $\tau \geq 1$. In this case, the tropical interference is $\mathcal{T} := 2H_x^{-\alpha}$. The distribution of the interference is

$$F_{\mathcal{T}}(x) = \mathbb{P}(2H_x^{-\alpha} \leq x) = \mathbb{P}(H_x \geq (x/2)^{-1/\alpha}).$$

The coverage probability is computed similarly to (78) and (79) and using formula (19) as

$$\begin{aligned} p_{x, \tau}^c &= \mathbb{E}_{H_x, R_x}^0 \left[F_{\mathcal{T}} \left(\left(\frac{R_x^{-\alpha}}{\tau} - \sigma^2 \right) \vee 0 \right) \right] \\ &= \mathbb{P}^0 \left(H_x \geq 2^{\frac{1}{\alpha}} \left(\left(\frac{R_x^{-\alpha}}{\tau} - \sigma^2 \right) \vee 0 \right)^{-\frac{1}{\alpha}} \right) \\ &= \mathbb{P}^0 \left(R_x \leq (\tau(2H_x^{-\alpha} + \sigma^2))^{-1/\alpha} \right) \\ &= \tau^{-2/\alpha} \mathbb{E}_{H_x}^0 \left[H_x^{-2} (2H_x^{-\alpha} + \sigma^2)^{-2/\alpha} \right] \\ &= \tau^{-2/\alpha} \mathbb{E}_{H_x}^0 \left[(2 + \sigma^2 H_x^\alpha)^{-2/\alpha} \right]. \end{aligned}$$

APPENDIX IV

PROOFS: COMPARISON OF PERFORMANCE METRICS

A. Theorem 6 (with fading)

Part 1. All these inequalities can be obtained by comparing the coverage probabilities

$$p_v^c = \frac{1}{1 + \tau} \int_0^\infty e^{-\mu \tau h^\alpha \sigma^2 - \pi \lambda h^2 \kappa(\tau, \alpha)} f_{H_v}(h) dh,$$

$$p_t^c = \int_0^\infty e^{-\mu \tau r^\alpha \sigma^2 - \pi \lambda r^2 \kappa(\tau, \alpha)} f_R(r) dr,$$

$$p_s^c = \int_0^\infty e^{-\mu \tau h^\alpha \sigma^2 - \pi \lambda h^2 \kappa(\tau, \alpha)} f_{H_s}(h) dh,$$

and comparing the densities of H_v, R, H_s . Note that the integrand in all the integrals are same and we define

$$G(h) := e^{-\mu \tau h^\alpha \sigma^2 - \pi \lambda h^2 \kappa(\tau, \alpha)}, \quad (81)$$

writing it in same variable h . Recall the probability densities of the random variables H_v, R and H_s , $f_{H_v}(h) = 4\pi \lambda^{3/2} h^2 e^{-\lambda \pi h^2}$, $f_R(h) = 2\lambda \pi h e^{-\lambda \pi h^2}$ and $f_{H_s}(h) = 2\lambda^{1/2} e^{-\lambda \pi h^2}$, for $h \geq 0$, respectively. Observe that $f_{H_v}(h) \leq$

$f_R(h)$ on $[0, 1/2\sqrt{\lambda}]$ and $f_{H_V}(h) > f_R(h)$ on $(1/2\sqrt{\lambda}, \infty)$. Hence

$$\begin{aligned} p_t^c - (1+\tau)p_v^c &= \int_0^{1/2\sqrt{\lambda}} G(h) [f_R(h) - f_{H_V}(h)] dh \\ &\quad - \int_{1/2\sqrt{\lambda}}^{\infty} G(h) [f_{H_V}(h) - f_R(h)] dh \\ &\geq G(1/2\sqrt{\lambda}) \int_0^{\infty} [f_{H_V}(h) - f_R(h)] dh = 0, \end{aligned}$$

which implies that $p_t^c \geq (1+\tau)p_v^c \geq p_v^c$, since $G(1/2\sqrt{\lambda}) \geq 0$ and $\tau \geq 0$.

For the other inequality, note that $f_R(h) \leq f_{H_S}(h)$ on $[0, 1/\pi\sqrt{\lambda}]$ and $f_R(h) > f_{H_S}(h)$ on $(1/\pi\sqrt{\lambda}, \infty)$. Then by similar comparison we have that $p_s^c \geq p_t^c$.

For the second part, we compare the coverage probabilities

$$p_I^c = \mathbb{E}_{H_I, R_I}^0 \left[\frac{H_I^\alpha}{H_I^\alpha + \tau R_I^\alpha} e^{-\mu\tau R_I^\alpha \sigma^2 - 2\pi\lambda \int_{H_I}^{\infty} \frac{\tau R_I^\alpha}{r^\alpha + \tau R_I^\alpha} r dr} \right],$$

$$p_{\mathcal{I}}^c = \mathbb{E}_{H_{\mathcal{I}}, R_{\mathcal{I}}}^0 \left[\left(\frac{H_{\mathcal{I}}^\alpha}{H_{\mathcal{I}}^\alpha + \tau R_{\mathcal{I}}^\alpha} \right)^2 e^{-\mu\tau R_{\mathcal{I}}^\alpha \sigma^2 - 2\pi\lambda \int_{H_{\mathcal{I}}}^{\infty} \frac{\tau R_{\mathcal{I}}^\alpha}{v^\alpha + \tau R_{\mathcal{I}}^\alpha} v dv} \right].$$

The densities of H_I and $H_{\mathcal{I}}$ are

$$f_{H_I}(h) = 4\pi\lambda^{3/2} h^2 e^{-\lambda\pi h^2}, \quad f_{H_{\mathcal{I}}}(h) = \frac{8}{3}\pi^2 \lambda^{5/2} h^4 e^{-\lambda\pi h^2},$$

respectively for all $h \geq 0$. Note that $f_{H_{\mathcal{I}}}(h) \leq f_{H_I}(h)$ on $[0, \sqrt{3/2\lambda\pi}]$ and $f_{H_{\mathcal{I}}}(h) > f_{H_I}(h)$ on $(\sqrt{3/2\lambda\pi}, \infty)$. Define

$$G_1(h, r) := \frac{h^\alpha}{h^\alpha + \tau r^\alpha} e^{-\mu\tau r^\alpha \sigma^2 - 2\pi\lambda \int_h^{\infty} \frac{\tau r^\alpha}{v^\alpha + \tau r^\alpha} v dv},$$

$$G_2(h, r) := \left(\frac{h^\alpha}{h^\alpha + \tau r^\alpha} \right)^2 e^{-\mu\tau r^\alpha \sigma^2 - 2\pi\lambda \int_h^{\infty} \frac{\tau r^\alpha}{v^\alpha + \tau r^\alpha} v dv}.$$

Observe that $G_2(h, r) \leq G_1(h, r)$ for all pair (h, r) , because of the extra factor of the form $\frac{h^\alpha}{h^\alpha + \tau r^\alpha} \leq 1$, in $G_2(h, r)$, for all $h, r, \tau \in \mathbb{R}^+$. Let us define

$$G_1(h) := \mathbb{E}_{R_I|h}[G_1(h, R_I|h)], \quad G_2(h) := \mathbb{E}_{R_{\mathcal{I}}|h}[G_2(h, R_{\mathcal{I}}|h)], \quad (82)$$

where $G_2(h) \leq G_1(h)$ for all $h \geq 0$. Then

$$\begin{aligned} p_I^c - p_{\mathcal{I}}^c &= \int_0^{\infty} \int_0^h G_1(h, r) f_{R_I|h}(r) dr f_{H_I}(h) dh \\ &\quad - \int_0^{\infty} \int_0^h G_2(h, r) f_{R_{\mathcal{I}}|h}(r) dr f_{H_{\mathcal{I}}}(h) dh \\ &= \int_0^{\infty} \mathbb{E}_{R_I|h}[G_1(h, R_I|h)] f_{H_I}(h) dh \\ &\quad - \int_0^{\infty} \mathbb{E}_{R_{\mathcal{I}}|h}[G_2(h, R_{\mathcal{I}}|h)] f_{H_{\mathcal{I}}}(h) dh \\ &\stackrel{(82)}{=} \int_0^{\infty} G_1(h) f_{H_I}(h) dh - \int_0^{\infty} G_2(h) f_{H_{\mathcal{I}}}(h) dh \\ &\geq \int_0^{\infty} G_2(h) f_{H_I}(h) dh - \int_0^{\infty} G_2(h) f_{H_{\mathcal{I}}}(h) dh \\ &= \int_0^{\sqrt{3/2\lambda\pi}} G_2(h) [f_{H_I}(h) - f_{H_{\mathcal{I}}}(h)] dh \\ &\quad - \int_{\sqrt{3/2\lambda\pi}}^{\infty} G_2(h) [f_{H_{\mathcal{I}}}(h) - f_{H_I}(h)] dh \\ &\geq G_2(\sqrt{3/2\lambda\pi}) \int_0^{\infty} [f_{H_I}(h) - f_{H_{\mathcal{I}}}(h)] dh = 0, \end{aligned}$$

since $G_2(\sqrt{3/2\lambda\pi}) \geq 0$. This proves the result for the non-tropical case. \square

Part 2. The results in the tropical case

$$p_{v;\tau}^c \leq p_{t;\tau}^c \leq p_{s;\tau}^c \quad \text{and} \quad p_{\mathcal{I};\tau}^c \leq p_{I;\tau}^c$$

can be proved similarly. \square

B. Theorem 6 (without fading)

Part 1. The proof essentially follows by comparing the the random variables H_V , R and H_S . Note that $F_{I_{H_V}}(x) \leq F_{I_R}(x) = F_{I_S}(x)$ for any $x \geq 0$, since

$$I_{H_V=h} = h^{-\alpha} + \sum_i D_i^{-\alpha}, \quad I_{R=h} = \sum_i D_i^{-\alpha} \stackrel{d}{=} I_{H_S=h}.$$

We prove the result by comparing the coverage probabilities

$$p_v^c = \mathbb{E}_{H_V}^0 \left[F_{I_{H_V}}(0 \vee (H_V^{-\alpha}/\tau - \sigma^2)) \right],$$

$$p_t^c = \mathbb{E}_R^0 \left[F_{I_R}(0 \vee (R^{-\alpha}/\tau - \sigma^2)) \right],$$

$$p_s^c = \mathbb{E}_{H_S}^0 \left[F_{I_{H_S}}(0 \vee (H_S^{-\alpha}/\tau - \sigma^2)) \right],$$

and using the technique similar to the first part of Theorem 6, with $G(h) = F_{I_{H=h}}(0 \vee (h^{-\alpha}/\tau - \sigma^2))$, for any $H \in \{H_V, R, H_S\}$.

For this part, we use a comparison argument similar to second part of Theorem 6 for

$$p_I^c = \mathbb{E}_{H_I, R_I}^0 \left[F_{I_{H_I}}(0 \vee (R_I^{-\alpha}/\tau - \sigma^2)) \right],$$

$$p_{\mathcal{I}}^c = \mathbb{E}_{H_{\mathcal{I}}, R_{\mathcal{I}}}^0 \left[F_{I_{H_{\mathcal{I}}}}(0 \vee (R_{\mathcal{I}}^{-\alpha}/\tau - \sigma^2)) \right].$$

Take

$$G_1(h, r) = F_{I_{H_I=h}}(0 \vee (r^{-\alpha}/\tau - \sigma^2)),$$

$$G_2(h, r) = F_{I_{H_I=h}} \left(0 \vee \left(r^{-\alpha} / \tau - \sigma^2 \right) \right),$$

for $r \leq h$ and observe that by definition of $I_{H_I=h}$ and $I_{H_I=h}$ we have $G_2(h, r) \leq G_1(h, r)$ for all pairs (h, r) . Moreover

$$\begin{aligned} G_2(h) &:= \mathbb{E}_{R_I|h} [G_2(h, R_I|h)] \\ &\leq \mathbb{E}_{R_I|h} [G_1(h, R_I|h)] =: G_1(h). \end{aligned} \quad (83)$$

Then by comparing the two densities

$$f_{H_I}(h) = 4\pi\lambda^{3/2}h^2e^{-\lambda\pi h^2}, f_{H_I}(h) = \frac{8}{3}\pi^2\lambda^{5/2}h^4e^{-\lambda\pi h^2},$$

we have

$$\begin{aligned} p_I^c - p_I^c &= \int_0^\infty \int_0^h G_1(h, r) f_{R_I|h}(r) dr f_{H_I}(h) dh \\ &\quad - \int_0^\infty \int_0^h G_2(h, r) f_{R_I|h}(r) dr f_{H_I}(h) dh \\ &= \int_0^\infty \mathbb{E}_{R_I|h} [G_1(h, R_I|h)] f_{H_I}(h) dh \\ &\quad - \int_0^\infty \mathbb{E}_{R_I|h} [G_2(h, R_I|h)] f_{H_I}(h) dh. \end{aligned} \quad (84)$$

Using the definition (83), the last term in (84) is equal to

$$\begin{aligned} &\int_0^\infty G_1(h) f_{H_I}(h) dh - \int_0^\infty G_2(h) f_{H_I}(h) dh \\ &\geq \int_0^\infty G_2(h) f_{H_I}(h) dh - \int_0^\infty G_2(h) f_{H_I}(h) dh \\ &= \int_0^{\sqrt{3/2\lambda\pi}} G_2(h) [f_{H_I}(h) - f_{H_I}(h)] dh \\ &\quad - \int_{\sqrt{3/2\lambda\pi}}^\infty G_2(h) [f_{H_I}(h) - f_{H_I}(h)] dh \\ &\geq G_2(\sqrt{3/2\lambda\pi}) \int_0^\infty (f_{H_I}(h) - f_{H_I}(h)) dh = 0, \end{aligned}$$

where, by definition of G_2 , it can be shown that $G_2(\sqrt{3/2\lambda\pi}) \geq 0$. Indeed for $h = \sqrt{3/2\lambda\pi}$, R_I^2 is uniformly distributed in $[0, 3/2\lambda\pi]$, and hence

$$\begin{aligned} G_2(\sqrt{3/2\lambda\pi}) &= \sqrt{2\lambda\pi/3} \int_0^{\sqrt{3/2\lambda\pi}} F_{I_{H_I=\sqrt{3/2\lambda\pi}}} \left(0 \vee \left(\frac{r^{-\alpha}}{\tau} - \sigma^2 \right) \right) dr \\ &= \sqrt{2\lambda\pi/3} \int_0^{(\tau\sigma^2)^{-1/\alpha} \wedge \sqrt{3/2\lambda\pi}} F_{I_{H_I=\sqrt{3/2\lambda\pi}}} \left(\frac{r^{-\alpha}}{\tau} - \sigma^2 \right) dr, \end{aligned}$$

which is non-negative and hence we have the result. \square

Part 3. The result $p_{I;\tau}^c \leq p_{I;\tau}^c$ in the tropical case can be proved similarly.

In contrast, the ordering among $p_{I;\tau}^c, p_{I;\tau}^c$ and $p_{I;\tau}^c$ depends on the parameter values τ, λ and α , which can be justified as follows and also validated in Figure 13. From (73) and (75), $p_{I;\tau}^c - p_{I;\tau}^c$ is positive or negative depending on the sign of the partial integral of the difference $f_{R_I|h}(r) f_R(h) - f_{R_S|h}(r) f_{H_S}(h)$ of joint probability densities, which depends on the parameters λ, σ and α .

Similarly, using (70) and (73), the difference

$$\begin{aligned} p_{I;\tau}^c - p_{I;\tau}^c &= \int_0^\infty \mathbb{1} \left\{ h < \left(\frac{1-\tau}{\tau\sigma^2} \right)^{\frac{1}{\alpha}} \right\} f_{H_I}(h) dh \\ &\quad - \int_0^{(\tau\sigma^2)^{-1/\alpha}} \int_{\left(\frac{h-\alpha}{\tau} - \sigma^2\right)^{-1/\alpha} \vee h}^\infty f_{R_S|h}(r) dr f_{H_S}(h) dh, \end{aligned}$$

is positive or negative depending on the parameters. \square

APPENDIX V COMPARISON OF INTERFERENCE

A. Theorem 7 (with fading)

For $I_V \geq_L I_t \geq_L I_S$ we compare the Laplace transforms

$$\mathbb{E}^0 [e^{-\gamma I_V}] = \mathbb{E}_{H_V}^0 \left[\frac{\mu}{\mu + \gamma H_V^{-\alpha}} e^{-2\pi\lambda \int_{H_V}^\infty \frac{\gamma r^{-\alpha}}{\mu + \gamma r^{-\alpha}} r dr} \right], \quad (85)$$

$$\mathbb{E}^0 [e^{-\gamma I_t}] = \mathbb{E}_R^0 \left[e^{-2\pi\lambda \int_R^\infty \frac{\gamma r^{-\alpha}}{\mu + \gamma r^{-\alpha}} r dr} \right],$$

$$\mathbb{E}^0 [e^{-\gamma I_S}] = \mathbb{E}_{H_S}^0 \left[e^{-2\pi\lambda \int_{H_S}^\infty \frac{\gamma r^{-\alpha}}{\mu + \gamma r^{-\alpha}} r dr} \right],$$

similarly to the proof of Theorem 6 in Subsection IV-A, in the case of an environment with fading, by comparing the densities of H_V, H_S and R , using the function G analogous to (81) as

$$G(h) := e^{-\lambda\pi h^2 \kappa(\gamma h^{-\alpha} / \mu, \alpha)}, \quad (86)$$

using the function κ from (96), along with the fact that $\frac{\gamma}{\mu + \gamma h^{-\alpha}} \leq 1$, for all $h \geq 0$.

To prove $I_T \geq_L I_I$, we compare

$$\mathbb{E}^0 [e^{-\gamma I_I}] = \mathbb{E}_{H_I}^0 \left[\frac{\mu}{\mu + \gamma H_I^{-\alpha}} e^{-2\pi\lambda \int_{H_I}^\infty \frac{\gamma u^{-\alpha}}{\mu + \gamma u^{-\alpha}} u du} \right],$$

$$\mathbb{E}^0 [e^{-\gamma I_T}] = \mathbb{E}_{H_T}^0 \left[\left(\frac{\mu}{\mu + \gamma H_T^{-\alpha}} \right)^2 e^{-2\pi\lambda \int_{H_T}^\infty \frac{\gamma u^{-\alpha}}{\mu + \gamma u^{-\alpha}} u du} \right],$$

from (55) and (62), by comparing the densities of H_I and H_T , and using the G function as

$$G(h) = \frac{\mu}{\mu + \gamma h^{-\alpha}} e^{-2\pi\lambda \int_h^\infty \frac{\gamma u^{-\alpha}}{\mu + \gamma u^{-\alpha}} u du}, \quad (87)$$

along with the fact that $\frac{\gamma}{\mu + \gamma h^{-\alpha}} \leq 1$, for all $h \geq 0$.

For proving $\mathcal{T}_V \geq_{st} \mathcal{T}_t \geq_{st} \mathcal{T}_S$, we compare

$$\mathbb{P}^0(\mathcal{T}_V \leq x) = \mathbb{E}_{H_V}^0 \left[\left(1 - e^{-\mu H_V^\alpha x} \right) e^{-2\lambda\pi K_\alpha(\mu, x, H_V)} \right],$$

$$\mathbb{P}^0(\mathcal{T}_t \leq x) = \mathbb{E}_R^0 \left[e^{-2\lambda\pi K_\alpha(\mu, x, R)} \right],$$

$$\mathbb{P}^0(\mathcal{T}_S \leq x) = \mathbb{E}_{H_S}^0 \left[e^{-2\lambda\pi K_\alpha(\mu, x, H_S)} \right],$$

by again comparing the densities of H_V, H_S and R . In the proof we use the function G similarly to (81) as $G(h) :=$

$e^{-2\lambda\pi K_\alpha(\mu, x, h)}$ and the fact that $(1 - e^{-\mu h^\alpha x}) \leq 1$ for any $h \geq 0$.

For $\mathcal{T}_x \geq_{\text{st}} \mathcal{T}_I$, we compare

$$\mathbb{P}^0(\mathcal{T}_I \leq x) = \mathbb{E}_{H_I}^0 \left[\left(1 - e^{-\mu H_I^\alpha x}\right) e^{-2\lambda\pi K_\alpha(\mu, x, H_I)} \right],$$

$$\mathbb{P}^0(\mathcal{T}_x \leq x) = \mathbb{E}_{H_x}^0 \left[\left(1 - e^{-\mu H_x^\alpha x}\right)^2 e^{-2\lambda\pi K_\alpha(\mu, x, H_x)} \right],$$

by comparing the densities of H_I and H_x , and using the G function as $G(h) := (1 - e^{-\mu h^\alpha x}) e^{-2\lambda\pi K_\alpha(\mu, x, h)}$. \square

B. Theorem 7 (without fading)

The comparison of the interference at different typical epochs in the no-fading scenario can be proved using same type of comparisons as in the case with fading and using the proof of Theorem 6 in no-fading case. For the first part, $I_v \geq_L I_t \geq_L I_s$, we compare

$$\mathbb{E}^0 [e^{-\nu I_v}] = \mathbb{E}_{H_v}^0 \left[e^{-\nu H_v^{-\alpha} - \pi\lambda L_\nu(H_v, \alpha)} \right],$$

$$\mathbb{E}^0 [e^{-\nu I_t}] = \mathbb{E}_R^0 \left[e^{-\pi\lambda L_\nu(R, \alpha)} \right],$$

$$\mathbb{E}^0 [e^{-\nu I_s}] = \mathbb{E}_{H_s}^0 \left[e^{-\pi\lambda L_\nu(H_s, \alpha)} \right],$$

by a similar comparison of the densities of H_v, R and H_s , using the function $G(h) = e^{-\pi\lambda L_\nu(h, \alpha)}$, where $L_\nu(r, \alpha)$ is as defined in (99). Also for proving $I_x \geq_L I_I$, we compare

$$\mathbb{E}^0 [e^{-\nu I_I}] = \mathbb{E}_{H_I}^0 \left[e^{-\nu H_I^{-\alpha} - \pi\lambda L_\nu(H_I, \alpha)} \right],$$

$$\mathbb{E}^0 [e^{-\nu I_x}] = \mathbb{E}_{H_x}^0 \left[e^{-2\nu H_x^{-\alpha} - \pi\lambda L_\nu(H_x, \alpha)} \right],$$

using the densities of H_I and H_x and the function $G(h) = e^{-\nu h^{-\alpha} - \pi\lambda L_\nu(h, \alpha)}$. \square

APPENDIX VI PROOFS: SCALE INVARIANCE

A. Theorem 8 (with fading)

Recall the coverage probabilities for the typical handover case in (39) with $\sigma = 0$ as

$$p_v^c = \frac{1}{1+\tau} \mathbb{E}_{H_v}^0 \left[e^{-\pi\lambda H_v^2 \kappa(\tau, \alpha)} \right] = \frac{1}{1+\tau} (1 + \kappa(\tau, \alpha))^{-3/2},$$

using the Laplace transform of H_I^2 from Proposition 3. The coverage probability p_v^c in this case depends only on τ, α . By a similar computation we can show that

$$p_t^c = (1 + \kappa(\tau, \alpha))^{-1} \text{ and } p_s^c = (1 + \kappa(\tau, \alpha))^{-\frac{1}{2}},$$

both of which depend only on τ, α . This shows the scale invariance property of the coverage probabilities with respect to the parameter λ, μ .

For the case of typical max interference epoch, the coverage probability with $\sigma = 0$ is

$$p_I^c = \frac{2\tau^{-2/\alpha}}{\alpha} \int_0^\tau \frac{z^{2/\alpha-1}}{1+z} \mathbb{E}_{H_I}^0 \left[e^{-\pi\lambda H_I^2 \kappa(z, \alpha)} \right] dz. \quad (88)$$

from (59). Using the density of H_I , after exchanging the integrals in (88), we have

$$p_I^c = \frac{2\tau^{-2/\alpha}}{\alpha} \int_0^\tau \frac{z^{2/\alpha-1}}{1+z} (1 + \kappa(z, \alpha))^{-3/2} dz, \quad (89)$$

using the Laplace transform of H_I^2 from Proposition 3. The last expression for p_I^c in (89) is independent of λ, μ . Similarly we can show from (63) that

$$p_x^c = \frac{2\tau^{-2/\alpha}}{\alpha} \int_0^\tau \frac{z^{2/\alpha-1}}{(1+z)^2} (1 + \kappa(z, \alpha))^{-5/2} dz, \quad (90)$$

which is independent of λ, μ and hence we have the result. The same scale invariance can be shown to hold for the tropical case as well. \square

Remark 23 Similarly to (44) we also obtain closed form for the coverage probability in the interference limited regime from (89), $p_I^c = 0$ with $\alpha = 2$, since $\kappa(z, 2) = \infty$. For $\alpha = 4$ we have $\kappa(z, 4) = z^{\frac{1}{2}} \arctan(z^{\frac{1}{2}})$ and hence

$$p_I^c = \frac{\tau^{-1/2}}{2} \int_0^\tau \frac{z^{-1/2}}{1+z} \left(1 + z^{\frac{1}{2}} \arctan(z^{\frac{1}{2}})\right)^{-3/2} dz. \quad (91)$$

Remark 24 Similarly to (91) we also obtain closed form for p_x^c in the interference limited regime from (90), $p_x^c = 0$ with $\alpha = 2$. For $\alpha = 4$

$$p_x^c = \frac{\tau^{-1/2}}{2} \int_0^\tau \frac{z^{-1/2}}{(1+z)^2} \left(1 + z^{\frac{1}{2}} \arctan(z^{\frac{1}{2}})\right)^{-5/2} dz,$$

B. Theorem 8 (without fading)

At the typical handover we have

$$p_v^c = \mathbb{P}^0 (H_v^{-\alpha} / I_{H_v} \geq \tau).$$

Since the ratio $\frac{H_v^{-\alpha}}{I_{H_v}}$ is independent of λ , so is the coverage probability. The same reasoning applies for the scale invariance of the coverage probabilities in the four other cases:

- typical time: $p_t^c = \mathbb{P}^0 (R^{-\alpha} / I_R \geq \tau)$,
- typical MS: $p_s^c = \mathbb{P}^0 (H_s^{-\alpha} / I_{H_s} \geq \tau)$,
- typical MI: $p_I^c = \mathbb{P}^0 (H_I^{-\alpha} / I_{H_I} \geq \tau)$,
- typical mI: $p_x^c = \mathbb{P}^0 (H_x^{-\alpha} / I_{H_x} \geq \tau)$,

from (68), (71), (74) and (77), respectively. For typical mS-MI, from (70), we have

$$p_{v, \tau}^c = \int_0^\infty \mathbb{1}_{h^{-\alpha} > \tau h^{-\alpha}} f_{H_v}(h) dh = \begin{cases} 1 & \text{if } \tau < 1 \\ 0 & \text{if } \tau = 1, \end{cases}$$

since $\tau \leq 1$. At a typical time from (72), for any $\tau \geq 0$ we have

$$\begin{aligned} p_{t, \tau}^c &= \int_0^\infty \mathbb{P} (R_1 > \tau^{1/\alpha} r) f_R(r) dr \\ &= \int_0^\infty \int_{\tau^{1/\alpha} r}^\infty 2\lambda\pi h e^{-\lambda\pi(h^2 - r^2)} dh f_R(r) dr. \end{aligned}$$

For $\tau \leq 1$, we have $\tau^{1/\alpha} \leq 1$ and hence $p_{t;\tau}^c = 1$ in this case. For $\tau > 1$, we have $\tau^{1/\alpha} > 1$ and

$$\begin{aligned} p_{t;\tau}^c &= \int_0^\infty \int_{\tau^{1/\alpha r}}^\infty 2\lambda\pi h e^{-\lambda\pi(h^2-r^2)} dh f_R(r) dr \\ &= \int_0^\infty \int_{\lambda\pi\tau^{2/\alpha} r^2}^\infty e^{-z} e^{\lambda\pi r^2} dz f_R(r) dr \\ &= \int_0^\infty e^{-\lambda\pi r^2(\tau^{2/\alpha}-1)} f_R(r) dr \\ &= \int_0^\infty e^{-\lambda\pi r^2\tau^{2/\alpha}} 2\lambda\pi r dr = \tau^{-2/\alpha}. \end{aligned}$$

We can similarly prove from (72) that $p_{s;\tau}^c$ is also independent of λ , as follows:

$$\begin{aligned} p_{s;\tau}^c &= \int_0^\infty \mathbb{P}\left(R_S > \tau^{1/\alpha} h\right) f_{H_S}(h) dh \\ &= \int_0^\infty \int_{\tau^{1/\alpha} h \vee h}^\infty f_{R_S|H_S=h}(r) dr f_{H_S}(h) dh. \end{aligned}$$

For $\tau \leq 1$, we have $p_{s;\tau}^c = 1$. For $\tau > 1$ we have

$$\begin{aligned} p_{s;\tau}^c &= \int_0^\infty \int_{\tau^{1/\alpha} h}^\infty f_{R_S|H_S=h}(r) dr f_{H_S}(h) dh \\ &= \int_0^\infty \int_{\tau^{1/\alpha} h}^\infty \frac{\lambda^{1/2} r}{(r^2 - h^2)^{1/2}} e^{-\lambda\pi(r^2-h^2)} dr f_{H_S}(h) dh \\ &= \int_0^\infty \int_{\lambda\pi(\tau^{2/\alpha}-1)h^2}^\infty \frac{1}{2\sqrt{\pi}} z^{-1} e^{-z} dz f_{H_S}(h) dh \\ &= \frac{1}{2\sqrt{\pi}} \mathbb{E}_{H_S}^0 \left[\Gamma\left(0, \lambda\pi(\tau^{2/\alpha}-1)H_S^2\right) \right]. \end{aligned}$$

In case of $\tau \leq 1$, at the typical max-interference, we have from (79) that

$$\begin{aligned} p_{I;\tau}^c &= \mathbb{P}^0\left(H_I \geq R_I \tau^{1/\alpha}\right) \\ &= \int_0^\infty \mathbb{P}^0\left(h^{-2} R_I^2 \leq \tau^{-2/\alpha}\right) f_{H_I}(h) dh \\ &= \int_0^\infty \tau^{-2/\alpha} f_{H_I}(h) dh = \tau^{-2/\alpha}, \end{aligned}$$

using Corollary 3. The final expression is independent of λ . For the typical min interference, from (80) we have

$$\begin{aligned} p_{\mathcal{I};\tau}^c &= \mathbb{E}_{H_{\mathcal{I}}, R_{\mathcal{I}}}^0 \left[F_{I_{H_{\mathcal{I}}}}(R_{\mathcal{I}}^{-\alpha}/\tau) \right] \\ &= \mathbb{P}^0\left(2H_{\mathcal{I}}^{-\alpha} \leq R_{\mathcal{I}}^{-\alpha}/\tau\right) \\ &= \int_0^\infty \mathbb{P}^0\left(h^{-2} R_{\mathcal{I}}^2 \leq (2\tau)^{-2/\alpha}\right) f_{H_{\mathcal{I}}}(h) dh \\ &= \int_0^\infty (2\tau)^{-2/\alpha} f_{H_{\mathcal{I}}}(h) dh = (2\tau)^{-2/\alpha}, \end{aligned}$$

using Corollary 5, where the last expression is independent of λ . \square

APPENDIX VII OTHER ATTENUATION FUNCTIONS

A. Bounded path-loss function

In the case of bounded attenuation function $\ell(r) = (1+r)^{-\alpha}$ as in IV-F1, given $H = h$ we have the coverage probability as

$$\begin{aligned} \mathbb{P}(S > \tau | H = h) &= \mathbb{E}_{I_h} [\mathbb{P}(S > \tau | I_h)] \\ &= \mathbb{E}_{I_h} [\mathbb{P}(\rho > \tau(1+h)^\alpha (\sigma^2 + I_h))] \\ &= \mathbb{E}_{I_h} \left[e^{-\mu\tau(1+h)^\alpha (\sigma^2 + I_h)} \right] \\ &= e^{-\mu\tau(1+h)^\alpha \sigma^2} \mathcal{L}_{I_h}(\mu\tau(1+h)^\alpha). \end{aligned}$$

For example, in the case of signal handover $I_h := \rho(1+h)^{-\alpha} + \sum_i \rho_i(1+D_i)^{-\alpha}$. Computing the PGFL with respect to the point process η_h we have the Laplace transform of I_h for any $\gamma \geq 0$ as

$$\mathbb{E}_{I_h} [e^{-\gamma I_h}] = \frac{\mu}{\mu + \gamma(1+h)^{-\alpha}} e^{-2\pi\lambda \int_h^\infty \frac{\gamma(1+r)^{-\alpha}}{\mu + \gamma(1+r)^{-\alpha}} r dr}. \quad (92)$$

Hence for $\gamma = \mu\tau(1+h)^\alpha$, we re-write the integral in the exponent in (92) as

$$\int_h^\infty \frac{\tau}{\tau + (1+r)^\alpha(1+h)^{-\alpha}} r dr := M_\alpha(h, \tau)$$

and we have the required Laplace transform as

$$\mathbb{E}_{I_h} [e^{-\mu\tau(1+h)^\alpha I_h}] = \frac{1}{1+\tau} e^{-2\lambda\pi M_\alpha(h, \tau)}.$$

The coverage probability is

$$p_{\mathcal{V}}^c = \frac{1}{1+\tau} \mathbb{E}_{H_{\mathcal{V}}}^0 \left[e^{-\mu\tau(1+H_{\mathcal{V}})^\alpha \sigma^2} e^{-2\lambda\pi M_\alpha(H_{\mathcal{V}}, \tau)} \right].$$

Similarly for the typical time and typical MS, we have

$$p_t^c = \mathbb{E}_R^0 \left[e^{-\mu\tau(1+R)^\alpha \sigma^2} e^{-2\lambda\pi M_\alpha(R, \tau)} \right],$$

$$p_s^c = \mathbb{E}_{H_S}^0 \left[e^{-\mu\tau(1+H_S)^\alpha \sigma^2} e^{-2\lambda\pi M_\alpha(H_S, \tau)} \right].$$

A comparison result similar to Theorem 6 can be shown to hold true, which is $p_{\mathcal{V}}^c \leq p_t^c \leq p_s^c$. Similarly, for the other two typical epochs

$$\begin{aligned} p_i^c &= \mathbb{E}_{H_I, R_I}^0 \left[Q_\alpha(H_I, R_I, \tau) e^{-\mu\tau(1+R_I)^\alpha \sigma^2} \right. \\ &\quad \left. \times e^{-2\pi\lambda \int_{H_I}^\infty Q_\alpha(R_I, u, \tau) u du} \right], \end{aligned}$$

$$\begin{aligned} p_{\mathcal{I}}^c &= \mathbb{E}_{H_{\mathcal{I}}, R_{\mathcal{I}}}^0 \left[(Q_\alpha(H_{\mathcal{I}}, R_{\mathcal{I}}, \tau))^2 e^{-\mu\tau(1+R_{\mathcal{I}})^\alpha \sigma^2} \right. \\ &\quad \left. \times e^{-2\pi\lambda \int_{H_{\mathcal{I}}}^\infty Q_\alpha(R_{\mathcal{I}}, u, \tau) u du} \right], \end{aligned}$$

where $Q_\alpha(x, y, \tau) := \frac{(1+x)^\alpha}{(1+x)^\alpha + \tau(1+y)^\alpha}$. It can be proved similarly that $p_{\mathcal{I}}^c \leq p_t^c$.

B. Step attenuation function

Consider the step attenuation function $\ell(r) = p\mathbb{1}_{r \leq d}$ as in IV-F2. The SINR is defined as

$$S \equiv \text{SINR} := \frac{\rho p \mathbb{1}_{H \leq d}}{\sigma^2 + \sum_i \rho_i p \mathbb{1}_{H \leq D_i \leq d}}.$$

Then the coverage probability with respect to the Palm probability distribution of epoch of interest is

$$p^c(\tau, \mu, \lambda, \alpha) = \mathbb{E}_H^0[\mathbb{P}(S > \tau | H)], \quad (93)$$

where f_H is the density of the distance H to the serving station. Conditioned on $H = h$ the inner term (93) is

$$\begin{aligned} \mathbb{P}(S > \tau | h) &= \mathbb{E}_{I_h}[\mathbb{P}(S > \tau | h, I_h)] \left(1 - e^{-\lambda \pi d^2}\right) \\ &= \mathbb{E}_{I_h} \left[\mathbb{P} \left(\rho > \frac{\tau}{p} (\sigma^2 + I_h) \right) \right] \left(1 - e^{-\lambda \pi d^2}\right) \\ &= \mathbb{E}_{I_h} \left[e^{-\frac{\mu \tau}{p} (\sigma^2 + I_h)} \right] \left(1 - e^{-\lambda \pi d^2}\right) \\ &= e^{-\frac{\mu \tau \sigma^2}{p}} \left(1 - e^{-\lambda \pi d^2}\right) \mathbb{E}_{I_h} \left[e^{-\frac{\mu \tau}{p} I_h} \right]. \end{aligned}$$

Using the PGFL of the max-shot noise of a Poisson point process, we get

$$\mathbb{E}_{I_h} \left[e^{-\frac{\mu \tau}{p} I_h} \right] = \begin{cases} \frac{1}{1+\tau} e^{-2\lambda \pi (d-h)\tau/(1+\tau)}, & \text{for typical ms-MI,} \\ e^{-2\lambda \pi (d-h)\tau/(1+\tau)}, & \text{for typical MS,} \\ e^{-2\lambda \pi (d-h)\tau/(1+\tau)}, & \text{for typical time.} \end{cases}$$

As a result the coverage probabilities are

$$p^c(\tau, \mu, \lambda, \alpha) = \begin{cases} \frac{C}{1+\tau} \mathbb{E}_{H_V}^0 [e^{\gamma H_V}], & \text{for typical ms-MI,} \\ C \mathbb{E}_{H_S}^0 [e^{\gamma H_S}], & \text{for typical MS,} \\ C \mathbb{E}_R^0 [e^{\gamma R}], & \text{for typical time,} \end{cases}$$

where $\gamma = 2\lambda \pi \tau / (1 + \tau)$ and

$$C \equiv C(\tau, d, \mu, \lambda, \sigma) := e^{-\frac{\mu \tau \sigma^2}{p}} \left(1 - e^{-\lambda \pi d^2}\right) e^{-2\lambda \pi \tau / (1 + \tau)}.$$

Even though we have $H_V \geq_{\text{mgf}} R \geq_{\text{mgf}} H_S$ from Lemma 3, this shows that no distinct ordering holds true among p_V^c, p_t^c and p_S^c , for all values of τ . Similarly using

$$\text{SINR} := \frac{\rho p \mathbb{1}_{R \leq d}}{\sigma^2 + \sum_i \rho_i p \mathbb{1}_{H \leq D_i \leq d}},$$

with $R \in \{R_I, R_{\bar{x}}\}$ and $H \in \{H_I, H_{\bar{x}}\}$ at typical mI and MI, respectively, one can show different ordering between $p_{\bar{x}}^c$ and p_I^c depending for different values of τ , even though we have $H_{\bar{x}} \geq_{\text{mgf}} H_I$ and $R_{\bar{x}} \geq_{\text{mgf}} R_I$, from Lemma 3.

It is also evident that in the interference limited regime, the coverage probabilities are not scale invariant with respect to λ , as the constant

$$C(\tau, d, \mu, \lambda, \sigma)|_{\sigma=0} = \left(1 - e^{-\lambda \pi d^2}\right) e^{-2\lambda \pi \tau / (1 + \tau)}$$

is not. On the other hand, the μ -scale invariance holds true.

APPENDIX VIII SPECIAL INTEGRALS

A. The integral in (43)

We determine the integral in (43) of the form $\int_h^\infty \frac{\tau h^\alpha}{r^\alpha + \tau h^\alpha} r dr$ for some h, τ and α positive. Taking a change of variable $\tau^{-2/\alpha} h^{-2} r^2 = z$ we obtain that

$$\begin{aligned} \int_h^\infty \frac{\tau h^\alpha}{r^\alpha + \tau h^\alpha} r dr &= \frac{1}{2} \tau^{2/\alpha} h^2 \int_{\tau^{-2/\alpha}}^\infty \frac{1}{1 + z^{\alpha/2}} dz \\ &= \frac{1}{2} h^2 \kappa(\tau, \alpha), \end{aligned}$$

where

$$\kappa(\tau, \alpha) := \tau^{2/\alpha} \int_{\tau^{-2/\alpha}}^\infty \frac{1}{1 + z^{\alpha/2}} dz. \quad (94)$$

B. The integral (85)

We compute the integral $\int_h^\infty \frac{\gamma r^{-\alpha}}{\mu + \gamma r^{-\alpha}} r dr$ in the exponent in (85) by a change of variable $(\gamma/\mu)^{-2/\alpha} r^2 = z$

$$\begin{aligned} \int_h^\infty \frac{\gamma r^{-\alpha}}{\mu + \gamma r^{-\alpha}} r dr &= \frac{1}{\mu} \int_h^\infty \frac{\gamma/\mu}{\gamma/\mu + r^\alpha} r dr \\ &= \frac{1}{2\mu} (\gamma/\mu)^{2/\alpha} \int_{(\gamma/\mu)^{-2/\alpha}}^\infty (1 + z^{\alpha/2})^{-1} dz \\ &= \frac{h^2}{2\mu} (\gamma h^{-\alpha}/\mu)^{2/\alpha} \int_{(\gamma h^{-\alpha}/\mu)^{-2/\alpha}}^\infty (1 + z^{\alpha/2})^{-1} dz \\ &= \frac{1}{2\mu} h^2 \kappa(\gamma h^{-\alpha}/\mu, \alpha), \end{aligned} \quad (95)$$

from (94). Note from (95) that $h^2 \kappa(\gamma h^{-\alpha}/\mu, \alpha)$ is a non-increasing function of h for fixed α, γ and μ .

C. The integral in (58)

For the integral $\int_h^\infty \frac{\tau r^\alpha}{u^\alpha + \tau r^\alpha} u du$ in (58), by the change of variable $\tau^{-2/\alpha} r^{-2} u^2 = z$ we have

$$\begin{aligned} \int_h^\infty \frac{\tau r^\alpha}{u^\alpha + \tau r^\alpha} u du &= \frac{\tau^{2/\alpha} r^2}{2} \int_{\tau^{-2/\alpha} (r/h)^{-2}}^\infty \frac{1}{z^{\alpha/2} + 1} dz \\ &= \frac{h^2}{2} (\tau(r/h)^\alpha)^{2/\alpha} \int_{\tau(r/h)^\alpha}^\infty \frac{1}{z^{\alpha/2} + 1} dz \\ &= \frac{h^2}{2} \kappa(\tau(r/h)^\alpha, \alpha), \end{aligned} \quad (97)$$

from (94).

D. The integral in (45)

For the integral $\int_h^\infty e^{-\mu r^\alpha} x r dr$ in (45) we have

$$\begin{aligned} \int_h^\infty e^{-\mu r^\alpha} x r dr &= \frac{1}{\alpha} \int_{\mu h^\alpha x}^\infty e^{-z} \left(\frac{z}{\mu x}\right)^{2/\alpha} \frac{1}{z} dz \\ &= \frac{1}{\alpha} (\mu x)^{-2/\alpha} \int_{\mu h^\alpha x}^\infty z^{2/\alpha - 1} e^{-z} dz \\ &= \frac{1}{\alpha} (\mu x)^{-2/\alpha} \Gamma(2/\alpha, \mu h^\alpha x) \\ &:= K_\alpha(\mu, x, h), \end{aligned} \quad (98)$$

where $\Gamma(\cdot, \cdot)$ is the upper incomplete gamma function defined as $\Gamma(a, b) := \int_b^\infty z^{a-1} e^{-z} dz$

E. The integral in (66)

The integral $\int_h^\infty (1 - e^{-\nu r^{-\alpha}}) r dr$ in (66) is computed as

$$\begin{aligned} & \int_h^\infty (1 - e^{-\nu r^{-\alpha}}) r dr \\ &= \frac{1}{\alpha} \nu^{2/\alpha} \int_0^{\nu h^{-\alpha}} (1 - e^{-z}) z^{-\frac{2}{\alpha}-1} dz \\ &= -\frac{1}{2} h^2 (1 - e^{-\nu h^{-\alpha}}) + \frac{1}{2} \nu^{2/\alpha} \gamma \left(1 - \frac{2}{\alpha}, \nu h^{-\alpha} \right) \\ &:= \frac{1}{2} L_\nu(h, \alpha), \end{aligned} \quad (99)$$

where $\gamma(\cdot, \cdot)$ is the lower incomplete gamma function defined as $\gamma(a, b) := \int_0^b z^{a-1} e^{-z} dz$.

ACKNOWLEDGEMENT

The authors are thankful to the ERC-NEMO grant, under the European Union's Horizon 2020 research and innovation program, grant agreement number 788851 to INRIA Paris. This research was also funded in part by the France 2030 BPI "5G NTN mmWave" project to Télécom Paris.

REFERENCES

- [1] C. E. Shannon, "A Mathematical Theory of Communication," *Bell System Technical Journal*, vol. 27, no. 3, pp. 379–423, 1948. [Online]. Available: <https://onlinelibrary.wiley.com/doi/abs/10.1002/j.1538-7305.1948.tb01338.x>
- [2] J. G. Andrews, F. Baccelli, and R. K. Ganti, "A Tractable Approach to Coverage and Rate in Cellular Networks," *IEEE Transactions on Communications*, vol. 59, no. 11, pp. 3122–3134, 2011.
- [3] J. G. Andrews, A. K. Gupta, and H. S. Dhillon, "A Primer on Cellular Network Analysis Using Stochastic Geometry," *ArXiv*, 2016. [Online]. Available: <https://arxiv.org/abs/1604.03183>
- [4] H. S. Dhillon, R. K. Ganti, F. Baccelli, and J. G. Andrews, "Modeling and Analysis of K-Tier Downlink Heterogeneous Cellular Networks," *IEEE Journal on Selected Areas in Communications*, vol. 30, no. 3, pp. 550–560, 2012.
- [5] H.-S. Jo, Y. J. Sang, P. Xia, and J. G. Andrews, "Heterogeneous Cellular Networks with Flexible Cell Association: A Comprehensive Downlink SINR Analysis," *IEEE Transactions on Wireless Communications*, vol. 11, no. 10, pp. 3484–3495, 2012.
- [6] H. ElSawy, E. Hossain, and M. Haenggi, "Stochastic Geometry for Modeling, Analysis, and Design of Multi-Tier and Cognitive Cellular Wireless Networks: A Survey," *IEEE Communications Surveys & Tutorials*, vol. 15, no. 3, pp. 996–1019, 2013.
- [7] N. Okati, "Modeling and Analysis of Massive Low Earth Orbit Communication Networks," *Ph.D. Thesis, Tempere University*, 2023. [Online]. Available: <https://trepo.tuni.fi/handle/10024/146346>
- [8] N. Okati, T. Riihonen, D. Korpi, I. Angervuori, and R. Wichman, "Downlink Coverage and Rate Analysis of Low Earth Orbit Satellite Constellations Using Stochastic Geometry," *IEEE Transactions on Communications*, vol. 68, no. 8, pp. 5120–5134, 2020.
- [9] C.-S. Choi and F. Baccelli, "A Novel Analytical Model for LEO and MEO Satellite Networks Based on Cox Point Processes," *IEEE Transactions on Communications*, vol. 73, pp. 2265–2279, 2022.
- [10] —, "Cox Point Processes for Multi Altitude LEO Satellite Networks," *IEEE Transactions on Vehicular Technology*, vol. 73, no. 10, pp. 15916–15921, 2024.
- [11] F. Baccelli and S. Zuyev, "Stochastic geometry models of mobile communication networks," *Frontiers in Queueing: Models and Applications in Science and Engineering*, ed. J. Dshalalow, CRC Press, 1996.
- [12] P. Nain, D. Towsley, B. Liu, and Z. Liu, "Properties of random direction models," in *Proceedings IEEE 24th Annual Joint Conference of the IEEE Computer and Communications Societies.*, vol. 3, 2005, pp. 1897–1907.
- [13] D. Josep, M. Dieter, and P. Xavier, "Dynamic random geometric graphs," *arXiv preprint cs/0702074*, 2007.
- [14] N. S. Ramesan and F. Baccelli, "How Wireless Queues Benefit from Motion: An Analysis of the Continuum Between Zero and Infinite Mobility," *IEEE Transactions on Wireless Communications*, vol. 20, no. 12, pp. 8149–8162, 2021.
- [15] X. Lin, R. K. Ganti, P. J. Fleming, and J. G. Andrews, "Fundamentals of Mobility in Cellular Networks: Modeling and Analysis," in *Proceedings of IEEE International Conference on Communications (ICC)*, 2012, pp. 5433–5437.
- [16] Z. Gong and M. Haenggi, "Mobility and fading: Two sides of the same coin," in *2010 IEEE Global Telecommunications Conference (GLOBECOM 2010)*. IEEE, 2010, pp. 1–5.
- [17] R. K. Ganti and M. Haenggi, "Spatial and temporal correlation of the interference in ALOHA ad hoc networks," *IEEE Communications Letters*, vol. 13, no. 9, pp. 631–633, 2009.
- [18] A. Balakrishnan, F. Baccelli, S. K. Jhavar, and P. Martins, "Doppler-Shannon Association in Vehicular Networks: A Stochastic Geometry Analysis," *HAL*, 2026. [Online]. Available: <https://hal.science/hal-05597638/>
- [19] P. Madadi, F. Baccelli, and G. de Veciana, "Shared Rate Process for Mobile Users in Poisson Networks and Applications," *IEEE Transactions on Information Theory*, vol. 64, no. 3, pp. 2121–2141, 2018.
- [20] H. K. Armeniakos, A. G. Kanatas, and H. S. Dhillon, "Comprehensive Analysis of Maximum Power Association Policy for Cellular Networks Using Distance and Angular Coordinates," *IEEE Transactions on Wireless Communications*, vol. 23, no. 9, pp. 12 189–12 205, 2024.
- [21] F. Baccelli and S. K. Jhavar, "On a Class of Dynamical Poisson-Voronoi Tessellations," *arXiv e-prints*, p. arXiv:2511.15893, Nov. 2025.
- [22] G. Nigam, P. Minero, and M. Haenggi, "Coordinated multipoint joint transmission in heterogeneous networks," *IEEE Transactions on Communications*, vol. 62, no. 11, pp. 4134–4146, 2014.
- [23] V. Baumstark and G. Last, "Some distributional results for poisson-voronoi tessellations," *Advances in Applied Probability*, vol. 39, no. 1, p. 16–40, 2007.
- [24] J. F. C. Kingman, *Poisson processes*, ser. Oxford Studies in Probability. New York: The Clarendon Press Oxford University Press, 1993, vol. 3, oxford Science Publications.
- [25] F. Baccelli and B. Błaszczyszyn, *Stochastic Geometry and Wireless Networks, Volume II - Applications*, ser. Foundations and Trends in Networking: Vol. 4: No 1-2, pp 1-312. NoW Publishers, 2009. [Online]. Available: <https://inria.hal.science/inria-00403040>
- [26] M. Haenggi and R. K. Ganti, "Interference in Large Wireless Networks," *Foundations and Trends in Networking*, vol. 3, no. 2, pp. 127–248, 11 2009. [Online]. Available: <https://doi.org/10.1561/13000000015>
- [27] A. Giovanidis and F. Baccelli, "A Stochastic Geometry Framework for Analyzing Pairwise-Cooperative Cellular Networks," *IEEE Transactions on Wireless Communications*, vol. 14, p. 794–808, 2015.
- [28] M. Shaked and J. G. Shanthikumar, "Stochastic Orders", ser. Springer Series in Statistics. New York, NY: Springer, 2007.
- [29] K. A. Hamdi, "Capacity of MRC on Correlated Rician Fading Channels," *IEEE Transactions on Communications*, vol. 56, no. 5, pp. 708–711, 2008.
- [30] A. AlAmmouri, J. G. Andrews, and F. Baccelli, "A Unified Asymptotic Analysis of Area Spectral Efficiency in Ultradense Cellular Networks," *IEEE Transactions on Information Theory*, vol. 65, no. 2, pp. 1236–1248, 2019.
- [31] T. Amdeberhan, M. L. Glasser, M. C. Jones, V. H. Moll, R. Posey, and D. Varela, "The Cauchy-Schlömilch transformation," *arXiv e-prints*, p. arXiv:1004.2445, Apr. 2010.